FNP

JOURNAL OF FOOD PROCESS ENGINEERING

D.R. HELDMAN
and
R.P. SINGH
COEDITORS

FOOD & NUTRITION PRESS, INC.

VOLUME 12, NUMBER 1 JANUARY 1990

JOURNAL OF FOOD PROCESS ENGINEERING

Coeditors: **D.R. HELDMAN,** National Food Processors Association, 1401 New York Ave., N.W., Washington, D.C.
R.P. SINGH, Agricultural Engineering Department, University of California, Davis, California

Editorial Board:
A.L. BRODY, Princeton, New Jersey (1991)
SOLKE, BRUIN, Vlaardingen, 1 Nederland (1991)
M. CHERYAN, Urbana, Illinois (1990)
J.P. CLARK, Chicago, Illinois (1991)
R.L. EARLE, Palmerston, North New Zealand (1991)
B. HALLSTROM, Lund, Sweden (1992)
M. KAREL, New Brunswick, New Jersey (1992)
J.L. KOKINI, New Brunswick, New Jersey (1990)
M. LEMAGUER, Edmonton, Alberta, Canada (1990)
R.G. MORGAN, Glenview, Illinois (1990)
M. PELEG, Amherst, Massachusetts (1990)
M.A. RAO, Geneva, New York (1992)
S.S.H. RIZVI, Ithaca, New York (1991)
E. ROTSTEIN, Minneapolis, Minnesota (1991)
I. SAGUY, Minneapolis, Minnesota (1990)
S.K. SASTRY, Columbus, Ohio (1992)
W.E.L. SPIESS, Karlsruhe, Germany (1990)
J.F. STEFFE, East Lansing, Michigan (1992)
K.R. SWARTZEL, Raleigh, North Carolina (1991)
A.A. TEIXEIRA, Gainesville, Florida (1992)
G.R. THORPE, Victoria, Australia (1992)

All articles for publication and inquiries regarding publication should be sent to DR. D.R. HELDMAN, COEDITOR, *Journal of Food Process Engineering,* National Food Processors Association, 1401 New York Ave., N.W., Washington, D.C. 20005 USA: or DR. R.P. SINGH, COEDITOR, *Journal of Food Process Engineering,* University of California, Davis, Department of Agricultural Engineering, Davis, CA 95616 USA.

All subscriptions and inquiries regarding subscriptions should be sent to Food & Nutrition Press, Inc., 6527 Main Street, P.O. Box 374, Trumbull, CT 06611 USA.

One volume of four issues will be published annually. The price for Volume 12 is $92.00 which includes postage to U.S., Canada, and Mexico. Subscriptions to other countries are $109.00 per year via surface mail, and $118.00 per year via airmail.

Subscriptions for individuals for their own personal use are $72.00 for Volume 12 which includes postage to U.S., Canada, and Mexico. Personal subscriptions to other countries are $89.00 per year via surface mail, and $98.00 per year via airmail. Subscriptions for individuals should be sent direct to the publisher and marked for personal use.

The *Journal of Food Process Engineering* (ISSN: 0145-8876) is published quarterly (March, June, September and December) by Food & Nutrition Press, Inc.—Office of Publication is 6527 Main Street, P.O. Box 374, Trumbull, Connecticut 06611 USA. (Current issue is January 1990.)

Second class postage paid at Bridgeport, CT 06602.

POSTMASTER: Send address changes to Food & Nutrition Press, Inc., 6527 Main Street, P.O. Box 374, Trumbull, CT 06611.

JOURNAL OF FOOD PROCESS ENGINEERING

JOURNAL OF FOOD PROCESS ENGINEERING

Coeditors:

D.R. HELDMAN, National Food Processors Association, 1401 New York Ave., N.W., Washington, D.C.

R.P. SINGH, Agricultural Engineering Department, University of California, Davis, California.

Editorial Board:

A.L. BRODY, Schotland Business Research, Inc., Princeton Corporate Center, 3 Independence Way, Princeton, New Jersey

SOLKE, BRUIN, Unilever Research Laboratorium, Vlaardingen, Oliver van Noortland 120 postbus 114, 3130 AC Claardingen 3133 AT Vlaardingen, 1 Nederland

M. CHERYAN, Department of Food Science, University of Illinois, Urbana, Illinois

J.P. CLARK, Epstein Process Engineering, Inc., Chicago, Illinois

R.L. EARLE, Department of Biotechnology, Massey University, Palmerston North, New Zealand

B. HALLSTROM, Food Engineering Chemical Center, S-221 Lund, Sweden

M. KAREL, Department of Food Science, Rutgers, The State University, Cook College, New Brunswick, New Jersey

J.L. KOKINI, Department of Food Science, Rutgers University, New Brunswick, New Jersey

M. LEMAGUER, Department of Food Science, University of Alberta, Edmonton, Canada

R.G. MORGAN, Kraft, Inc., Glenview, Illinois

M. PELEG, Department of Food Engineering, University of Massachusetts, Amherst, Massachusetts

M.A. RAO, Department of Food Science and Technology, Institute for Food Science, New York State Agricultural Experiment Station, Geneva, New York

S.S.H. RIZVI, Department of Food Science, Cornell University, Ithaca, New York

E. ROTSTEIN, The Pillsbury Co., Minneapolis, Minnesota

I. SAGUY, The Pillsbury Co., Minneapolis, Minnesota

S.K. SASTRY, Department of Agricultural Engineering, Ohio State University, Columbus, Ohio

W.E.L. SPIESS, Bundesforschungsanstalt fuer Ernaehrung, Karlsruhe, Germany

J.F. STEFFE, Department of Agricultural Engineering, Michigan State University, East Lansing, Michigan

K.R. SWARTZEL, Department of Food Science, North Carolina State University, Raleigh, North Carolina

A.A. TEIXEIRA, Agricultural Engineering Department, University of Florida, Gainesville, Florida

G.R. THORPE, CSIRO Australia, Highett, Victoria 3190, Australia

Journal of
FOOD PROCESS ENGINEERING

VOLUME 12
NUMBER 1

Coeditors: D.R. HELDMAN
R.P. SINGH

FOOD & NUTRITION PRESS, INC.
TRUMBULL, CONNECTICUT 06611 USA

© Copyright 1990 by
Food & Nutrition Press, Inc.
Trumbull, Connecticut USA

All rights reserved. No part of this publication may be reproduced, stored in a retrieval system or transmitted in any form or by any means: electronic, electrostatic, magnetic tape, mechanical, photocopying, recording or otherwise, without permission in writing from the publisher.

ISSN 0145-8876

Printed in the United States of America

CONTENTS

ห้องสมุดกรมวิทยาศาสตร์บริการ
-2 พค. 2533

RHEOLOGICAL MODELING OF POTATO FLOUR DURING EXTRUSION COOKING

KEVIN L. MACKEY[1], ROBERT Y. OFOLI[2,4], RON G. MORGAN[3] and JAMES F. STEFFE[2]

Accepted for Publication February 8, 1989

ABSTRACT

A generalized model for predicting the effects of shear rate, temperature, moisture content, time-temperature history and strain history on viscosity has been evaluated for extruded potato flour doughs. An Instron Capillary Rheometer and a 50 mm Baker Perkins co-rotating twin screw extruder were used to evaluate all effects incorporated in the model, except strain history. The power law model was used to describe shear rate effects in the range 10-10000 s^{-1}. The generalized model fit observed data for temperatures of 25–95°C and moisture contents ranging from 22 to 50%, wet basis. Since potato flour by its manufacturing process is pregelatinized, it was unnecessary to evaluate the effects of time-temperature history. Strain history was found to have an insignificant influence on the viscosity.

INTRODUCTION

Commercialization of extrusion processes is constrained by lack of adequate scale-up information. Two important elements in extrusion scale-up and design are effective process engineering analysis methods, and comprehensive rheological models. During cooking extrusion, starch granules undergo many changes leading to molecular rearrangement, including loss of crystallinity and formation of amylose lipid complexes. These changes in the starch granule significantly affect viscosity. Temperature, moisture, shear, and feed ingredient composition are important factors in these structural changes (Harper 1986). Accurate characterization of their effects on extrudates is, therefore, important.

[1]USDA-ARS, ERRC, Philadelphia, PA.
[2]Michigan State University, East Lansing, MI.
[3]Kraft, Inc., Glenview, IL.
[4]All correspondence to: Dr. Robert Y. Ofoli, 102 A.W. Farrall Hall, Michigan State University, East Lansing, Michigan 48824-1323.

Journal of Food Process Engineering *12(1989) 1–11. All Rights Reserved.*
©Copyright 1989 by Food & Nutrition Press, Inc., Trumbull, Connecticut.

Several extrusion models for flour and protein doughs have been proposed in the published literature (Bhattacharya and Hanna 1986; Cervone and Harper 1978; Janssen 1986; Jao *et al.* 1978; Remsen and Clark 1978). Of these, only the model proposed by Remsen and Clark (1978) incorporates effects of temperature, shear rate, time-temperature history and moisture content.

The most comprehensive rheological model yet has been proposed by Morgan *et al.* (1989). This generalized model describes the rheological changes which occur during the cooking extrusion of protein doughs. The mathematical relationship predicts viscosity as a function of temperature-time history, strain history, temperature, shear rate and moisture content.

Dolan *et al.* (1989) used the model by Morgan *et al.* (1989) as the basis for predicting changes in starch viscosity during the gelatinization of high moisture starch solutions. The model was found to predict changes in viscosity due to different time-temperature histories when shear rate, moisture content, temperature and strain history are held constant. While the changes that occur in the starch granules are different for high moisture systems than low moisture systems, it is important to note that time-temperature history is an important factor contributing to viscosity changes in both systems.

Recently, Mackey (1989) modified the expression of Morgan *et al.* (1989), and used it to describe the viscosity of low to intermediate moisture starch-based doughs during cooking extrusion. The major modification involved the substitution of starch kinetics (gelatinization) in place of protein kinetics (denaturation).

The purpose of this paper is to evaluate Mackey's (1989) expression for potato flour extruded at low to intermediate moisture. In particular, the significance of the modular effects of time-temperature history, moisture content, temperature, shear-strain history, and shear rate will be assessed.

THEORETICAL DEVELOPMENT

Mackey's (1989) modification of the model presented by Morgan *et al.* (1989) made it suitable for use in describing the viscosity of low to intermediate moisture starch-based products. The effect of time-temperature history on viscosity was modified to account for starch gelatinization kinetics. The resulting expression for time-temperature history effects is (Mackey 1989)

$$\eta = 1 + A\left(1 - e^{-k_a \psi}\right)^{\alpha} \tag{1}$$

Incorporating the above expression, the generalized viscosity model for extrusion of starch-based doughs becomes (Mackey 1989):

$$\eta = \exp\left[\frac{\Delta E_v}{R}(T^{-1} - T_r^{-1}) + b\,(MC - MC_r)\right] f(\dot{\gamma})\left[1 + A\left(1 - e^{-k_a \psi}\right)^{\alpha}\right] \cdot \left[1 - \beta(1 - e^{-d\phi})\right] \tag{2}$$

where

$$\psi = \int_0^t T \exp\left(\frac{\triangle E_g}{RT(t)}\right) dt \qquad for \quad T \geq T_g \tag{3a}$$

$$\psi = 0 \qquad for \quad T < T_g \tag{3b}$$

$$\phi = \int_0^t \dot{\gamma}(t) \; dt \tag{3c}$$

and

$$A = \frac{\eta_\infty}{\eta_{\dot{\gamma},T,MC}} - 1 \tag{3d}$$

The first term on the right hand side of Eq. 2 incorporates the effects of temperature and moisture content on viscosity. It is important to note that $\triangle E_v/R$ is not a measure of gelatinization kinetics but rather of how temperature affects the flow of the material. Lubricating effects of water are described by b(MC-MC_r). The $f(\dot{\gamma})$ term represents any apparent shear rate model (power law, Casson, Herschel-Bulkley, etc.) of the dough at the reference temperature, moisture content, and $\psi = \phi = 0$. The next term describes the effects of gelatinization on the viscosity of starch dough.

Time-temperature history (ψ) can range from zero for temperatures below the gelatinization threshold to infinity for either very high temperatures, long exposure times or a combination of the two. Also included is the energy of activation for gelatinization ($\triangle E_g$) which may be affected by moisture content. The final term incorporates strain history (ϕ), which is a measure of the effects of irreversible shear thinning. As strain history increases, the viscosity approaches a finite value (η_∞).

If any of the effects in Eq. 2 is absent or negligible, the term which incorporates that effect reduces to unity.

MATERIALS AND METHODS

Potato flour (Lamb-Weston, Portland, Oregon) was mixed at room temperature with tap water to 25, 35, and 45% moisture (wb) in a large institutional kitchen mixer. The doughs were allowed to equilibrate at 7 °C overnight in Ziploc bags (Dow Chemical, Indianapolis, Indiana). Final moisture content of the doughs were determined by drying in a vacuum oven overnight at 70 °C and 686 mm Hg.

An Instron Capillary Rheometer and a Model 4202 Instron Universial Testing Machine (Instron Corp., Canton, Massachusetts) were used to measure the apparent viscosity of the doughs. Die lengths of 50.8 mm (2 in) and 6.35 mm (¼ in) and diameters of 3.175 mm (1/8 in) and 1.59 mm (1/16 in) were used, giving

L/D ratios ranging from 2 to 32. Two replicates for each plunger velocity and L/D ratio were performed. Force versus plunger displacement curves were collected and force at the die entrance was calculated by extrapolation of the force versus displacement curves to the die as described by Einhorn and Turetzky (1964). Barrel drag was then substracted from the corrected force.

Temperatures of 25, 50, 65, and 95 °C were used in this study. At 50 and 65 °C, doughs were compressed in the capillary barrel and were held for 10 min. Moisture contents of 25, 35, and 45%, wet basis, were used. Tests were conducted at 50 °C for 25% (wb) moisture samples. Cook times of 2, 4, 6 and 12 min at 95 °C were performed on 35% (wb) moisture samples after compression. The 45% moisture samples were cooked for 4 and 12 min after compression. Effects of temperature on viscosity ($\triangle E_v$) was determined by a linear regression of log η versus inverse temperature; the effect of moisture content on viscosity (b) was determined by a linear regression of log η versus moisture content at constant temperature.

Experimental extrusion tests were conducted using a Baker Perkins MPF-50D (APV Baker, Grand Rapids, Michigan) co-rotating twin screw extruder with the screw configuration given in Table 1. Moisture contents were 40 and 50% (wb) and temperatures at the die ranged from 40 to 75 °C depending on extruder operating conditions. Feed rates of 1.26×10^{-1}, 2.00×10^{-2}, and 8.69×10^{-3} kg/s; and screw speeds of 100, 220, and 350 RPM were used. Die diameter was 3.17×10^{-3} m and die lengths were 4.00×10^{-3}, 1.50×10^{-2} and 2.60×10^{-2} m. Pressure drop and extrudate temperature at the die were recorded two minutes after extruder operating conditions had been changed to allow equilibrium conditions to be attained. Equilibrium conditions were assumed to exist when die pressure and barrel zone temperatures were stabilized.

RESULTS AND DISCUSSION

Correction for entrance effects was made using the technique described by Bagley (1957). Shear rate and shear stress were calculated using the Rabinowitsch equation (Whorlow 1980)

$$\dot{\gamma}_w = \frac{3Q}{\pi R_o^3} + \sigma_w \left[\frac{d \frac{Q}{\pi R_o^3}}{d\sigma_w} \right] \tag{4}$$

and the standard expression for shear stress at the wall of a capillary:

$$\sigma_w = \frac{\Delta P R_o}{2L} \tag{5}$$

TABLE 1.
SCREW CONFIGURATIONS (L/D RATIO: 15)

Length (cm)	Screw Type*	Location
17.2	FS	Feed Inlet
7.6	30F	
7.6	FS	
5.1	30F	
2.5	45F	
5.1	FS	
6.2	30F	
5.1	FS	
5.1	30F	
12.7	SL	Die

*Key to screw notation
FS Feed screws
30F 30 degree forwarding paddles
45F 45 degree forwarding paddles
SL Single lead screws

Viscosities of the extrudates were calculated by measuring the pressure drop at the die. Plotting pressure drop versus the three die L/D ratios at constant temperature, moisture, and mass flow rate allowed correction for end effects as described by Bagley (1957) for capillary dies. Shear rate was calculated using the Rabinowitsch equation (Whorlow 1980) and shear stress was calculated using Eq. 5 for each die, temperature, moisture and mass flow rate. Temperature and moisture correction on extruder data was performed using $\triangle E_v$ and b estimated from the capillary rheometer.

There was apparent slip at some moisture contents, temperatures and shear rates, as indicated by the presence of a "shark skin" on the extrudate. Slip analysis was performed using the method described by Darby (1976); however, the results were not meaningful. The inability to correct for slip is probably due to a friction coefficient between the wall of the capillary die and the food material which could not be measured.

The effect of temperature on viscosity (adjusted to 35% moisture content and a shear rate of 100 s^{-1}) is shown in Fig. 1. The effect of moisture content on viscosity (adjusted to 50 °C and 100 s^{-1}) is shown in Fig. 2. The actual moisture contents of the 25, 35, and 45% doughs were determined to be 0.282 (22% wb), 0.507 (33.7% wb), and 0.772 (43.6% wb) g water per g potato flour, respectively. As illustrated, a simple logarithmic relationship may not be adequate for broad ranges of moisture content. This is similar to the data for defatted soy flour adjusted to 95 °C from Morgan *et al.* (1989).

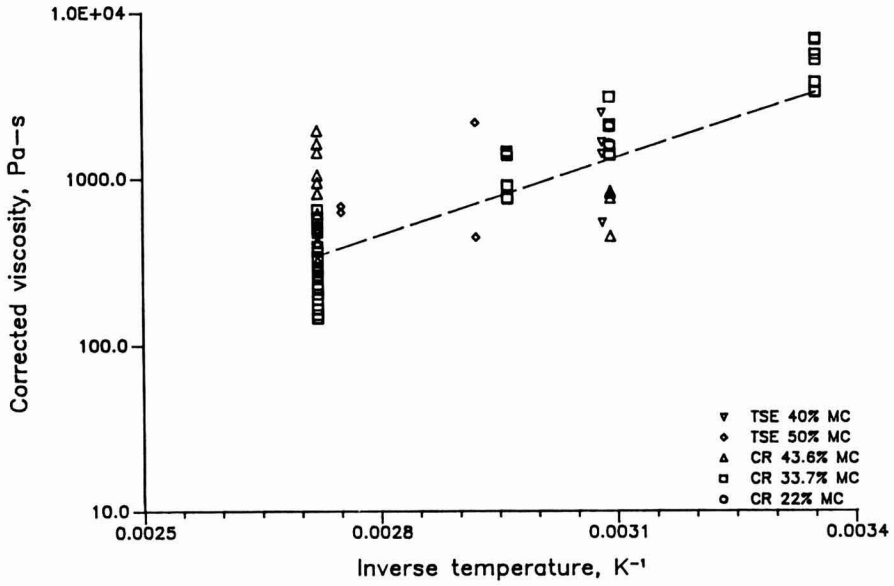

FIG. 1. EFFECT OF TEMPERATURE ON VISCOSITY OF POTATO FLOUR
(Viscosities adjusted to 35% MC and 100 s^{-1})

Apparent viscosity versus shear rate for potato flour cooked at 95 °C for 0, 2, 4, 6, and 12 min are plotted in Fig. 3. The power law model was found to provide accurate characterization for shear rate effects. Data for 2, 4, and 6 min show similar slopes (flow behavior indices) and apparent viscosities. The 12 min cook data exhibits more shear thinning. This is, most likely, due to degradation of overcooked starch, which would indicate that time-temperature had little effect on viscosity for cooking times less than 6 min.

Since potato flour is pregelatinized in the process of making it, there is no relative increase in viscosity from gelatinization effects, therefore, $A = 0$ (see Eq. 3c). The term in Eq. 2 accounting for the effects of time-temperature history

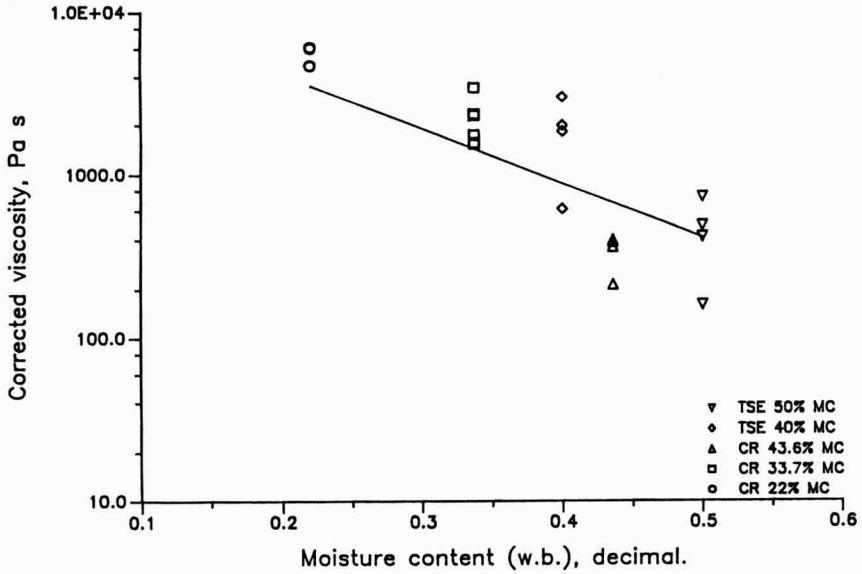

FIG. 2. CORRECTED VISCOSITY OF POTATO FLOUR VERSUS MOISTURE CONTENT
(Viscosities adjusted to 50C and 100s^{-1})

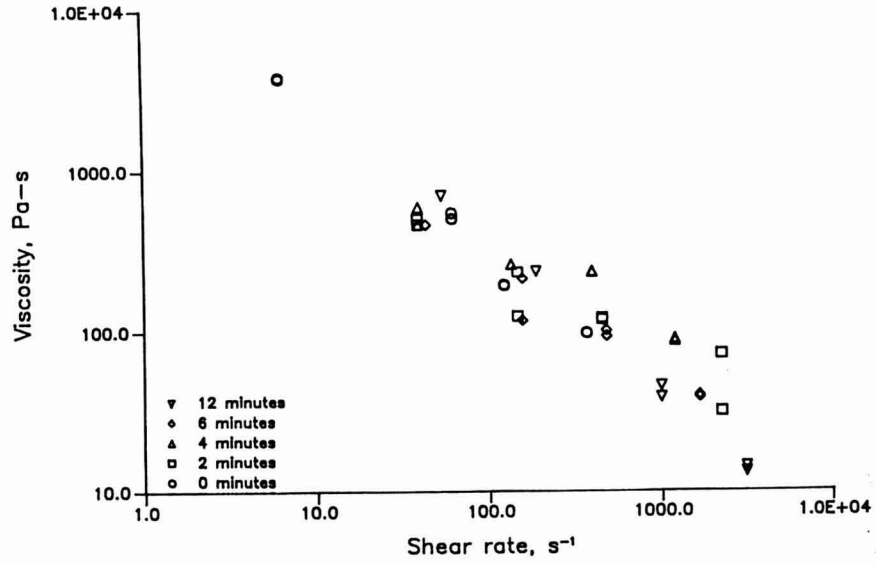

FIG. 3. VISCOSITY OF POTATO FLOUR DOUGHS COOKED OVER VARIOUS TIMES AT 95 °C

accordingly reduces to unity. Comparison of these data with uncooked viscosities adjusted to the same temperature and moisture content verifies that the potato flour is pregelatinized. Strain history did not significantly affect the viscosity of the potato flour and therefore this parameter was also set to unity.

All capillary rheometer and twin-screw extrusion data were then fit to a final model of

$$\eta = K\dot{\gamma}^{n-1}\exp\left[\frac{\Delta E_v}{R}(T^{-1} - T_r^{-1}) + b\,(MC - MC_r)\right] \quad (6)$$

which, essentially, is equivalent to the model presented by Cervone and Harper (1978).

Equation 6 gives an R^2 of 0.951. The parameters in Eq. 6 which provided the best fit are given in Table 2.

TABLE 2.
REGRESSED VALUES AND LITERATURE COMPARISONS

Parameter	Regressed value	Literature value*	Type of material
ΔE_v	8729	4967	Cooked cereal dough
		8723	Pregelatinized corn flour
		7300	Soy grits
		6900	Defatted soy flour dough
b	8.63	6.7	Defatted soy four
		7.9	Corn flour dough
		0.19	Soy grits
n	0.25	0.24	Defatted soy flour
		0.34	Soy grits
		0.36	Pregelatinized corn flour
		0.51	Cooked cereal dough
K	34903	4880	Cooked cereal dough
		4982	Pregelatinized corn flour
		16930	Soy grits
		28800	Soy grits

*Harper (1981).

The values of the free energy of activation ($\triangle E_v$), the moisture constant (b), and the shear thinning index (n) are within the ranges observed by other researchers for similar cereal and soy products (Table 2). The lower value of the power law index compared to pregelatinized corn flour is to be expected since

native potato starch is highly shear thinning. The means of the predicted versus observed data are plotted in Fig. 4 for all data. Note that the data obtained during twin-screw extrusion fit with the same degree of accuracy as the data obtained from capillary rheometry.

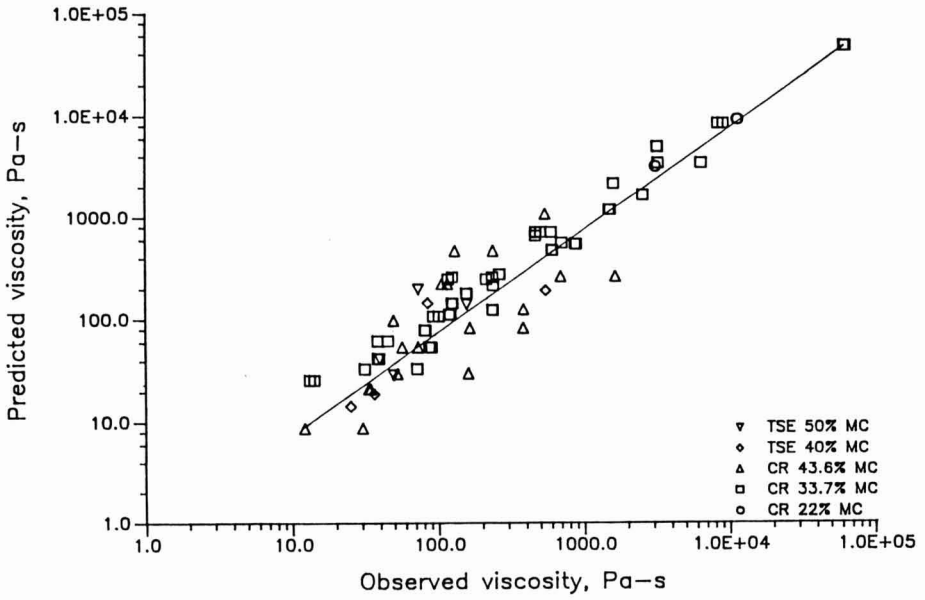

FIG. 4. PREDICTED VERSUS OBSERVED VISCOSITY OF POTATO FLOUR DOUGHS

CONCLUSIONS

The generalized model of Mackey (1989) has been evaluated for extruded potato flour. The model incorporates the effects of shear rate, temperature, moisture content, time-temperature history and strain history. Viscosity data were obtained by capillary rheometry and twin screw extrusion of low moisture potato flour doughs.

The model was experimentally tested with potato flour doughs over a wide range of experimental conditions; a temperature range of 25–95 °C, a moisture content range of 0.28–0.77 g water per g potato flour (22–44% wb), and shear rate range of 10–10000 s^{-1}.

Results from the capillary rheometer and twin screw extruder are similar over a wide range of shear rates, moisture contents, and temperatures. It appears, therefore, that the capillary rheometer could be used to obtain the appropriate

model parameters to describe the effects of shear rate, moisture content and temperature. Since potato flour is pregelatinized during the process of making it, time-temperature and strain history effects were absent.

Future research must focus on assessing the kinetics of ungelatinized starches, on the relationship of time-temperature history and strain history to starch gelatinization, and on the understanding of slip phenomena in capillary and extruder dies.

NOMENCLATURE

A	relative viscosity increase due to gelatinization
b	constant related to moisture effects on viscosity, dimensionless
d	constant related to strain history effects on viscosity, s
$\triangle E_v$	free energy of activation, kcal [g mole]$^{-1}$
k_a	reaction transmission coefficient, K^{-1} s^{-1}
K	power law consistency coefficient, Pa s^n
L	capillary length, m
MC	moisture content, dry weight basis, decimal
MC_r	reference moisture content, dry weight basis, decimal
n	flow behavior index, dimensionless
Q	volume flow rate, m^3 s^{-1}
R	universal gas constant, 1.987 cal [g mole K]$^{-1}$
R_o	die or capillary radius, m
t	time, s
T	temperature, K
T_g	Threshold temperature for starch gelatinization, K
T_r	reference temperature, K

Greek Symbols

α	index of molecular weight effects on viscosity
$\dot{\gamma}$	shear rate, s^{-1}
$\triangle E_g$	Activation energy of gelatinization, cal/g-mol
$\triangle P$	pressure drop, Pa
η	apparent viscosity, Pa s
η_∞	viscosity at infinite time-temperature history, Pa s
$\eta_{\dot{\gamma},T,MC}$	viscosity corrected for shear rate, moisture and temperature, Pa s

σ_w	shear stress at the wall, Pa
ϕ	strain history, dimensionless
ψ	time-temperature history, K s

REFERENCES

BAGLEY, E.B. 1957. End corrections in the capillary flow of polyethylene. *J. Applied Phys. 28*, 624–627.

BHATTACHARYA, M. and HANNA, M.A. 1986. Viscosity modeling of dough in extrusion. *J. Food Tech. 21*(2), 167–174.

CERVONE, N.W. and HARPER, J.M. 1978. Viscosity of an intermediate moisture dough. *J. Food Proc. Eng. 2*, 83–95.

DARBY, R. 1976. *Viscoelastic Fluids: An Introduction to Their Properties and Behavior*, Marcel Dekker, p. 283–296, New York.

DOLAN, K.D., STEFFE, J.F. and MORGAN, R.G. 1989. Back extrusion and simulation of viscosity development during starch gelatinization. *J. Food Proc. Eng. 11*, 79–101.

EINHORN, S.C. and TURETZKY, S.B. 1964. Rheological properties of SBR polymers by capillary extrusion. *J. Appl. Polym. Sci. 8*, 1257–1273.

HARPER, J.M. 1981. *Extrusion of Foods*, Vol. 1. CRC Press, Boca Raton, Florida.

HARPER, J.M. 1986. Extrusion of foods. *Food Tech. 40*, 70–76.

JANSSEN, L.P.B.M. 1986. Models for cooking extrusion. In *Food Engineering and Process Applications*, Vol.2, Unit Operations. (M. Le Maguer and P. Jelen, eds.) pp. 115–129. Elsevier Applied Science, London and New York.

JAO, Y.C., CHEN, A.H., LEWANDOWSKI, D. and IRWIN, W.E. 1978. Engineering analysis of soy dough rheology in extrusion. *J. Food Proc. Eng. 2*, 97–112.

MACKEY, K.L. 1989. *A Generalized Viscosity Model for the Cooking Extrusion of Starch Based Products.* Ph.D. Dissertation, Department of Food Science and Human Nutrition, Michigan State University, East Lansing, Michigan.

MORGAN, R.G., STEFFE, J.F. and OFOLI, R.Y. 1989. A generalized viscosity model for extrusion of protein doughs. *J. Foods Proc. Eng. 11*, 55–78.

REMSEN, C.H. and CLARK, J.P. 1978. A viscosity model for a cooking dough. *J. Food Proc. Eng. 2*, 39–64.

WHORLOW, R.W. 1980. *Rheological Techniques*, Ellis Howwood., Chichester, England.

PERFORMANCE OF HEAT RECOVERY SYSTEM FOR A SPRAY DRYER

D.P. DONHOWE[1], C.H. AMUNDSON[2,4] and C.G. HILL, JR.[3]

University of Wisconsin
Madison, Wisconsin 53706

Accepted for Publication February 22, 1989

ABSTRACT

A factorial experimental design was used to study the effect of exhaust heat recovery, air flow rate and outlet temperature on the energy consumption of a spray dryer. A commercial-scale cocurrent flow dryer with pressure atomization was used to dry 15 wt% sodium sulfate solutions. The inlet air to the dryer was preheated by using a shell-and-tube heat exchanger to recover energy from the exhaust air. Heat recovery reduced the energy consumption of the dryer by 12−28%, with the largest reduction occurring at the high levels of air flow rate (13,000 kg/h) and outlet temperature (104°C). The energy consumption of the dryer was lowest when heat was recovered at the low air flow rate (6500 kg/h) and low outlet temperature (82°C).

No problems were encountered with fouling or cleaning of the heat exchanger. The total pressure drop across the heat exchanger varied from 0.05−0.2 kPa depending on the air flow rate. This additional flow restriction resulted in an estimated 8% decrease in air flow rate but had negligible effect on energy consumption. The warm-up time and the space required by the heat recovery unit were insignificant factors for this dryer. The payback period of the heat recovery system was estimated as 4.1−5.4 years with a rate of return of 21−28%.

INTRODUCTION

Spray drying is one of the most energy intensive unit operations in the food industry. In the production of dried milk, for example, the spray dryer can consume 16–20 time the energy that an evaporator requires to evaporate a pound of water (Knipschildt 1986). Thus, there has been a considerable effort to improve the thermal efficiency of spray dryers.

[1]Department of Food Science
[2]Departments of Food Science and Agricultural Engineering
[3]Department of Chemical Engineering
[4]Address correspondence to Dr. C.H. Amundson, Department of Food Science, University of Wisconsin, 1605 Linden Drive, Madison, Wisconsin 53706.

Journal of Food Process Engineering *12(1989) 13–32. All Rights Reserved.*
©Copyright 1989 by Food & Nutrition Press, Inc., Trumbull, Connecticut.

Advances in the technology of producing powdered food products have centered on the use of an additional fluidized bed or perforated plate to accomplish the final drying of the product (Pisecky 1985; Youngs 1986). These improvements have lowered energy consumption by as much as 30%. Other drying technologies showing promise include acoustic drying (Chowdhury 1984; Muralidhara 1985; Swientek 1986), drying in the presence of superheated steam (Amelot and Gauvin 1986) and drying under vacuum (Hayashi 1983).

Improvements can also be made in the design and operation of the spray dryer, including the use of direct air heating (Jansen and Elgersma 1985; Shebler 1977), optimization of process parameters (Cook and Dumont 1988; Gronlund 1984), foaming the feed solution (Romero-Ferrer *et al.* 1986; Okazaki and Crosby 1984) and establishing good operational practices (Baker and Bahu 1983).

However, these methods of improving the thermal efficiency are limited by the loss of energy with the exhaust air from the dryer, particularly the latent heat associated with its water vapor. If the energy in the exhaust air could be fully recovered, then spray dryers would have thermal efficiencies approaching those of modern evaporators employing vapor recompression (Bimbenet 1982).

There are many options for recovering the energy in the exhaust air of a spray dryer (Kragh and Kraglund 1981; Reay 1980). Scrubbers use part of the this energy to preheat the feed to the evaporator or dryer. However, these systems have often resulted in bacterial contamination of the product and are less effective than other systems at reducing overall energy consumption (Kessler 1980; Knipschildt 1986; Richardt 1980). Another option is sending clean and humid exhaust air to a flue gas evaporator (Kragh and Kraglund 1981; Richardt 1980). The inlet air to the dryer, meanwhile, could be preheated by waste gas from a boiler (Energy Technology Support Unit 1986a) or steam condensate (Pisecky and Shell 1979). However, the operating schedule of the dryer should match that of the other processes being considered.

Heat recovery systems for preheating the inlet air to the dryer with the exhaust air offer the advantage of simultaneous operation of energy source and energy sink. Single-stage air-air heat exchangers and air-liquid-air exchangers are the most commonly used systems, and the choice between the two types of systems often depends on the powder loading in the exhaust air (Kragh and Kraglund 1981).

Air-air heat exchangers are usually of the tubular (Energy Technology Support Unit 1986c; Masters 1983), plate (Jansen and Steenbergen 1979; Reay 1980) or heat pipe types (Jansen and Steenbergen 1979; Vasiliev *et al.* 1984). These heat exhangers often incorporate smooth surfaces (e.g., straight tubes or flat plates) for resistance to fouling and ease of cleaning (Reay 1980, Kragh and Kraglund 1981). They are usually quite large, though, due to the poor heat transfer properties of air.

Air-liquid-air heat exchangers or "run-around coils" consist of two air-liquid heat exchangers connected by a recirculating liquid (Reay 1980). Run-around coils typically use extended surfaces to decrease the size of the unit (Hansen 1982). The inlet and exhaust air ducts of the dryer may also be located far apart without the additional expense of ductwork which might be prohibitive with air-air heat exchangers. Run-around coils are thus often used when retrofitting dryers. However, they are more sensitive to fouling, more complicated and less efficient than air-air heat exchangers (Energy Technology Support Unit 1986b; Holland 1980).

Other potential heat recovery systems include two-stage heat exchangers (Kragh and Kraglund 1980; Milton 1981) and heat pumps in an open (Jebson 1977) or closed (Pendyala 1986) cycle. These systems recover part or all of the latent heat available in the exhaust air as well as its sensible heat, which could greatly increase the efficiency of spray drying. However, these units are generally more complex and expensive.

The purpose of the research presented here was to assess the performance of a shell-and-tube heat exchanger for recovering energy from a commercial-scale spray dryer.

MATERIALS AND METHODS

Spray Dryer

Experiments were conducted on a one-stage cocurrent flow spray dryer operating with pressure atomization (Fig. 1). It is capable of evaporating 900 kg/h of water when drying a 45 wt% skim milk concentrate. The cylindrical drying chamber has a height of 11.3 m and a diameter of 2.4 m.

A two-speed exhaust fan provides air flow through the dryer. A damper can be used to vary the flow rate from 14–283 std m^3/h. The incoming ambient air stream first passes through a recuperative heat exchanger. After passing through some louvers and an air filter, the air can be heated indirectly by steam coils or directly by a natural gas burner. For this research the air was heated primarily by the gas burner.

The inlet air is split between two ducts before entering the drying chamber. The air in the upper inlet duct enters the drying chamber immediately around the feed nozzle and aids the atomization and spray-air contacting processes. The air in the lower inlet duct enters the outer annular plenum chamber and helps to prevent powder buildup on the dryer walls. The ability to change the velocity and temperature of each inlet air stream gives the dryer versatility for drying various foodstuffs.

The liquid feed is held in a 760-L tank equipped with steam and cooling water jackets for temperature control. A small centrifugal pump is used to prime a high

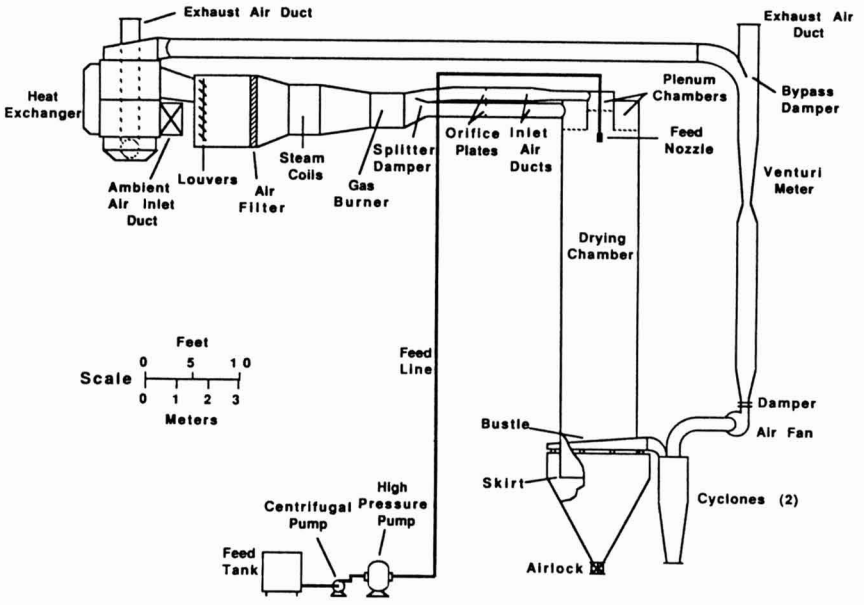

FIG. 1.

pressure pump, which transports the feed under pressure to a spray nozzle positioned in the center of the inner plenum chamber.

The atomized feed and inlet drying air mix in the plenum chamber and travel cocurrently down the drying chamber in approximately plug flow. Most of the dried product falls through the main cone and airlock when the air stream reverses its direction of flow at the dryer skirt. The product fines are recovered by two cyclones connected in parallel. The exhaust air is then either rejected to the atmosphere or sent to the heat recovery unit.

The experimental spray dryer is described in greater detail by Amundson (1967).

Heat Recovery Unit

A shell-and-tube heat exchanger was used to preheat the inlet air to the dryer by recovering energy from the exhaust air (Fig. 2). The heat exchanger has two tube-side passes and one shell-side pass in counter-cross flow. The tube-side fluid is the cold ambient air which is to be preheated, while the shell-side fluid is the hot exhaust air from the dryer. The tubes are made of borosilicate glass, and the shell is constructed of 304 stainless steel.

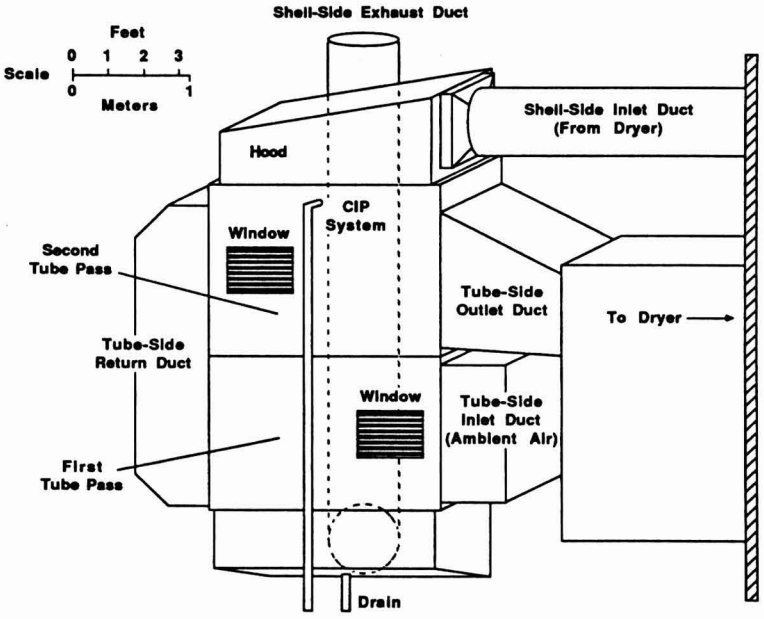

FIG. 2.

The tube arrangement in the heat exchanger is shown in Fig. 3. Each tube pass contains 31 rows of 40 tubes; the heat exchanger thus contains a total of 2480 tubes. The tubes are arranged horizontally and vertically "in-line". The geometric parameters of the heat exchangers are also summarized in Fig. 3.

A clean-in-place (CIP) system was used to clean the shell side of the heat exchanger. The outsides of the tubes were cleaned by feeding hot water or cleaning solution to a perforated pipe at the top of the heat exchanger (inside the hood), with the holes in the pipe pointed downward over the tubes. A pneumatic system was used to move the pipe back and forth over the tubes. A separate hot water line was connected to a spray nozzle for cleaning the hood. An automatic system was provided for controlling the CIP procedure, although manual control was used for this research. Filters were installed before the first tube pass to remove any dust in the ambient air.

Experimental Measurements

The flow rate, temperature and composition of each process stream (air, feed or product) and the energy supplied to the dryer were measured.

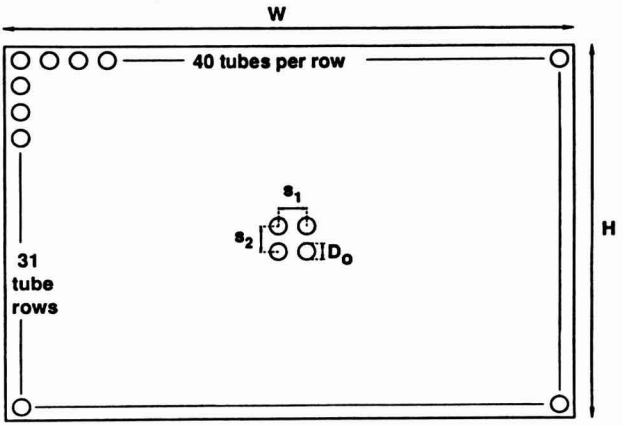

Geometric Parameters of the Heat Exchanger

Tube diamater, inner (D_i)	0.026 m
outer (D_o)	0.028 m
Transverse pitch (s_1)	0.0443 m
Longitudinal pitch (s_2)	0.0367 m
Tube length, tube-side	2.00 m
shell-side (L)	1.97 m
Width of pass (W)	1.776 m
Height of pass (H)	1.22 m
Space between passes (shell-side)	0.18 m
Total number of tubes in heat exchanger	2480

FIG. 3.

Flow Rate. Air flow rates were measured using orifice meters in the inlet ducts to the dryer and a Venturi meter in the exhaust duct. These meters were calibrated by injecting a known amount of ammonia into the air duct upstream of the meter and simultaneously measuring the time-averaged concentration of ammonia in the air immediately downstream of the meter (Woodhams 1970; Donhowe 1988).

In addition, the negative pressure differential created by the exhaust fan caused room air to leak into the dryer. This leakage occurred primarily in the inlet ductwork around the steam coils and gas burner, and in the exhaust ductwork between the bustle and cyclones. Air leakage in the inlet ducts was determined from ammonia calibration of the air flow rate upstream and downstream of the leaks. The exhaust duct leakage was estimated as the difference between the measured flow rates of the inlet and exhaust air streams.

Manometers were used to measure the pressure drops over the flow meters, heat exchanger and exhaust fan.

The flow rate of the sodium sulfate feed solution was determined by calibrating the nozzle for a given feed pressure before and after a set of experimental runs. The flow rates were determined by measuring the time required to collect a known amount of feed from the nozzle. Since the nozzle wore out rather quickly due to the abrasive nature of the feed solution, the flow rate through the nozzle at a given pressure increased about 2% between calibrations. The feed flow rate for an experimental run was estimated by linear interpolation between calibrations.

The total flow rate of product was determined using a mass balance on sodium sulfate.

Temperature. Air temperatures were measured using copper-constantan thermocouples connected to a potentiometer (Model #156X63V30, Honeywell, Inc.). The thermocouples were generally located at the center of an air duct or passage. However, temperature and velocity profiles were measured in the ducts around the heat exchanger to determine where to locate thermocouples to obtain a good estimate of the average temperature. The thermocouples were calibrated against a National Bureau of Standards thermometer over the operational temperature range.

The air temperature was measured at the following locations: before and after the heat exchanger on both shell and tube sides, in the upper and lower inlet ducts, in the dryer bustle (where extensive mixing of the air stream gives a reliable estimate of the outlet dryer temperature), at the entrance to the cyclones, and at the Venturi meter.

A calibrated thermocouple was used to measure the temperature of the solution in the feed tank. The product temperature was estimated as the temperature of the air passing through the dryer bustle. Although the product leaving the dryer was substantially cooler than the exhaust air, the effect of this inaccuracy on the energy calculations was negligible.

Composition. Air humidities were determined from measurements of wet-bulb and dry-bulb temperatures. These measurements were taken at three locations: the ambient inlet to the heat exchanger, downstream of the Venturi meter in the exhaust duct, and in the outlet duct from the heat exchanger on the shell (exhaust) side. The ambient air pressure was measured using a mercury barometer. Psychrometric formulae were used to calculate the humidity from these measurements (ASME 1968; Pallady 1984; Treybal 1980).

The moisture contents of the feed solution and the product were determined by drying samples to a constant weight in a vacuum oven.

Energy Input. The energy input to the dryer came from three sources: the gas burner, the steam coils, and work effects associated with the pumps and fan. The

flow rate of gas to the burner was determined from timed readings of a Rockwell 1000 gas meter. The energy input from the steam coils was estimated from measurements of the flow rate of condensate and the steam pressure. The electrical energy consumption of the dryer was determined by measuring the voltage and current drawn by the pumps and fan.

RESULTS AND DISCUSSION

The objectives of this research were to determine: (1) the effect of heat recovery on the energy consumption of the spray dryer; (2) the technical and economic feasibility of installing the heat recovery system on this dryer (if it were operated as a commercial dryer); and (3) the economic feasibility of installing the heat recovery system on this dryer.

Effect of Heat Recovery on Energy Consumption

A 2^3 factorial design (Box *et al.* 1978a) was used to study the effect of heat recovery on the energy consumption of the dryer for various operating conditions. The process variables investigated were: (1) whether or not heat was recovered (H); (2) the exhaust air flow rate (F); and (3) the outlet temperature of the dryer (T).

The experimental design was run in blocks four, with the block factor confounded with the three-factor interaction HFT. Each block was replicated at least once. The experimental levels of the process variables and the blocking arrangement are shown in Table 1.

Attempts were made to maintain all other operating parameters at constant values during the execution of the factorial design. However, some variation in these parameters was unavoidable, as can be seen in Table 2. The effect of these variations was reduced by executing the runs within a block in a random order.

Additional precautions were taken to minimize the effect of variation of the feed flow rate and ambient air temperature. First, all results were referenced to an ambient temperature of 10 °C. Second, since the flow rate of feed solution increased almost linearly as the factorial design progressed, the blocks were run in the order I, II, II, I. Third, the energy consumption of the dryer was divided by the amount of water evaporated from the feed. This quantity is called "specific energy consumption" or SEC and has units of kJ/kg.

Since the levels of the factorial variables could not be achieved precisely, the data were regressed to a linear model of the factors and their interactions (Box *et al.* 1978b). The SEC values obtained from this model for the design levels of -1 and $+1$ were then analyzed as though the factorial had been executed perfectly (Donhowe 1988).

TABLE 1.
2^3 FACTORIAL DESIGN FOR ASSESSING EFFECT OF HEAT RECOVERY ON ENERGY CONSUMPTION OF DRYER

Variables and levels

Level	Heat Recovered? H	Air Flow Rate F	Dryer Outlet Temperature T
-1	NO	6455 kg/h	82.2 °C
1	YES	13010 kg/h	104.4 °C

Blocking arrangement

Standard Order					Blocking Arrangement				
Test Condition	Variables H	F	T	Block HFT	Test Condition	Variables H	F	T	Block
A	-	-	-	-	A	-	-	-	I
B	+	-	-	+	D	+	+	-	
C	-	+	-	+	F	+	-	+	
D	+	+	-	-	G	-	+	+	
E	-	-	+	+	B	+	-	-	II
F	+	-	+	-	C	-	+	-	
G	-	+	+	-	E	-	-	+	
H	+	+	+	+	H	+	+	+	

TABLE 2.
EXPERIMENTAL RANGES OF "CONSTANT" PARAMETERS FOR FACTORIAL DESIGN

Parameter	Experimental Range
Feed - wt. % Na_2SO_4	14.83 - 14.95
- temperature (°C)	53 - 56
- nozzle	SX-58/21
- pressure	2000 psig
- flow rate (kg/hr)	255 - 274
Ambient - temperature (°C)	-2 to 23
- humidity (kg/kg)	0.005 - 0.011
- pressure (mm Hg)	727 - 743
Energy from steam coils* (kW)	4.4 - 13.2

* Energy input from the steam coils for Run 21 was 35 kW since steam heating was needed to achieve the desired outlet temperature.

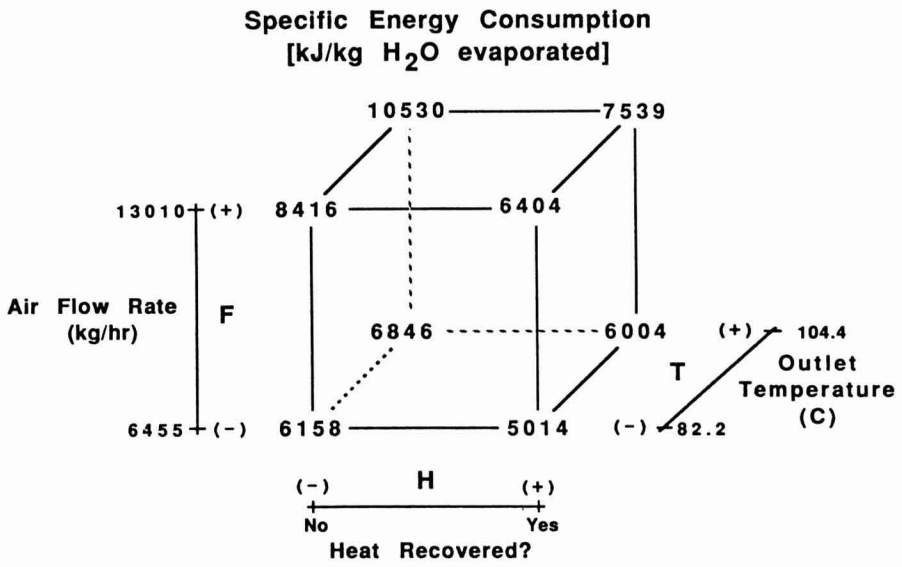

FIG. 4.

A cube plot of the regressed data is shown in Fig. 4. The specific energy consumption of the dryer was lowest for the combination of heat recovery, low air flow rate and low outlet temperature. The combination of no heat recovery, high air flow rate and high outlet temperature required the most energy.

The effects of the various factors on the energy consumption of the dryer was shown in Table 3. All three main factors (H.F.T) and the two-factor interaction HF were statistically significant at the $p < 0.005$ level.

The use of heat recovery (H) reduced the specific energy consumption by 1746 kJ/kg evaporated compared to the mean of 7114 kJ/kg. The average reduction in energy consumption due to heat recovery was thus

$$\frac{1746}{7114 + 1746/2} \times 100 = 21.9\%$$

with the factor of 2 being introduced because the mean represents a point midway between the low and high levels for heat recovery.

The reduction in energy consumption by using heat recovery at an operating condition F,T is given by

$$\% \text{ Reduction in Energy Consumption} = \frac{SEC_{H=-1,F,T} - SEC_{H=1,F,T}}{SEC_{H=-1,F,T}} * 100$$

TABLE 3.
ESTIMATED EFFECTS OF THE VARIABLES AND THEIR INTERACTIONS ON THE ENERGY CONSUMPTION OF THE DRYER

	Estimate ± Standard Error	
	Specific Energy Consumption (kJ/kg evap.)	Reduction in Energy Consumption (%)
Average	7114 ± 62	-------
Main Effects:		
Heat Recovery H	-1746 ± 123	-21.9 ± 1.7 ***
Air Flow Rate F	2216 ± 123	27.0 ± 1.7 ***
Outlet Dryer Temperature T	1230 ± 123	15.9 ± 1.7 ***
Two-Factor Interactions:		
H x F	-753 ± 123	-10.0 ± 1.7 ***
H x T	-170 ± 123	-2.4 ± 1.7
F x T	391 ± 123	5.4 ± 1.7
Three-Factor Interaction (Block):		
H x F x T = B	-319 ± 123	-4.4 ± 1.7

*** Statistically significant at $p < 0.005$ level.

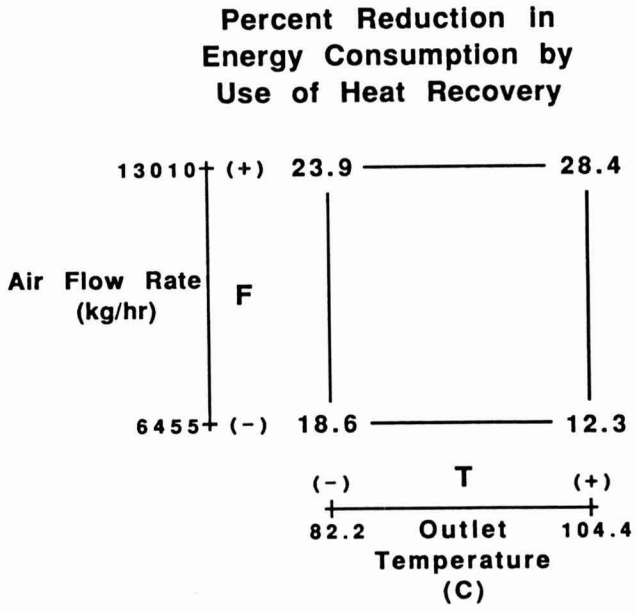

FIG. 5.

The reduction in energy consumption varied from 12–28%, with the largest reduction occurring at the high levels of air flow rate and outlet temperature (see Fig. 5).

The specific energy consumption was 2216 kJ/kg or 27.0% greater for high air flow rate (F) compared to low air flow rate. This result was probably due to a combination of two effects. First, for a given energy input, the temperature of air downstream of the gas burner (i.e., the inlet drying temperature) is lower for the high air flow rate. Second, the residence time of the air in the dryer at the high flow rate is about half the residence time for the low flow rate. Both have an adverse effect on the efficiency of the dryer and more than counteract the positive effect of increased atomization and spray-air contact at the high air flow rate.

The specific energy consumption was 1230 kJ/kg or 15.9% greater at the higher outlet temperature (T). This result has been frequently cited in the literature (Masters 1979; Cook and Dumont 1988).

The interaction between heat recovery and air flow rate (HF) was also significant, as shown by Fig. 6. The reduction in energy consumption by use of heat recovery was 26.4% and 15.3% at the high and low air flow rates, respectively. This situation resulted from two phenomena: (1) the temperature of the air decreased less between the dryer outlet and heat exchanger at the high air flow rate (heat losses from the exhaust duct were lower relative to flow rate); and (2) the effectiveness of the heat exchanger was greater at the high air flow rate. Commercial dryers are normally operated at full capacity, which corresponds to the high air flow rate.

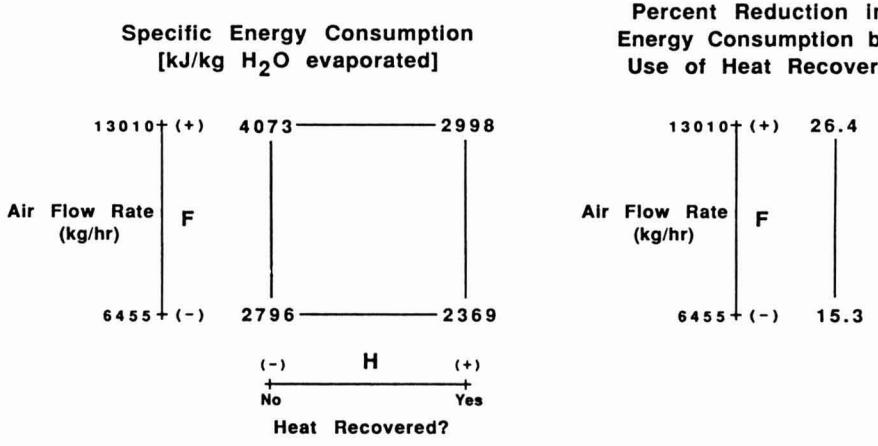

FIG. 6.

The effect of heat recovery on the energy consumption of the dryer is summarized by the Sankey diagram given in Fig. 7. The values in this diagram represent percentages of the total energy entering or leaving the dryer. These values were obtained by averaging the results from all runs with heat recovery.

An average of 19% of the energy leaving the system was recovered by the heat exchanger. However, 54% of the total energy was still lost with the exhaust air leaving the heat exchanger, due to its high content of water vapor. Heat losses accounted for about 26% of the energy leaving the system, with the heat loss from the uninsulated drying chamber most significant (14%). The heat loss from the ductwork between the dryer outlet and the heat exchanger was relatively small but still significant (about 6%). This value may be somewhat lower than would be encountered in industry, since the heat recovery unit is located inside a building.

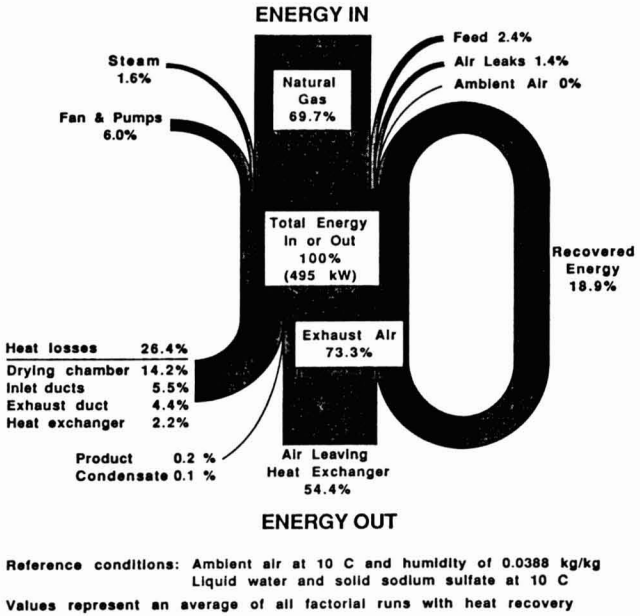

Fig. 7.

The values for the heat losses, particularly the inlet duct loss, are slightly inflated since all energy input devices were assumed to be 100% efficient. The efficiency of the steam coils, the pumps and the fan would be expected to be

somewhat less than 100%. However, these devices contribute far less energy than the gas burner, which probably has an efficiency close to 100%.

Technical Feasibility of Heat Recovery System

Assessment of the technical feasibility of installing the heat recovery system on this spray dryer involved considering aspects associated with: (1) fouling and cleaning of the heat exchanger; (2) the additional pressure drop over the heat exchanger; (3) the warm-up time of the heat exchanger; and (4) the size of the heat recovery unit and its associated ductwork.

No problems were encountered with fouling of the heat exchanger. Although sodium sulfate powder built up on the tubes, this fouling had no noticeable impact on the effectiveness of the heat exchanger. This result is not surprising, as the estimated resistance to heat transfer from the tube wall was less than 3% and any additional build-up on the tubes would increase this value only slightly (Donhowe 1988). Fouling also had no noticeable effect on the pressure drop of the heat exchanger.

For the experimental runs with sodium sulfate, the tubes were easily cleaned by a periodic rinse with hot water. However, test runs with other products, such as fat-based foods, required the use of a soap solution during the cleaning cycle.

It should be noted that the dryer was not operated continuously for extended periods of time, as is usually the case in industry, and the dried product was usually easy to clean.

The individual pressure drops over the shell and tube sides of the heat exchanger ranged from 0.02 to 0.1 kPa. The maximum cumulative pressure drop over the heat exchanger was 0.2 kPa, which is small relative to the pressure drop across the fan (2.0 kPa). The additional power requirement of the fan due to the pressure drop across the heat exchanger was estimated as 0.7 kW at the high air flow rate (Perry and Chilton 1973). This value represents a 2% increase in the energy consumption of the fan, but only a 0.2% increase in the total energy consumption of the dryer. However, the maximum flow rate of the fan decreased by an estimated 8% due to the presence of the heat exchanger.

The time required for the temperature of the preheated air leaving the heat exchanger to reach 95% of its maximum value was less than 20 min for both low and high air flow rates. Since the dryer structure is normally warmed up for at least 30 min before drying product, the warm-up time of the heat exchanger has no effect on the operation of the dryer.

Although the heat recovery unit was relatively large, it was easily installed on the roof of the building containing the spray dryer. The building containing the spray dryer was eventually extended to enclose the heat recovery unit, but this would probably not be feasible in a commercial setting. The additional expense of this building extension was thus not included in the economic analysis of the unit. The inlet and exhaust ducts of the dryer were fairly close together (10 m), so the associated ductwork was not extensive nor difficult to install.

Economic Feasibility of Heat Recovery System

An economic analysis of the heat recovery system is summarized in Table 4. For this analysis, the energy saved by heat recovery was determined at conditions similar to those normally used for producing dried skim milk with this dryer. The operating conditions of the dryer and other assumptions for the economic analysis are listed in Table 5.

TABLE 4.
ECONOMIC ANALYSIS OF HEAT RECOVERY UNIT

Case	A	B	C	D
Conditions:				
Dryer capacity ($kg\ H_2O$ evap/h)	350	350	568	568
Cleaning	easy	hard	easy	hard
Initial investment ($):				
Heat exchanger	40000	40000	40000	40000
Ductwork, installation, etc.	35000	35000	35000	35000
CIP installation	2000	10000	2000	10000
Total	77000	85000	77000	85000
Annual Net Profit:				
Operating costs ($/yr)				
Cleaning	450	3100	450	3100
Repairs, maintenance	2700	3000	2700	3000
Total	3150	6100	3150	6100
Energy savings ($/yr)	21800	21800	35400	35400
Net profit ($/yr)	18600	15700	32200	29300
Payback period (yr)	4.13	5.42	2.39	2.90
Rate of Return (%)	27.8	21.5	46.0	38.5

Economic assessments of the heat recovery system were carried out for two levels of cleaning difficulty (easy and hard) and for two dryer capacities (350 and 568 kg H_2O/h). The lower capacity value was obtained experimentally for the conditions given in Table 5. The higher capacity value was based on the air flow rate for which the heat exchanger was designed (20,400 kg dry air/h)(Tucker 1988). The experimental capacity was therefore about 38% less than the design capacity. This difference is substantially greater than the estimated 8% decrease in capacity resulting from the additional pressure drop over the heat exchanger. Thus, the heat exchanger was considerably oversized.

TABLE 5.
ASSUMPTIONS FOR ECONOMIC ANALYSIS OF HEAT RECOVERY UNIT

Operating conditions of dryer:	
Air parameters:	
Inlet temperature	204 °C
Outlet temperature	93 °C
Ambient temperature	10 °C
Ambient humidity	0.0135 lb/lb
Flow rate (dry basis)	12,600 kg/h
Feed parameters:	
Temperature	56 °C
Composition	pure water
Flow rate	350 kg/h
Energy savings (for above operating conditions):	
Energy consumption without heat recovery	742 kW
Energy consumption with heat recovery	577 kW
Reduction in energy consumption	164 kW
Cleaning costs (1–3):	
Cleaning difficulty: "easy": one cleaning cycle per week	
"hard": one cleaning cycle per day	
Each cleaning cycle requires 2650 L hot (54.4 °C) water and $5 of cleaning solution	
Cold (12.8 °C) city water costs $0.415/100 ft³ ($0.146/m³);	
disposal of water costs $0.4488/100 ft³ ($0.158/m³).	
Water is heated by natural gas with an efficiency of 85%.	
Cost of natural gas is $0.5326/10⁵ Btu ($0.0182/kW).	
Economic assumptions ([4]):	
Dryer operates 20 h/day, 365 days/year (7300 h/yr).	
Equipment life of 18 years, straight-line depreciation with no salvage value.	
Annual cost for repairs and maintenance is 3.5% of original investment.	
Net profit increases at an annual rate of 5%.	
Annual insurance premium is 1% of value of investment.	
Tax rate is zero.	
Working-capital investment in zero.	
Pay-back period only accounts for the annual net profit and the total initial investment.	
Rate of return is based on discounted cash flow;	
net profit is compounded on the basis of end-of-year income.	

Sources: [1]Tucker 1988
[2]Madison Water Utility, Madison, WI (1988)
[3]Madison Gas & Electric Co., Madison, WI (1988)
[4]Peters and Timmerhaus 1980

It was assumed that the amount of energy recovered by the heat exchanger increased proportionally with the dryer capacity. Actually, the manufacturer of the heat exchanger claims that the percent reduction in energy consumption should be even greater at the higher capacity, since the heat exchanger was designed for a higher flow rate of air (i.e., higher Reynolds number)(Tucker 1988). Experimental measurements appear to confirm this hypothesis, as the effectiveness of the heat exchanger increased with air flow rate (Donhowe 1988).

The payback period of the heat recovery system as installed was estimated as 4.1–5.4 years, depending on the costs associated with the cleaning of the heat exchanger. The system would have been more attractive from an economic sense if it had been sized correctly, as the payback period based on an optimum design criterion was 2.6–2.9 years. However, the payback periods tend to give unrealistic assessments of the process economics of the system, since they do not account for the long expected life of the system (18 years), the cost of money, depreciation, insurance, etc.

A better estimate is that given by the rate of return based on discounted cash flow (Peters and Timmerhaus 1980). The rate of return for the system as currently configured was 21–28%, while that for the optimum design case was 38.5–46.0%. These values indicate that the heat recovery system represents a good long-term investment.

CONCLUSIONS

The energy consumption of a small commercial-scale spray dryer was reduced by 12–28% by preheating the inlet air to the dryer with energy recovered from the exhaust air. The highest reduction in energy consumption occurred at the high levels of air flow rate and dryer outlet temperature. However, the energy consumption of the dryer was lowest when heat was recovered at the low levels of outlet temperature and flow rate.

The heat recovery system did not present any technical problems. From an economic standpoint, the heat recovery system is a good investment for this spray dryer if it were operated under conditions normally encountered in industry, and would be an even better investment if the heat recovery system had been correctly sized.

ACKNOWLEDGMENTS

This work was supported by the Food Engineering Pilot Plant, the College of Agricultural and Life Sciences, University of Wisconsin-Madison. The heat recovery system was provided by Air Frohlich, Inc. The authors would also like to thank Mr. Horst Gierke and Mr. Scott Wells for their assistance in this research.

REFERENCES

AMELOT, M.P. and GAUVIN, W.H. 1986. Spray drying with plasma-heated water vapor. In *Drying '86,* Vol. 1, (A.S. Mujumdar, ed.) pp. 285–290, Hemisphere Publ., Washington.

AMERICAN SOCIETY OF MECHANICAL ENGINEERS. *1967 ASME Steam Tables.* Reprinted by Combustion Engineering, Windsor, CT.

AMUNDSON, C.H. 1967. Spray drying dairy and food products. ASHRAE J. *9*, 70–73.

BAKER, C. and BAHU, R. 1983. A low-cost strategy for reducing fuel consumption of dryers. Process Eng. *64*(3), 42–45.

BIMBENET, J.J. 1982. Criteria of energetic performance for convective-type dryers. In *Drying '82*, (A.S. Mujumdar, ed.) pp. 121–128, Hemisphere Publ., Washington.

BOX, G.E.P., HUNTER, W.G. and HUNTER, J.S. 1978a. *Statistics for Experimenters,* Ch. 10, John Wiley & Sons, New York.

BOX, *et al.* 1978b. p. 503.

CHOWDHURY, J. 1984. Pulse combustion lowers drying costs. Chem. Eng. (NY) *91*(25), 44–45.

COOK, E.M. and DuMONT, H.D. 1988. New ideas to improve dryer performance. Chem. Eng. (NY) *95*(7), 71–78.

DONHOWE, D.P. 1988. Heat recovery from a spray dryer. M.S. Thesis, University of Wisconsin-Madison.

ENERGY TECHNOLOGY SUPPORT UNIT. 1986a. Heat recovery from a boiler exhaust to pre-heat air to a spray dryer. J. Heat Recovery Syst. *6*(1), 11–23.

ENERGY TECHNOLOGY SUPPORT UNIT. 1986b. Heat recovery from a spray dryer using a glass tube heat exchanger. J. Heat Recovery Syst. *6*(1), 25–31.

ENERGY TECHNOLOGY SUPPORT UNIT. 1986c. Heat recovery from a spray dryer using a run-around coil system. J. Heat Recovery Syst. *6*(1), 33–38.

GRONLUND, M. 1984. Optimizing evaporator and spray dryer performance in food processing. In *Profitability of Food Processing,* Inst. of Chem. Eng. Symp. Ser. n. 84, Pergamon Press, New York.

HANSEN, R. 1982. Heat recovery by means of Elektrogeno thermoplats. North Eur. Dairy J. *1*, 1–6.

HAYASHI, H., KUMAZAWA, E., SAEKI, Y. and ISHIOKA, Y. 1983. Continuous vacuum dryer for energy saving. Drying Technol. *1*(2), 275–284.

HOLLAND, C.R. and MCCANN, J.B. 1980. Heat recovery in spray drying systems. J. Food Technol. *15*, 9–23.

JANSEN, L.A. and STEENBERGEN, A.E. 1979. Recovery of heat from exhaust air of spray driers in the dairy industry. In *Conf. Energy Conserv. Dairy Ind.*, pp. 1–24, Dept. of Industry, Commerce and Energy, Dublin.

JANSEN, L.A. and ELGERSMA, R.H.C. 1985. Direct heating of drying air with natural gas in the preparation of milk powder. J. Soc. Dairy Technol. *38*(4), 134–139.

JEBSON, R.S. and LASCELLES, D.R. 1977. Applications of heat pumps in the dairy industry. N.Z.J. Dairy Sci. Technol. *12*, 116–122.

KESSLER, H.G. 1980. Heat conservation in concentration and spray-drying of milk products. In *Drying '80,* Vol. 1 (A.S. Mujumdar, ed.) pp. 339–342, Hemisphere Publ., Washington.

KNIPSCHILDT, M.E. 1986. Drying of milk and milk products. In *Modern Dairy Technology*, Vol. 1, (R.K. Robinson, ed.) pp. 131–234, Elsevier Applied Science, New York.

KRAGH, O.T. and KRAGLUND, A. 1981. Heat recovery in dryers. Chem. Eng. (London) *367*, 149–153.

MASTERS, K. 1983. Recent developments in spray drying. In *Developments in Food Preservation*, Vol. 2, (S. Thorne, ed.) pp. 95–121, Applied Science Publ., New York.

MASTERS, K. 1979. *Spray Drying Handbook*, 3rd ed., John Wiley & Sons, New York.

MILTON, B.J. 1981. Low energy milk drying plants. In *Conf. Energy Conserv. Dairy Ind.*, pp. 25–44, Dept. of Industry, Commerce and Energy, Dublin.

MURALIDHARA, H.S., ENSMINGER, D. and PUTNAM, A. 1985. Acoustic dewatering and drying (low and high frequency): State of the art review. Drying Technol. *3*(4), 529–566.

OKAZAKI, M. and CROSBY, E.J. 1984. Foam spray drying: Efficiency of energy utilization. In *Proc. 4th Int. Drying Symp.*, (R. Toie and A. Mujumbar, eds.) pp. 347–357, Society of Chem. Engineers, Tokyo.

PALLADY, P.H. and HENLEY, P.J. 1984. Evaluating moist air properties. Chem. Eng. (NY) *91*(22), 117.

PERRY, R.H. and CHILTON, C.H. (eds.) 1973. *Chemical Engineers' Handbook*, 5th ed., pp. 6–21, McGraw-Hill, New York.

PETERS, M.S. and TIMMERHAUS, K.D. 1980. *Plant design and Economics for Chemical Engineers*, 3rd ed., McGraw-Hill, New York.

PISECKY, J. and SHELL, J.F. 1979. The effective utilization of energy in the milk powder industry. Am. Dairy Rev. *41*(6), 52A–52F.

PISECKY, J. 1985. Technological advances in the production of spray dried milk. J. Soc. Dairy Technol. *38*(2), 60–64.

RAO PENDYALA, V., DEVOTTA, S. and PATWARDHAN, V.S. 1986. The economics of heat pump assisted drying systems. J. Heat Recovery Syst. *6*(6), 433–442.

REAY, D.A. 1980. A review of gas-gas heat recovery systems. Heat Recovery Syst. *1*(1), 3–41.

RICHARDT, K. 1980. Energy saving in dryers. In *Drying '80*, Vol. 2, (A.S. Mujumbar, ed.) pp. 379–386. Hemisphere Publ., Washington.

ROMERO-FERRER, D.E., AMUNDSON, C.H. and HILL, C.G., JR. 1986. The effects of gas injection on the efficiency of thermal energy utilization in spray drying. J. Food Process Eng. *8*, 171–191.

SHEBLER, K.J. 1977. Use of direct-fired natural gas heaters for spray drying. In *Proc. Jubilee Conf. Dairy Sci. Technol.*, New Zealand Society of Dairy Science & Technology and New Zealand Dairy Research Institute.

SWIENTEK, R.J. 1986. Sonic technology applied to food drying. Food Process. *47*(7), 62–63.

TREYBAL, R.E. 1980. *Mass Transfer Operations,* 3rd Ed., Ch. 7, McGraw-Hill, New York.

TUCKER, R. 1988. Personal Communication. Air Frohlich, Inc., Minneapolis.

VASILIEV, L.L., GRAKOVICH, L.P., KISELEV, V.G., MATVEEV, Y. and KHRUSTALEV, D.K. 1984. Heat pipes and heat pipe exchangers for heat recovery systems. J. Heat Recovery Syst. *4*(4), 227–233.

WOODHAMS, D.J. 1970. Spray dryer performance. Ph.D. Thesis, University of Wisconsin-Madison.

YOUNGS, R. 1986. The improved energy efficiency of modern spray dryers. J. Heat Recovery Syst. *6*(3), 217–223.

POTASSIUM SORBATE PERMEABILITY OF POLYSACCHARIDE FILMS: CHITOSAN, METHYLCELLULOSE AND HYDROXYPROPYL METHYLCELLULOSE

FAKHRIEH VOJDANI and J. ANTONIO TORRES[1]

Department of Food Science and Technology
Oregon State University
Corvallis, OR 97331

Accepted for Publication February 22, 1989

ABSTRACT

Edible coatings controlling preservative migration from surface to food bulk could control surface microbial growth which is often the main cause of spoilage for many food products. In this paper we examine the potassium sorbate permeability behavior of chitosan, methyl cellulose and hydroxypropyl methyl cellulose based films. To gain an understanding of the permeation process, permeability determinations were done at 5, 24, 32 and 40°C. Permeability rates followed the Arrhenius activation energy model. A lack of breaking points in Arrhenius plots indicated that no morphological changes occur within these films in the 5 to 40°C temperature range. Activation energy values were found to be independent of film composition and were affected only by the solvent embedded in the film. This behavior was confirmed by analysis of the same permeability data using a modified Stokes-Einstein equation.

Methyl cellulose was the most promising diffusion barrier with a permeability constant of 3.4 and 1.4×10^{-8} (mg/s cm^2)(cm)/(mg/cm^3) at 24 and 5°C, respectively. Electron microscopy was used to examine the morphological characteristics of these films and showed they have no visible pores or channels at magnifications up to 10,000.

INTRODUCTION

The quality and stability of foods is often affected by diffusion phenomena. The progress of chemical reactions depends on the reactants having sufficient mobility to move to the reaction site (Duckworth 1981; Simatos *et al.* 1981).

[1]To whom correspondence should be addressed.
[2]Oregon State University Agricultural Experiment Station, Technical Paper No. 8586.

Journal of Food Process Engineering *12(1989) 33–48.* *All Rights Reserved.*
©Copyright 1989 by Food & Nutrition Press, Inc., Trumbull, Connecticut.

The control and reduction of moisture, gas or other solutes from the environment into the food as well as their exchange between different regions of a heterogeneous food can be a main factor in the stability of a food product. In some cases it may be desirable to coat foods or food elements with an edible film or layer containing a high concentration of a given food additive. Recent work conducted by Fennema and coworkers (Kamper and Fennema 1984a,b, 1985; Kester and Fennema 1986) has centered on the control of moisture migration between regions with different water activities using modified cellulose based films.

A particularly interesting situation is the control of surface microbial growth which is often the main cause of spoilage for many refrigerated food products (Vitkov 1973, 1974; Gill 1979; Anderson *et al.* 1980; Maxcy 1981). For example, fresh broilers in retail outlets have an initial concentration of 10^4 to 10^5 microorganisms/cm^2 and can be stored only for a few days at 3–5 °C and still maintain their freshness (Cunningham 1979; Robach 1979). In the case of intermediate moisture foods (IMF), surface condensations caused by temperature fluctuations result in temporary and local increases in surface water activity (a_w) leading to microbial spoilage (Torres *et al.* 1985a,b; Torres 1987).

To cope with surface microbial problems, food processors have used preservatives as a surface treatment. The use of potassium sorbate dips has been shown to reduce the total number of viable bacteria at refrigeration and temperature abuse conditions (Robach and Ivey 1978; Cunningham 1979; D'Aubert *et al.* 1980; Holley 1981; Robach and Sofos 1982; Lueck 1984). However, the shelf-life extension achieved by this surface treatment is limited. Eventually, microorganisms overcome the sorbate induced bacteriostasis due to diffusion of the preservative into the bulk of the food. Diffusion results in preservative concentration reduction on the surface where microbial spoilage is occurring (Greer 1981; Torres 1987). A tenfold reduction in sorbic acid diffusion rate (D) has been obtained by adjusting the a_w of a model food system (Guilbert *et al.* 1985). Lowering the a_w of the model system from 1.0 to 0.88 using 40% w/w glycerol or 16% w/w salt reduced the apparent diffusivity at room temperature from 6.7 $\times$ 10^{-6} to 2.0 $\times$ 10^{-6} cm^2/s. At 70% glycerol the a_w was 0.64 and D was 5 $\times$ 10^{-7} cm^2/s.

The diffusion of sorbic acid in zein films has also been measured and found to be in the order of 3–7 $\times$ 10^{-9} cm^2/s, i.e., about a 300 fold decrease as compared to the agar model with $a_w = 1.0$. The diffusion barrier properties of zein films were confirmed in microbial tests using a model food system with $a_w = 0.88$ coated with zein and *Staphylococcus aureus* as the challenge microorganisms (Torres *et al.* 1985a; Torres and Karel 1985). The use of edible coatings for this and other purposes has been recently reviewed by Guilbert (1986).

In this paper we report on the use of methylcellulose, hydroxypropyl methylcellulose, a mixture of both, and chitosan as coatings to retard sorbic acid diffusion from food surface into food bulk. Polysaccharides were chosen for their ability to form strong, clear films using relatively low price ingredients as compared to proteins such as zein. These films were characterized by electron microscopy and by measuring K-sorbate permeability in films soaked in water and in aqueous glycerol.

MATERIALS AND METHODS

Preparation of Films

Chitosan Films. 0.5 g chitosan (Bioshell Inc., Albany, OR) was dissolved in 100 mL of a 1.5% v/v acetic acid aqueous solution using continuous mechanical stirring. To avoid chitosan agglomeration, chitosan was slowly added to the solution. A clear solution was achieved after three hours of continuous mixing. The solution was then filtered through a medium porosity fritted disk Buchner type filtration funnel using a slight vacuum. About 25 g solution was poured into 100 × 15 mm disposable Petri dishes after allowing the solution to rest for 30 min. A film was formed after 7 h drying in an oven at 45–47 °C. When the film had cooled to room temperature the film was removed from the Petri dish and immersed in 25 mL 1 N sodium hydroxide for 1 h. Finally the film was washed four times with 250 mL distilled water to remove excess reagents and then soaked in 50% v/v glycerol solution for 15–30 min (CHI/G films). In the case of permeability determinations in pure water this last step was not necessary (CHI/W films).

Cellulose Ether Films. 5 g of hydroxypropyl methylcellulose (HPMC, Methocel F50, Premium, Dow Chemical Co., Midland, MI), methyl cellulose (MC, Methocel A 15-LV, Premium) or a 3:1 mixture of HPMC and MC were suspended in 30 mL ethanol. The latter mixture had been reported to provide optimum retention of micronutrients entrapped in fortified rice coatings (Peil *et al.* 1982).

While stirring the suspension with a mechanical agitator 70 mL distilled water was then added. After 20 min mixing the solution was allowed to rest for 30 min to remove entrapped air. 10 g of solution was then poured into the same Petri dishes and dried at room temperature for 24–48 h. The film was then removed from the dish and soaked for 1 h in 50% v/v glycerol solution before measuring its thickness.

Film Thickness Measurement

The thickness of the films soaked in aqueous glycerol or water was measured using a top mounted Best Test Indicator (EDP No. 45987, Brown and Sharp Mfg. Co., N. Kingston, RI). The reported thickness values are the average of at least 20 measurements. Films were mounted on the permeability cell immediately after thickness measurement.

Permeability Test

Permeability values were determined using a cell similar to the one described by Torres (1987). It consisted of two mechanically agitated chambers separated by the film to be tested. The upper chamber contained 50% (v/v) glycerol solution or pure water. The lower chamber contained the same solution with 2.5% w/v potassium sorbate. The cell was placed in an oven at 40 or 32 °C, left at room temperature (24 °C) or placed in a walk-in refrigerator at 5 °C. All determinations were done at least in triplicates.

When mounted on the permeability cell the top side (air drying side) of the film faced the high K-sorbate concentration. Aqueous glycerol was used as the solvent to reduce a_w and to serve as a film plasticizer. Samples were taken from the upper chamber and the K-sorbate concentration was measured spectrophotometrically at 255 nm.

Films were inspected before and after every test to assure that results were not affected by cracks or other types of visually detectable failures. It should be noted that the permeability test is not a gentle experimental procedure and that the films are subjected to the mechanical abuse of stirrers and compression between the two permeability cell chambers.

Determination of Permeability Coefficients

Permeability coefficients (K) were calculated as described by Torres *et al.* (1985a). K-sorbate determinations were used to obtain plots of total amount of preservative transferred through the film as a function of time. After a time lag, a linear relationship is obstained. The slope of this curve is the steady state rate of K-sorbate transfer through the film (Crank 1976; Rogers 1985).

$$K = Fl/c \tag{1}$$

where:

K = permeability rate
F = amount of K-sorbate permeated per unit time
1 = thickness of the film
c = concentration in the high K-sorbate concentration chamber

These determinations were confirmed by using the following expression (Crank 1976; Rogers 1985):

$$L = l^2/6K \tag{2}$$

L is obtained as an intercept on the time axis by extrapolation of the steady state rate of K-sorbate transfer through the film.

Effect of Temperature on Permeability

The permeability phenomenon is a combination of two types of physical processes. First, there are sorption and desorption processes on both sides of the membrane which depend on the solubility of the diffusing molecule in the film and the nature of the adhesive forces at the interface (Karel 1975). In addition, we have the diffusion of the permeate in the film. In most cases, the latter process is the controlling step and explains why permeability rates follow the Arrhenius activation energy model (McElhaney *et al.* 1970; Colton *et al.* 1971; Karel 1975; Rha 1975).

$$K = K_0 \exp(-E_a/RT) \tag{3}$$

where:

K_0 = frequency constant
E_a = activation energy, Kcal/g-mole
R = universal gas constant
T = absolute temperature

Another approach to estimate the effect of temperature on permeability rate is by use of the following expression:

$$K\mu/T = \psi \tag{4}$$

where:

μ = solvent viscosity (Perry and Green 1984; Newman 1968)
T = absolute temperature
ψ = a constant

This expression is based on the Stokes-Einstein equation for the diffusion of a molecule in a medium of known viscosity (Guilbert *et al.* 1985). This equation should be used with caution when the solution viscosity is high. At high viscosity

this equation overestimates the effect of temperature on the diffusion constant (Perry and Green 1984). This is not the case with water and the aqueous glycerol solution at the temperatures used in this study.

Electron Microscopy Studies

Electron microscopy was used to evaluate film structure. Of particular interest were film uniformity and detection of pores. It was also used to confirm film thickness measurements.

The specimens were mounted on aluminum plancets using Avery Spot-O-Glue. The film was sectioned with a sharp razor blade and coated with approximately 100–200Å of 60:40 gold-palladium in a Varian VE-10 vacuum evaporator at a vacuum of 1×10^{-5} torr. The microscopic examination was made using an AMRAY 1000A SEM operated at 20KV at the Electron Microscope Facility, Oregon State University. Images were recorded on Polaroid type 55 positive/negative 4×5 format film.

Statistical Analysis

The statistical analysis of data was done on an IBM Personal Computer using SAS® (Anon. 1985).

RESULTS AND DISCUSSION

Film Casting

All films formed appeared strong and flexible. This observation suggests that they might not fail during distribution if used as edible coatings. It should be noted that although all toxicological tests on chitosan have been negative it has not been petitioned for human consumption to the U.S. Food and Drug Administration.

As shown in Table 1, the thickness variation for films with the same composition was less than 10%. Thickness ranged from 0.02 for chitosan films to 0.12 mm for methylcellulose ether films.

Permeability Determinations

Permeability determinations were done at a $a_w = 0.77$ (50% v/v aqueous glycerol). To examine the effect of higher a_w chitosan permeability was also determined at $a_w = 1.00$ (pure water).

Plots of total amount of K-sorbate diffused per unit area of film as a function of time at 5, 24, 32 and 40 °C are summarized in Fig. 1 and 2. These permeability curves followed the expected relationship with time. After a certain time

TABLE 1.
EFFECT OF TEMPERATURE ON THE POTASSIUM SORBATE PERMEABILITY THROUGH POLYSACCHARIDE FILMS

Film	40°C			32°C			24°C			5°C		
	K[a] x10[8]	l[b]	ψ[c] x10[11]	K x10[8]	l	ψ x10[11]	K x10[8]	l	ψ x10[11]	K x10[8]	l	ψ x10[11]
CHI/G[d]												
	13.7	21	285[q]	9.9	21	283[q]	8.6	24	320[pq]	3.6	20	355[p]
	17.1	25		11.4	23		8.5	24		3.5	27	
	13.7	20		11.4	23		8.8	23		3.6	22	
	Average ψ = (311 ± 34)x10^{-11}, P=.0088											
HPMC												
	13.9	98	269[r]	10.6	95	275[r]	8.1	98	308[q]	3.6	96	367[p]
	13.8	92		11.1	90		8.5	120		3.8	92	
	14.4	110		10.2	100		8.3	95		3.6	95	
	Average ψ = (305 ± 45)x10^{-11}, P=.0001											
MC												
	6.2	99	137[p]	5.0	113	131[p]	3.2	95	125[p]	1.4	140	144[p]
	6.5	100		5.7	112		3.3	103		1.4	110	
	7.5	104		4.6	90		3.6	120		1.5	120	
	Average ψ = (134 ± 8)x10^{-11}, P=.2228											
HPMC+MC												
	10.0	95	198[q]	8.5	98	214[q]	5.9	90	216[q]	2.6	114	244[p]
	10.5	110		8.1	110		5.6	95		2.2	115	
	10.4	100		8.2	104		6.0	85		2.5	111	
	Average ψ = (218 ± 19)x10^{-11}, P=.0072											
CHI/W												
	95.7	28	200[p]	77.7	28	208[p]	62.5	26	200[p]	39.0	25	208[p]
	83.7	24		75.1	26		63.7	24		39.9	29	
	82.2	23		76.8	27		61.8	25		40.0	26	
	Average ψ = (204 ± 5)x10^{-11}, P=.5579											

a Permeability, (mg/s cm^2)(cm)/(mg/cm^3)
b Film thickness, μm
c ψ = Kμ/T
d See text for definition of other terms
p,q,r ψ values for individual films with the same letter are not significantly different (α=.05)

period needed for the establishment of equilibrium conditions, straight lines indicating a constant permeation rate F were evident. As expected, the rate of permeation decreased with temperature. The slope and the thickness of the film for every individual run was measured and used with Eq. 1 to calculate individual permeability coefficients. The lowest permeability rate values were obtained for MC.

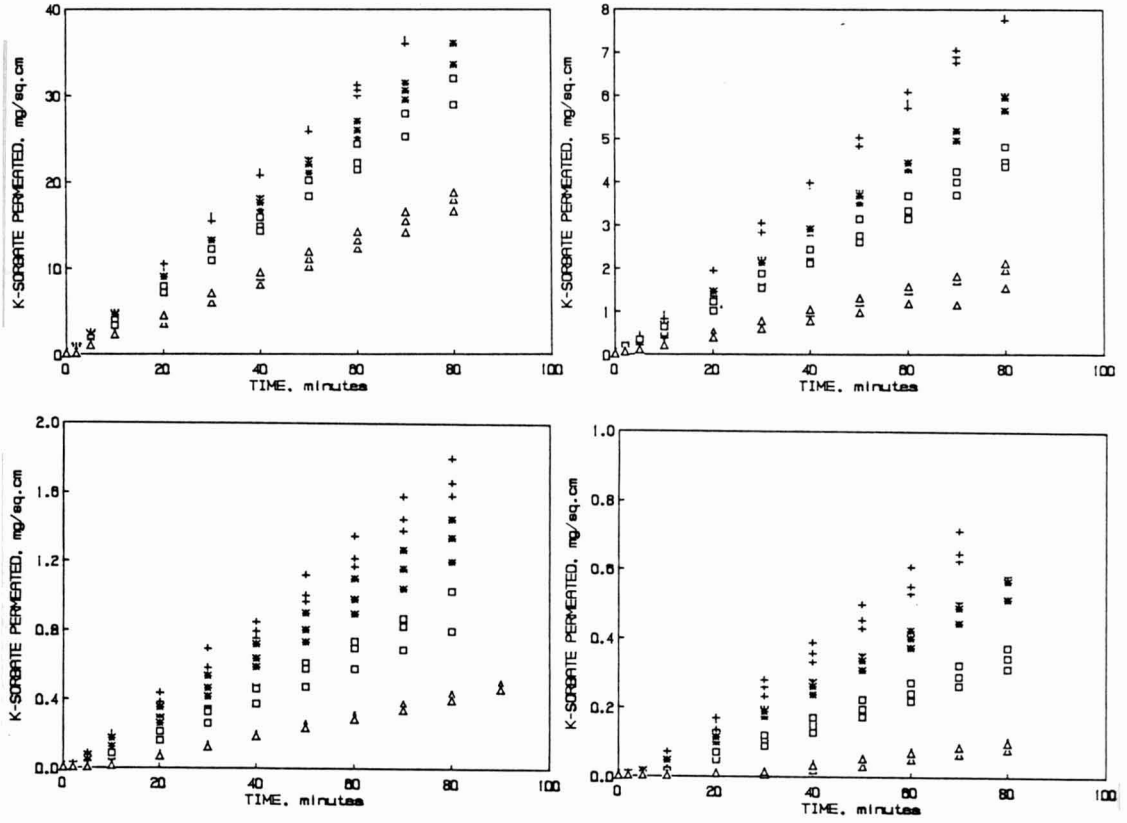

FIG. 1. EFFECT OF TEMPERATURE ON K-SORBATE PERMEABILITY
a. CHI at $a_w \cong 1.00$
b. CHI at $a_w \cong 0.77$
c. HPMC at $a_w \cong 0.77$
d. MC at $a_w \cong 0.77$
+, 40 °C; *, 32 °C; □, 24 °C; △, 5 °C

The comparison of Fig. 1a and 1b shows the dramatic effect of reducing the a_w from 1.0 to 0.77. The comparison of Fig. 1b with Fig. 1c and 1d shows that MC and HPMC films were superior to chitosan films. Finally, Fig. 2 shows that the mixture of MC and HPMC had a permeability behavior intermediate to that for the pure MC and HPMC films.

Average permeability values for experiments using aqueous glycerol were 8.6, 8.3, 3.4 and 5.8×10^{-8} at 24 °C and 3.6, 3.7, 1.4 and 2.4×10^{-8} (mg/s cm^2)(cm)/(mg/cm^3) at 5 °C for chitosan, HPMC, MC and the HPMC+MC mixture, respectively (Table 1). As described by Torres (1987, Table 14.2) it is possible to roughly estimate the effect of these films on increased surface

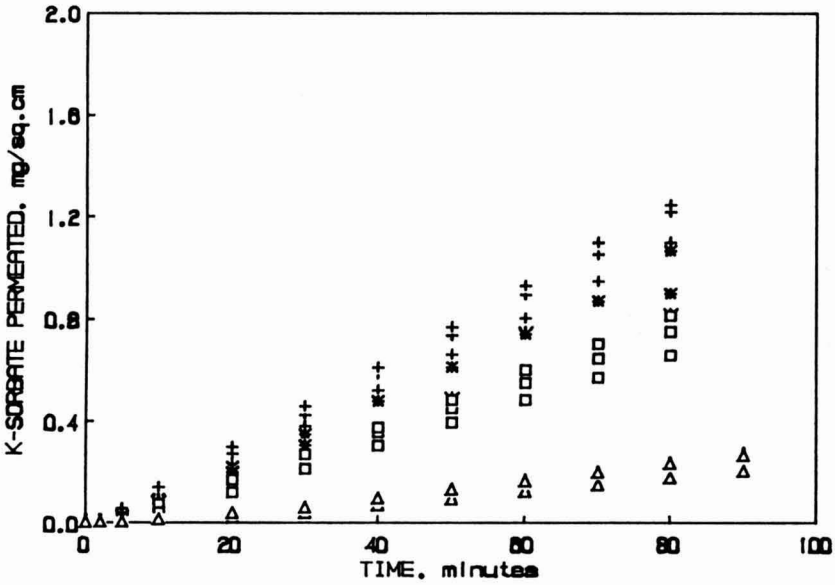

FIG. 2. EFFECT OF TEMPERATURE ON K-SORBATE PERMEABILITY:
HPMC + MC at $a_w \cong 0.77$
+, 40 °C; *, 32 °C; □, 24 °C; △, 5 °C

microbial stability. The surface protection of 0.5 mm CHI, HPMC, MC and HPMC+MC films applied on an IM food can be estimated to last 1.5, 1.5, 4 and 2 months at 24 °C and 3.5, 3.5, 8.5 and 5 months at 5 °C, respectively.

As shown in Table 1 (K values), an important parameter to be considered is the hydration status of the film which would depend upon the food a_w. When determinations were done in pure water at 24 and 5 °C the values were an order to magnitude higher than in aqueous glycerol. The values were 6.3 and 4×10^{-7} (mg/s cm^2)(cm)/(mg/cm^3) which would reduce the surface protection period from 1.5 and 3.5 months to 6 and 9 days at 24 and 5 °C, respectively. These estimations should be confirmed using specific food systems and challenging microorganisms. These studies would emphasize the importance of the food a_w.

Effect of Temperature on Permeability

Permeability values measured at 5, 24, 32 and 40 °C (Table 1) were used to obtain Arrhenius plots and to determine an activation energy for the overall permeation process. The lack of breaking points in the Arrhenius plots (Fig. 3) indicates that no morphological changes occur within these films in the 5 to 40 °C temperature range. A statistical analysis showed that there is no significant

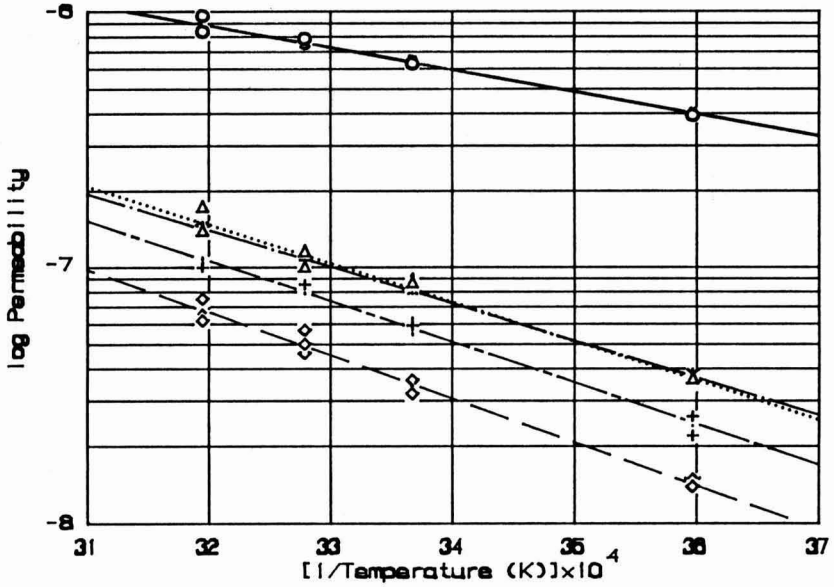

FIG. 3. ARRHENIUS PLOTS FOR PERMEABILITY OF K-SORBATE THROUGH EDIBLE COATING FILMS

○——○, CHI at high a_w
△ · · · · △, CHI at low a_w
——·——, HPMC at low a_w
+—— — ——+, HPMC+MC at low a_w
◇ —— ——◇ MC at low a_w

TABLE 2.
ACTIVATION ENERGY (E_a) OF K-SORBATE PERMEATION

Film	E_a, cal/g-mole
a. solvent = 50% v/v glycerol	
CHI/G	6980
HPMC	6620
MC	7710
HPMC+MC	7270
Average	7150 ± 460
b. solvent = water	
CHI/W	3950

[a] See text for definition of terms

difference (α = .05) between the slopes for CHI, MC, HPMC and HPMC+MC films when the permeability was measured using a glycerol solution. The slope difference between the chitosan film in water versus all films in aqueous glycerol was found to be highly significant. As shown in Table 2, a 45% reduction in activation energy results when the K-sorbate permeation rate was determined using water instead of aqueous glycerol. The observation that the permeability values follow the Arrhenius model and that the activation energy is affected by the solvent embedding the film suggests that the diffusion process in the film occurs through the aqueous phase. Consequently, the performance of edible coatings controlling surface preservative concentration will depend strongly on the aqueous phase of the coated food. On the other hand, K_0 values are affected by the nature of the polysaccharide. This effect will be quantified and analyzed in future studies.

Equation 4 was used to estimate ψ values. As expected, ψ was only slightly affected by temperature (Table 1). No significant differences (α = .05) were observed for CHI in water and MC in aqueous glycerol. Most of the significant differences for the other film/solvent combinations were observed only at 5 °C.

ψ was normalized by dividing the value for a film-temperature combination by the average ψ for all temperatures for a specific film. As shown in Fig. 4 these values show very little dependence with temperature and for practical estimation purposes ψ can be assumed to be a constant. This observation suggests again that the permeability process is controlled by diffusion in the aqueous glycerol phase. The Stokes-Einstein equation was derived for diffusion in a liquid medium.

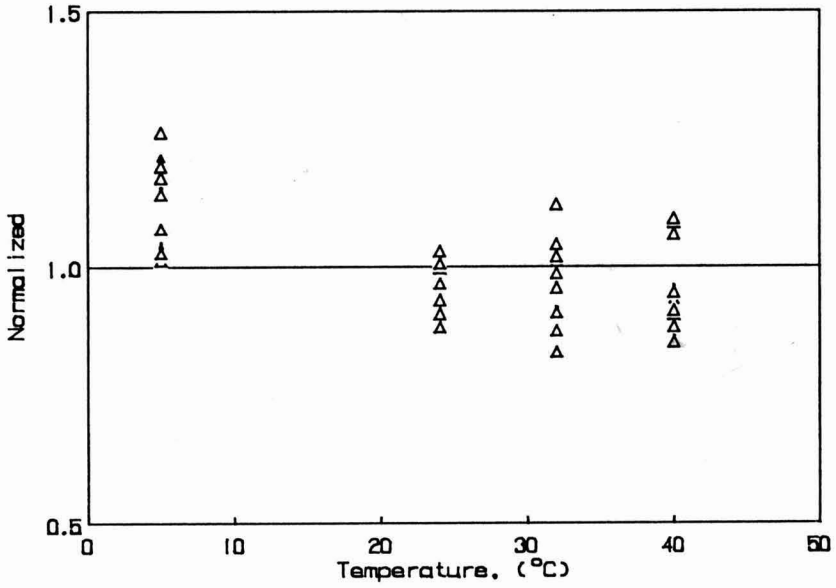

FIG. 4. NORMALIZED ψ FOR ALL EDIBLE COATING FILMS
See text for further details.

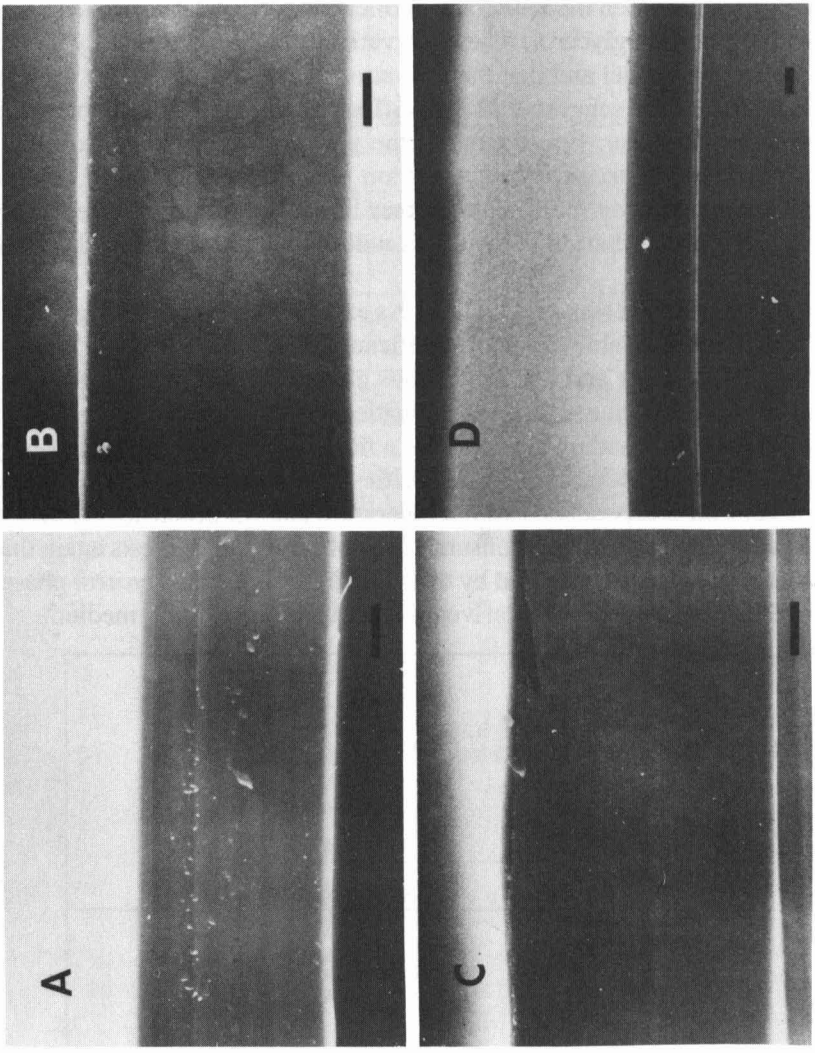

FIG. 5. ELECTRON MICROSCOPY PHOTOMICROGRAPHS OF CROSS SECTIONS OF EDIBLE COATING FILMS (BAR = 20μm)
a. MC
b. HPMC
c. HPMC + MC
d. CHI

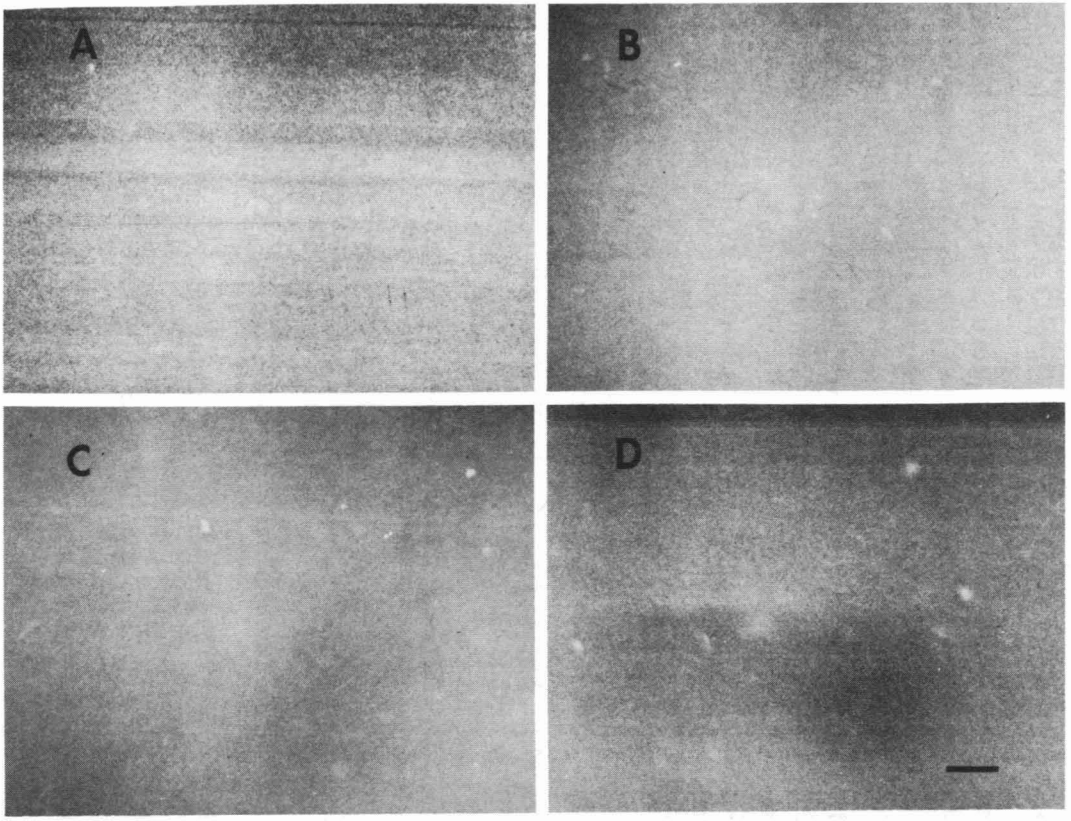

FIG. 6. ELECTRON MICROSCOPY PHOTOMICROGRAPHS OF EDIBLE COATING FILM SURFACES (BAR = 1μm)
a. MC
b. HPMC
c. HPMC + MC
d. CHI

Electron Microscopy Studies

The morphological characteristics of CHI, MC, HPMC, and HPMC+MC films after soaking in aqueous glycerol were observed by electron microscopy. As shown in Fig. 5 these films were homogeneous and of uniform thickness. Examination of the film surface at the maximum magnification possible without film damage, 10,000x (Fig. 6), showed an absence of pores or other type of defects. The same lack of features were observed in examinations of film cross sections. This means that if pores or channels exist they should be less than 0.1 μm.

CONCLUSIONS

This study confirms that it is possible to develop coatings that will enhance surface microbial stability. Based on the observation that the diffusion process occurs through the solvent phase, future papers will examine the effect on potassium sorbate permeation by reducing the hydrophilicity of polysaccharide based coatings.

REFERENCES

ANDERSON, M.E., SEGAUGH, J.L., MARSHALL, R.T. and STRINGER, W.C. 1980. A method for decreasing sampling variance in bacteriological analysis of meat surfaces. J. Food Protec. *43*, 21.

ANON. 1985. *SAS® Language Guide for Personal Computers,* Version 6 Edition, SAS Institute, Cary, NC.

COLTON, C.K., SMITH, K.A., MERRILL, E.W. and FARRELL, P.C. 1971. Permeability studies with cellulosic membranes. J. Biomed. Mater. Res. *5*, 459.

CRANK, J. 1976. *The Mathematics of Diffusion,* 2nd. ed., Clarendon Press, Oxford.

CUNNINGHAM, F.E. 1979. Shelf life and quality characteristics of poultry meat parts dipped in potassium sorbate. J. Food Sci. *44*, 863.

D'AUBERT, S., POLITI, P.G. and SIMONETTI, P. 1980. Potassio sorbato e conservabilita del pollame. Industries alimentari *19*(10), 759.

DUCKWORTH, R.B. 1981. Solute mobility in relation to water content and water activity. In *Water Activity: Influences on Food Quality,* (L.B. Rockland and G.F. Stewart, eds.) pp. 295, Academic Press, New York.

GILL, C.O. 1979. A review. Intrinsic bacteria in meat. J. Appl. Bact. *47*, 367.

GREER, G.G. 1981. A research note: Mechanism of beef shelf-life extension by sorbate. J. Food Protec. *45*, 82.

GUILBERT, S. 1986. Technology and application of edible protective films. Ch. 19. In *Food Packaging and Preservation. Theory and Practice,* (M. Mathlouthi, ed.) pp. 371, Elsevier Applied Science, London.

GUILBERT, S., GIANNAKOPOULOS, A. and CHEFTEL, J.C. 1985. Diffusivity of sorbic acid in food gels at high and intermediate water activities. In *Properties of Water in Foods*, (D. Simatos and J.L. Multon, eds.), pp. 343, Martinus Nijhoff Publishers, Dordrecht, Netherlands.

HOLLEY, R.A. 1981. Prevention of surface mold growth on Italian dry sausage by natamycin and potassium sorbate. Appl. Env. Microbial, *41*, 422.

KAREL, M. 1975. Protective packaging of foods. Ch. 12. In *Principles of Food Science. Part II. Physical Principles of Food Preservation,* (M. Karel, O.R. Fennema and D.B. Lund, eds.) pp. 399, Marcel Dekker, New York.

KAMPER, S.L. and FENNEMA, P. 1985. Use of an edible film to maintain water vapor gradients in foods. J. Food Sci. *50*, 382.

KAMPER, S.L. and FENNEMA, O. 1984a. Water vapor permeability of edible bilayer films. J. Food Sci. *49*, 1478.

KAMPER, S.L. and FENNEMA, P. 1984b. Water vapor permeability of an edible, fatty acid, bilayer film. J. Food Sci. *49*, 1482.

KESTER, J.J. and FENNEMA, O.R. 1986. Edible films and coatings: A review. Food Technol. *40*(12), 47.

LUECK, E. 1984. Sorbinsaeure und Sorbate. Fleischwirtsch. *64*(6), 727.

MAXCY, R.B. 1981. Surface microenvironment and penetration of bacteria into meat. J. Food Protec. *44*, 550.

McELHANEY, R.N., DE GIER, J. and VAN DEENEN, L.L.M. 1970. The effect of alterations in fatty acids composition and cholesterol content on the permeability of *Mycoplasma laidlawii* B cells and derived liposomes. Preliminary Notes. Biochim. Biophys. Acta *219*, 245.

NEWMAN, A.A. 1968. *Glycerol*, C.R.C. Press, Cleveland, OH.

PEIL, A., BARRETT, F., RHA, C. and LANGER, R. 1982. Retention of micronutrients by polymer coatings used to fortify rice. J. Food Sci. *47*, 260.

PERRY, R.H. and GREEN, D. (Ed.) 1984. *Perry's Chemical Engineers' Handbook*, 6th ed., McGraw-Hill, New York.

RHA, C. (Ed.) 1975. *Theory, Determination and Control of Physical Properties of Food Materials,* D. Reidel Publishing, Dordorecht, Holland.

ROBACH, M.C. 1979. Extension of shelf-life of fresh, whole broilers, using a potassium sorbate dip. J. Food Protec. *42*, 855.

ROBACH, M.C. and IVEY, F.J. 1978. Antimicrobial efficacy of a potassium sorbate dip on freshly processed poultry. J. Food Protec. *41*, 284.

ROBACH, M.C. and SOFOS, J.N. 1982. Use of sorbates in meat products, fresh poultry and poultry products. A review. J. Food Protec. *45*, 374.

ROGERS, C.E. 1985. Permeation of gases and vapors in polymers. Ch.2. In *Polymer Permeability*, (J. Comyn, ed.) pp. 11, Elsevier Applied Science, London.

SIMATOS, D., LE MESTE, M., PETROFF, D. and HALPHEN, B. 1981. Use of electron spin resonance for the study of solute mobility in relation to moisture content in model food systems. In *Water Activity: Influences on Food Quality,* (L.B. Rockland and G.F. Stewart, eds.) pp. 319, Academic Press, New York.

TORRES, J.A. 1987. Microbial stabilization of intermediate moisture food surfaces. Ch. 14. In *Water Activity: Theory and Applications to Food,* (L.B. Rockland and L.R. Beuchat, eds.), pp. 329, Marcel Dekker, New York.

TORRES, J.A., MOTOKI, M. and KAREL, M. 1985a. Microbial stabilization of intermediate moisture food surfaces. I. Control of surface preservative concentration. J. Food Proc. Pres. *9*, 75.

TORRES, J.A., BOUZAS, J.O. and KAREL, M. 1985b. Microbial stabilization of intermediate moisture food surfaces. II. Control of surface pH. J. Food Proc. Pres. *9*, 93.

TORRES, J.A. and KAREL, M. Microbial stabilization of intermediate moisture food surfaces. III. Effects of surface preservative concentration and surface pH control on microbial stability of an intermediate moisture cheese analog. J. Food Proc. Pres. *9*, 107.

VITKOV, M. 1974. Hygienic studies on the production of poultry meat. II. On the presence of salmonellae. Veteranarnomeditsinskis Nauki *11*(1), 17.

VITKOV, M. 1973. Hygienic studies on the production of poultry meat. I. On the superficial contamination of poultry meat. Veteranarnomeditsinski Nauki *10*(9), 55.

PIGMENTS MODIFICATIONS DURING FREEZING AND FROZEN STORAGE OF PACKAGED BEEF

M.C. LANARI, A.E. BEVILACQUA and N.E. ZARITZKY

Centro de Investigacion y Desarrollo en Criotecnologia de Alimentos (CIDCA)
Facultad de Ciencias Exactas - 47 y 116
(1900) La Plata - ARGENTINA

Accepted for Publication February 24, 1989

ABSTRACT

Muscle pigment modifications during freezing and frozen storage of beef wrapped in high (polyethylene) and low (EVA/SARAN/EVA) gaseous permeability films were analyzed. Myo (Mb), oxy (MbO_2) and metmyoglobin (MetMb) concentrations were determined using reflectance spectrophotometry. Results indicated that in polyethylene wrapped samples myoglobin oxygenation took place during freezing and the only reaction observed throughout frozen storage was MetMb production from MbO_2. Autoxidation was interpreted as a first order kinetic reaction. Storage temperature effect on kinetic and equilibrium constants was analyzed; reaction enthalpy and activation energy were calculated. MbO_2 and MetMb production during beef oxygenation was represented as a consecutive first order reaction system determining previous vacuum storage time and temperature influence on oxygenation capacity. Vacuum packaging of frozen beef increased color stability maintaining MetMb concentration levels lower than those corresponding to just frozen samples wrapped in polyethylene.

INTRODUCTION

Freezing, frozen storage and thawing produce undesirable changes on surface color of beef muscles packaged in high gaseous permeability films. Color of raw beef is mainly determined by the relative surface concentrations of purple myoglobin (Mb), bright red oxymyoglobin (MbO_2) and brown metmyoglobin (MetMb). The major factor leading to discoloration of beef is the accumulation of metmyoglobin at the surface, this process is affected by several factors including muscle type (O'Keefe and Hood 1980) partial pressure of oxygen (Ledward 1970), storage temperature (Hood 1980), microbial population (Lanier *et al.* 1977) oxygen consumption rate and activity of the enzymatic reducing systems present in muscles (MacDougall 1982). Zachariah and Saterlee (1973) showed that storage temperature, incident light, pH and buffer strength affected

Journal of Food Process Engineering *12(1989) 49-66.* *All Rights Reserved.*
©Copyright 1989 by Food & Nutrition Press, Inc., Trumbull, Connecticut.

the autoxidation rate of MbO_2 solutions at freezing temperatures. Ledward and MacFarlane (1971) working in frozen beef reported that MetMb production was accelerated by freeze-thawing treatments. Lentz (1979) and MacDougall (1982) informed that the major color problem encountered with frozen beef was photooxidation of the pigment and that the rate of fading was influenced by the illumination level, storage temperature, packaging methods and muscle type.

According to Dalhoff and Jul (1965), quality of frozen foods must be analyzed considering not only time, temperature, tolerance factors (TTT), but also product, process and packaging (PPP) concepts.

Packaging of beef muscles with low permeability films offers not only the advantage of decreasing oxidative rancidity but also to delay surface discoloration (Jul 1984). Hood (1983) reported that high vacuum packaging gives the best results with respect surface color. High vacuum also improves both the appearance of fat, which otherwise may be discolored by meat fluids and the color of meat on final exposure (Seideman *et al.* 1976; Taylor 1985).

Information about rate constants for MbO_2 and MetMb production in frozen beef tissues is scarce; Brown and Dolev (1963) and Zachariah and Saterleee (1973) analyzed storage temperature, buffer strength and pH effect on kinetic constant for the autoxidation of MbO_2 solutions and noticed the acceleration of this reaction upon freezing.

The objectives of the present work were (1) To study storage temperature and time effects on pigment relative surface concentrations of frozen beef packaged in different oxygen permeability films; (2) To analyze Mb oxygenation in vacuum packaged frozen beef samples and (3) To develop kinetic models appropriate to represent pigment behavior during oxygenation and oxidation processes.

MATERIALS AND METHODS

Samples

Beef samples were obtained from gluteus medium bovine muscles (eye of rump) removed from commercial steers classified as NT according to the Argentine National Meat Board Classification (carcass weight 240 kg) with 48 h post mortem at 4 °C from a local slaughter house. Muscle pH was within 5.5–5.9 (measured with an INGOLD LOT 450 M4 insertion electrode).

Samples of beef of 3.2 × 2.3 cm section and 2 cm thickness were cut maintaining muscle fibers parallel to the surface to be analyzed.

Packaging

Samples were tight wrapped using two types of films of different gaseous permeability: low-density polyethylene (thickness = 60 μm, oxygen permeability = 6.4 10^{-8} m^3/m^2 Pa day at 23 °C) and EVA-SARAN-EVA (E/S/E) coextruded film (thickness = 60 μm, oxygen permeability = 3.7 10^{-10} m^3/m^2 Pa day at 25 °C and relative humidity (RH) = 75%. Trade name: Super Cryovac, Darex SAIC, Buenos Aires, Argentina). SARAN is polyvinyl and polyvinylidene chloride copolymer and EVA is ethyl vinyl acetate. Cutting and packaging times were kept as short as possible to prevent conversion of Mb. Packaging was done with a Minidual Mw 4980 machine equipment (Schkolnick SAIC, Buenos Aires) with a single chamber at 0.6 kPa and thermal sealing. The degree of vacuum inside the packages was measured by the method of Seideman *et al.* (1976). Packaged samples were placed in an anaerobic jar (Oxoid; Hampshire, England) which was gradually evacuated, pressure at which the film detached from the sample was determined by manometric reading. The average pressure of the internal atmosphere in the packages was 5.3 kPa.

Freezing and Thawing

Wrapped samples were frozen using a contact plate freezer; methanol from a Lauda UK-50DW cryostat with a temperature control of ± 0.1 °C was circulated through each plate. Lateral insulation was provided using expanded polyestirene 5 cm thick in order to obtain an unidirectional heat flux. Thermal histories were monitored with copper-constantan thermocouples inserted in the border and the center of the samples and connected to a Data Logger model 2240-C (John Fluke M. Fg. Co., Mountlake Terrace, WA). Variations of the freezing rates were obtained interposing acrylic slabs of different thickness between the samples and the plate freezer.

Freezing rate was expressed in terms of:

(1) the ratio in cm/h between the minimum distance from the surface to the thermal center and the time elapsed between the surface reaching 0 °C and the thermal center reaching 10 °C colder than the initial ice formation at the thermal center (IIF 1972). For beef, initial freezing point is -1.1 °C.

(2) the local characteristic freezing time t_{7_c} defined as the period in which the temperature changes from -1 °C to -7 °C.

Equivalent expressions were used for thawing rates, inverting initial and final temperature levels.

Freezing and Thawing Rate Effect on Muscle Pigments Relative Surface Concentrations

The analysis of freezing and thawing rates effect on muscle pigment relative surface concentrations was performed on polyethylene wrapped samples. Two

different freezing rates were assayed: 43.4 and 0.3 cm/h combined with the following thawing rates: 34.0 cm/h (1 h in a waterbath at 25 °C) and 1.1 cm/h (12 h at 4 °C in still air chamber). Characteristic freezing and thawing times (t_{7c} and t_{7d}, respectively) evaluated at the samples surface and corresponding to the assayed conditions were: t_{7c} = 1 and 37 min; t_{7d} = 1 and 36 min. These freezing rates were selected because they represent average conditions in meat pieces of different sizes industrially processed (IIR 1972); thermal surface conditions were simulted since they govern meat color. As regards thawing rates, they corresponded to typical meat border situations of defrosting in refrigerated room at 4 °C and in cold water bath.

Storage

Pigment evolution during frozen storage was studied using beef samples from 11 animals, packaged in polyethylene and E/S/E, frozen at a determined rate (43.4 cm/h) up to a final temperature of −25 °C and stored in freezers with no air circulation at −5 °C, −10 °C, −13 °C, and −20 °C in darkness to avoid photooxidation (MacDougall 1982) for periods between 150 and 400 days. Storage times for polyethylene packaged samples were selected taking into account practical storage life data informed by Van Arsdel (1969) and Jul (1984).

Samples packaged in polyethylene were hanged in such a way that all exposed areas were in contact with air to permit oxygenation. Pigments modifications during aerobic storage were analyzed on polyethylene wrapped samples. Previous vacuum storage time (tps) and temperature effect on oxygenation capacity (blooming) was studied in samples packaged in E/S/E, which were removed from the film and exposed to air for 30 to 40 min at different storage periods; during blooming variations in Mb, MbO_2 and MetMb levels were recorded.

Analytical Techniques

Mb, MbO_2 and MetMb relative surface concentrations were determined on samples thawed at 1.1 cm/h (12 h at 4 °C). Relative surface concentrations of pigments were measured with a VARIAN SUPERSCAN 3 spectrophotometer equipped with integrating sphere reflectance attachment. Reflectance spectra were recorded between 400 and 800 nm, using barium sulfate coating as reference standard.

Meat samples were placed on special sample holders, with muscle fibers parallel to the surface to be analyzed, and were covered with an optical glass (the absorbance of which was considered in further calculations) in such a way that no occluded air remained. Samples thickness (2 cm) was chosen to satisfy the requirements of the R_∞ measurement, R_∞ is the reflectance of a layer so thick that an increase on thickness does not change this value (Bevilacqua and Zaritzky 1986).

Equations derived from the Kubelka Munk theory (Wendlandt and Hecht 1966; Kortum 1969) were used to calculte the relative surface concentrations of Mb, MbO_2 and MetMb. For the purpose of Kubelka Munk analysis, meat can be considered to be a light scattering matrix of cellular material, myofibrillar proteins, connective tissue and light absorbing pigments (MacDougall 1970). The intensity of reflected light and therefore its color and appearance is governed by the interrelationship of the light scattering components in the system. The red pigments are absorbers of light and the uncolored structure and myofibrillar proteins both scatter and absorb.

By solving the Kubelka Munk function for specific wavelengths: 525 nm (isobestic point for all three derivatives), 572 nm (isobestic for MbO_2 and Mb), 473 nm (isobestic for MbO_2 and MetMb) and 580 nm (characteristic wavelength of MbO_2 absorption spectrum) and by determining the relationship between the absorption and scattering coefficients corresponding to each of the pigments at the different wavelengths used, Bevilacqua and Zaritzky (1986) obtained expressions, which allowed to determine the relative surface concentrations of the muscle pigments in the present study.

Statistical Analysis

Freezing and thawing rates effect on pigment surface concentration was analyzed using a 2×2 factorial design with 10 replicates; existence of significant differences between treatments ($P < 0.05$) was established.

To study the influence of the frozen storage time and temperature on Mb, MbO_2 and MetMb evolution a complete block design was followed considering each muscle as one block. Integral method of kinetic analysis was performed on pigment surface concentration versus time data. Parameters were estimated by nonlinear regression using Marquardt's (Draper and Smith 1981) and Quasi-Newton minimization methods (Wilkinson 1986) with a computer program; curves were compared statistically by a modification of the Neter and Wasserman method (1974), and the presence of significant differences ($P < 0.05$) between treatments was established.

RESULTS AND DISCUSSION

Freezing and Thawing Rate Effect on Surface Color

Relative surface concentrations of muscle pigments for freeze-thawed samples were compared (Fig. 1) with data corresponding to unfrozen beef refrigerated at 4 °C for 24 h.

These results indicated that freeze-thawing treatments increases MetMb production rate; a similar conclusion was postulated by Brown and Dolev (1963)

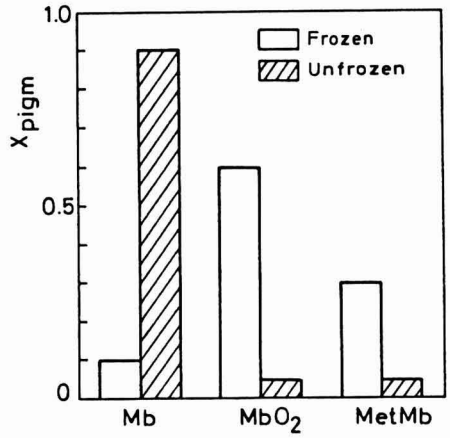

FIG. 1. COMPARISON BETWEEN PIGMENTS RELATIVE CONCENTRATIONS OF FROZEN-THAWED AND UNFROZEN REFRIGERATED SAMPLES (4 °C, 24 h) PACKAGED IN POLYETHYLENE
Each value is the mean of 10 replicates. Standard errors are within 10% and 20%.

working with MbO_2 solutions. Fennema (1975) informed that acceleration of reactions during freezing was not uncommon and could be explained on the basis of concentration of reactants in the unfrozen phase during freezing capable in some cases to overbalance temperature depressing effect. Hood (1983) reported that electrolyte concentration and presence of free transition metal ions contributed to the discoloration of frozen beef.

Statistical analysis showed that within the freezing and thawing rates range used in this work, variations in these parameters did not significantly affect ($P > 0.05$) relative surface concentration of muscle pigment of samples packaged in high permeability films. Similar results were reported by Jul (1984), this author informed that beef does not seem to be affected by variations in freezing rate between 0.2 cm/h (frozen slowly in still air) to 5 cm/h (quick frozen). A high freezing rate cause the meat to be slightly lighter in color (Zaritzky *et al.* 1983) but this effect can be attributed to the small crystals, formed by fast freezing that scatter more light than large crystals formed by slow freezing and hence fast frozen meat is opaque and pale and slow frozen is translucent and dark.

Pigment Interconversion Kinetic

Fox (1966) reported that interconversion of muscle pigments followed a dynamic color cycle in which oxygen is associating and dissociating continuously.

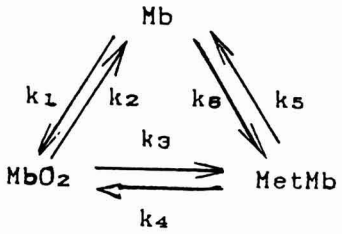

Integration of the differential equations obtained applying a first order kinetic led to the following general expression (Aris 1965)

$$x_i = A_{il}\, e^{(-L1\, t)} + A_{i2}\, e^{(-L2\, t)} + A_{ieq} \quad (1)$$

with i = 1, 2 and 3 for Mb, MbO_2 and MetMb respectively,

$$\text{being } x_1 + x_2 + x_3 = 1 \quad (2)$$

A_{i1} and A_{i2} are the amplitudes, L1 and L2 the time constants, A_{ieq} the equilibrium concentration of the i component. L1 and L2 are roots of the following second order equation:

$$L^2 + QL + M = 0 \quad (3)$$

$$\text{where } Q = k_1 (1 + 1/K_1) + k_3 (1 + 1/K_2) + k_5 (1 + 1/K_3) \quad (4)$$

$$\text{and } M = k_3k_5 (1 + 1/K_3 + 1/K_2K_3) + k_1k_5 (1 + 1/K_1 + 1/K_1K_3) + k_1k_3 (1 + 1/K_2 + 1/K_1K_2) \quad (5)$$

$$\text{with} \quad K_1 = k_1/k_2; \quad K_2 = k_3/k_4; \quad K_3 = k_5/k_6$$

Influence of Aeorbic Storage Time and Temperature on Pigment Surface Concentrations

Figures 2a, b, c and d represent pigment level modifications during storage in polyethylene film (aerobic conditions) at −5 °C, −10 °C, −13 °C and −20 °C, respectively. Results showed that xMb remained practically constant during

frozen storage and that equilibrium conditions for MbO_2 and MetMb were reached after 80 - 100 days of frozen storage.

Experimental data were satisfactorily fitted by the following expressions:

$$xMbO2 = A_{21}\, e^{(-L\,t)} + A_{2eq} \tag{6}$$

$$xMetMb = A_{31}\, e^{(-L\,t)} + A_{3eq} \tag{7}$$

Amplitudes, time constants and equilibrium concentration were calculated using nonlinear regression analysis (Draper and Smith 1981; Wilkinson 1986). Time constants and equilbrium concentrations values with their respective errors are shown in Table 1.

Results showed that Mb oxygenation took place during the freeze-thawing process since MbO_2 initial surface concentration corresponded to the highest value and xMb remained constant during the storage period, this would indicate that Mb does not participate in MetMb accumulation reaction. Thus, during aerobic frozen storage the following reversible reaction for pigment interconversion can be proposed:

$$MbO2 \underset{k_4}{\overset{k_3}{\rightleftharpoons}} MetMb$$

Considering a first order kinetic the integration of the differential equation led to:

$$xMetMb = k_3(1-A_{1eq})/(k_3+k_4) - ((k_3(1-A_{1eq}) - (k_3+k_4)xMetMbo)/(k_3+k_4))e^{-(k3+k4t)} \tag{8}$$

where xMetMbo corresponded to MetMb surface concentration at the beginning of frozen storage; Eq. (8) is similar to Eq. (7) considering:

$$L = k_3 + k_4 \tag{9}$$

$$A_{31} = -(k_3(1-A_{1eq}) - (k_3+k_4)xMetMb_0)/(k_3+k_4) \tag{10}$$

$$A_{3eq} = k_3\,(1-A_{1eq})/(k_3+k_4) \tag{11}$$

$$K = k_3/k_4 \text{ being } 1\text{-}A_{1eq} = xMetMbo + xMbO_{2o} \tag{12}$$

K represented the equilibrium conditions and k_4 can be related to the enzymatic reducing system present in muscle. Table 2 shows kinetic constants (k_3, k_4) calculated from Eq. (9) and (11) and equilbrium constant (K).

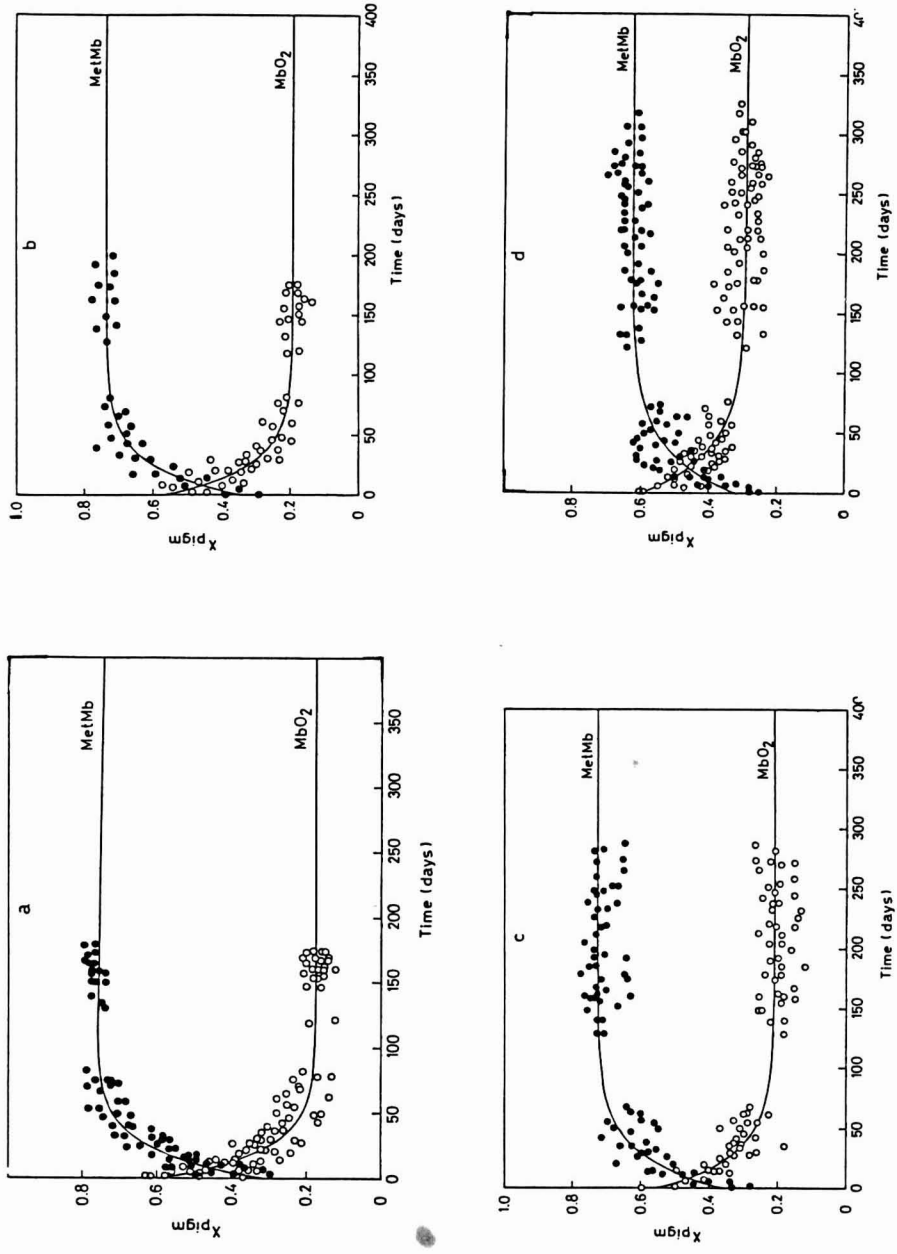

FIG. 2. PIGMENT CONCENTRATIONS CHANGES DURING FROZEN STORAGE OF POLYETHYLENE WRAPPED SAMPLES
Number of animals N = 11. Storage conditions: (a)T = −5 °C, (b) T = −10 °C, (c) T = −13 °C and (d) T = −20 °C. Solid lines represents pigment behavior predicted by the kinetic model.

TABLE 1.
TIME CONSTANTS (DAYS-1) AND EQUILIBRIUM CONCENTRATIONS OF MUSCLE PIGMENTS DURING FROZEN STORAGE OF POLYETHYLENE PACKAGED SAMPLES

T(°C)	L	A_{1eq}	A_{2eq}	A_{3eq}
-5	0.049	0.071	0.175	0.752
	(0.006)	(0.009)	(0.012)	(0.009)
-10	0.042	0.075	0.187	0.738
	(0.005)	(0.008)	(0.015)	(0.008)
-13	0.036	0.080	0.210	0.727
	(0.004)	(0.008)	(0.007)	(0.006)
-20	0.029	0.085	0.295	0.627
	(0.004)	(0.013)	(0.007)	(0.006)

$A_{1eq} = xMb_{eq}$; $A_{2eq} = xMbO_{2eq}$; $A_{3eq} = xMetMb_{eq}$
Standard deviations are given in parenthesis.

TABLE 2.
KINETIC AND EQUILIBRIUM CONSTANTS FOR METMYOGLOBIN ACCUMULATION DURING STORAGE OF FROZEN BEEF IN AEROBIC CONDITIONS

T(°C)	k_3 (days^{-1})	k_4 (days^{-1})	K
-5	3.97 10^{-2}	9.25 10^{-3}	4.30
-10	3.35 "	8.49 "	3.46
-13	3.35 "	8.07 "	3.46
-20	2.79 "	9.21 "	2.12

Reaction enthalpy for oxidation was calculated using Van't Hoff Equation $\triangle H = 27.142$ kJ/mol. This result indicated that MetMb production was an endothermic reaction, thus a decrease of storage temperature produced an enhancement of MbO_2 stability through a reduction of autoxidation rate (k_3) without affecting the activity of the enzymatic reducing system (k_4). The energy of activation for MetMb production was calculated assuming an Arrhenius-type temperature dependence of k_3, $E_a = 26.532$ kJ/mol. Chu *et al.* (1987) working with restructured beef steaks frozen up to $-34\,°C$ and stored at $-2\,°C$ postulated that the rapid increase in MetMb formation rate over the first month of storage was probably due to ice crystal formation and cell disruption; such changes permit catalysts of oxidative reactions to come into contact with Mb and lipids. Energy of activation values for MbO_2 oxidation obtained in the present study ($E_a = 26.532$kJ/mol) and the one informed by Martino and Zaritzky (1988) corresponding to the ice recristalization process in beef tissues ($E_2 = 42.370$ kJ/mol) are not comparable, from these results some doubts arise upon the validity of this theory.

Kinetic constant behavior with storage temperature obtained in the present study does not agree with the informed by Brown and Dolev (1963) and Zachariah and Satterlee (1973). These authors reported that autoxidation rates of bovine MbO_2 solutions frozen up to temperatures between $-5\,°C$ and $-25\,°C$ subsequently stored showed a slight maximum at $-11\,°C$ to $-12\,°C$. Results from a study performed in our laboratory about freezing final temperature effect on pigment surface concentration indicated that in a temperature range of $-5\,°C$ to $-15\,°C$ a significant increase in MetMb levels was produced that could be explained considering that within this range the largest variations in reactants concentration in the unfrozen phase were observed (Fennema 1975). Thus, differences in rate constant temperature dependence between reports from Brown and Dolev (1963) and Zachariah and Saterlee (1973) and the obtained in this work can be attributed to the different final freezing temperatures utilized.

As far as surface color is concerned there are different criteria regarding shelf-life of beef. Van den Oord and Wesdorp (1971) stated that meat becomes unacceptable for most consumers at xMetMb = 0.5. Hood and Riordan (1973) showed that when xMetMb is 0.2 the retail sale ratio of discolored to bright red meat was about 1:2. Considering xMetMb = 0.5 as limit of acceptablity, Lanari and Zaritzky (1988) reported that for refrigerated beef this value was attained in 30 and 15 days at 0 °C and 4 °C, respectively. In frozen beef these periods were: 14 days at $-5\,°C$ and $-10\,°C$, 16 days at $-13\,°C$ and 32 days at $-20\,°C$ because due to the freezing process initial values of MetMb were very high (xMetMb = 0.3).

From these results it can be concluded that freezing and frozen storage of beef samples wrapped in high permeability films produces discoloration, reaching in short times levels of MetMb higher than the acceptable values.

Effect of Previous Vacuum Frozen Storage on Meat Blooming

Figure 3a and b showed pigment evolution during oxygenation at 25 °C of thawed samples (1.1 cm/h; 12 h at 4 °C) previously vacuum wrapped in E/S/E, frozen and stored during 180 days at −5 °C and −20 °C, respectively. Similar curves were obtained at −10 °C and −13 °C for different tps values (tps = previous vacuum storage time). Oxygenation curves were statistically compared according to Neter and Wasserman (1974) to determine the degree of significance of the tps effect.

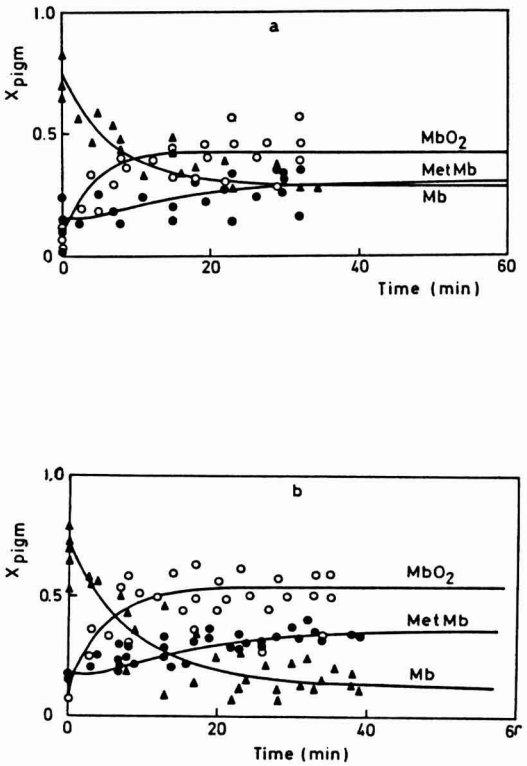

FIG. 3. PIGMENT MODIFICATIONS DURING BLOOMING OF E/S/E WRAPPED SAMPLES
Previous vacuum storage time (tps) = 180 days; number of animals N = 11. Storage temperature: (a) −5 °C, (b) −20 °C. Solid lines represents pigment concentrations predicted by the kinetic model.

When a meat sample is exposed to air, pigment interconversion can be interpreted with the following reaction scheme:

$$Mb \underset{k'_2}{\overset{k'_1}{\rightleftharpoons}} MbO_2 \underset{k'_4}{\overset{k'_3}{\rightleftharpoons}} MetMb$$

with equilibrium constants:

$$K'_1 = k'_1/k'_2 \qquad K'_2 = k'_3/k'_4 \tag{13}$$

K'_1 is related with the oxygenation capacity of the meat sample, K'_2 with the stability of MbO_2 complex and k'_4 with the activity of the enzymic reducing system present in meat. Assuming first order kinetics the following mass balances were obtained:

$$dxMb/dt = k'_2\, xMbO_2 - k'_1\, xMb \tag{14}$$
$$dxMbo_2/dt = k'_1\, xMb - (k'_2 + k'_3)\, xMbO_2 + k'_4\, xMetMb \tag{15}$$
$$dxMetMb/dt = k'_3\, xMbO_2 - k'_4\, xMetMb \tag{16}$$

$$\text{Where } xMb + xMbO_2 + xMetMb = 1 \tag{17}$$

Integration of the differential equations lead to a general expression similar to Eq.(1), where t represents oxygenation time. Experimental data were satisfactorily fitted by this expression, parameter values were calculated using Quasi-Newton method (Wilkinson 1986) in a computer program. Time constants and equilibrium concentrations with their respective standard deviations for the different temperatures and tps assayed are shown in Table 3.

MetMb equilibrium surface concentrations were not significantly affected by tps and storage temperature, these values were similar to those corresponding to just frozen samples wrapped in high permeability films; for storage temperatures of −13 °C and −20 °C and tps lower than 210 days, MbO_2 final levels after blooming were comparable to MbO_2 relative surface concentration values of just frozen polyethylene packed samples.

Kinetic constants were calculated from the following expressions derived from Eq. (3) to (5) considering k'_5 and $k'_6 = 0$.

$$L1 + L2 = k'_1 + k'_2 + k'_3 + k'_4 \tag{18}$$

$$L1 - L2 = \left\{(k'_1 + k'_2 + k'_3 + k'_4)^2 - 4\, k'_1 k'_3 (1 + 1/K'_2 + 1/(K'_1 K'_2)\right\}^{1/2} \tag{19}$$

Table 4 shows kinetic and equilibrium constants values for the oxygenation process. The increase of tps at each temperature (−5 °C, −13 °C and −20 °C) caused a decrease of the oxygenation capacity (K'_1) through the diminution of k'_1 and k'_4. This was reflected in a reduction of $xMbO_2eq$. At similar tps values

TABLE 3.
TIME CONSTANTS AND EQUILIBRIUM CONCENTRATIONS
OF MUSCLE PIGMENT FOR THE OXYGENATION PROCESS

T(°C)	tps	L1	L2	A_{1eq}	A_{2eq}	A_{3eq}
	9	0.205	0.343	0.120	0.580	0.300
		(0.065)	(0.090)	(0.032)	(0.021)	(0.032)
-5	30	0.115	0.195	0.150	0.564	0.330
		(0.019)	(0.065)	(0.027)	(0.027)	(0.035)
	180	0.106	0.181	0.280	0.419	0.301
		(0.045)	(0.038)	(0.060)	(0.103)	(0.029)
	30	0.111	0.188	0.120	0.563	0.320
		(0.039)	(0.042)	(0.068)	(0.044)	(0.033)
-13	180	0.108	0.149	0.140	0.520	0.340
		(0.026)	(0.070)	(0.032)	(0.035)	(0.042)
	210	0.090	0.130	0.150	0.520	0.330
		(0.012)	(0.030)	(0.045)	(0.040)	(0.040)
	250	0.080	0.117	0.180	0.463	0.360
		(0.009)	(0.027)	(0.023)	(0.054)	(0.040)
	30	0.098	0.197	0.117	0.553	0.330
		(0.024)	(0.040)	(0.040)	(0.033)	(0.037)
	180	0.088	0.172	0.120	0.540	0.351
		(0.027)	(0.050)	(0.040)	(0.039)	(0.034)
-20	210	0.090	0.151	0.132	0.530	0.340
		(0.010)	(0.046)	(0.050)	(0.035)	(0.033)
	250	0.085	0.123	0.149	0.506	0.345
		(0.015)	(0.022)	(0.044)	(0.043)	(0.034)
	390	0.082	0.106	0.170	0.500	0.330
		(0.020)	(0.023)	(0.054)	(0.036)	(0.033)

$A_{1eq} = xMb_{eq}$; $A_{2eq} = xMbO_{2eq}$; $A_{3eq} = xMetMb_{eq}$
tps = previous vacuum storage time in days.
Standard deviations are given in parenthesis.
L_1, L_2 in $days^{-1}$

TABLE 4.
KINETIC AND EQUILIBRIUM CONSTANTS FOR PIGMENT INTERCONVERSION DURING OXYGENATON

T(°C)	tps	k'1	k'2	k'3	k'4	Ki	Kż
	9	0.27	0.05	0.07	0.15	5.07	0.49
-5	30	0.12	0.03	0.06	0.10	4.67	0.62
	180	0.09	0.06	0.06	0.08	1.50	0.70
	30	0.12	0.03	0.05	0.09	4.67	0.57
-13	180	0.11	0.03	0.05	0.08	4.13	0.64
	210	0.09	0.03	0.04	0.07	3.47	0.63
	250	0.08	0.03	0.03	0.04	2.56	0.78
	30	0.12	0.02	0.05	0.09	5.70	0.58
	180	0.10	0.02	0.05	0.08	4.51	0.63
-20	210	0.10	0.02	0.05	0.07	4.01	0.63
	250	0.09	0.02	0.04	0.06	3.85	0.66
	390	0.07	0.03	0.04	0.06	2.94	0.66

tps = previous vacuum storage time in days. Kinetic constants in (min^1)

a decrease in storage temperature produced a higher MbO_2 stability. This was particularly notorius at tps longer than 30 days; at tps = 180 days MbO_2 levels at −5 °C were significantly lower ($P < 0.05$) than those corresponding to −13 °C and −20 °C. For storage temperature and time of −20 °C and 250 days. MbO_{2eq} were slightly higher than those at −13 °C.

These results showed that pigment surface concentration of frozen beef packed in low permeability films is maintained within acceptable values for more than 250 days at −20 °C and −13 °C. Color is the most important feature of frozen meat appearance. Therefore, use of vacuum wrapping could be a viable alternative in terms of cost, convenience and long term stability for marketing fresh meat in the frozen state.

CONCLUSIONS

The behavior of muscle pigments during oxygenation and oxidation processes of frozen beef samples was analyzed at different storage temperature samples packaged in high and low permeability films. Experimental results corresponding to relative pigment surface concentrations were adequately interpreted by kinetic models.

Within the freezing and thawing rates range used in the present study, variations in these parameters did not affect pigment surface concentration of samples packaged in high permeability films.

Freezing and frozen storage of beef samples wrapped in polyethylene produced a considerable enhancement of MetMb production, acceptability time values obtained for each storage temperature were lower than those corresponding to refrigerated beef stored at 0 °C and 4 °C.

Storage of vacuum-packaged frozen samples increased color stability; MbO_2 equilibrium surface concentration after blooming remained practically constant for more than 200 days at −13 °C and −20 °C. MetMb final levels were in all cases below the limit value of 0.5.

From these results it can be concluded that marketing vacuum packaged fresh meat in the frozen state is convenient since a considerable enlargement of color stability can be obtained offering great potential advantages in terms of cost and quality improvement.

REFERENCES

ARIS, R. 1965. *Introduction to the Analysis of Chemical Reactors,* pp. 94–101, Prentice Hall, Englewood Cliffs, New Jersey.

BEVILACQUA, A.E. and ZARITZKY, N.E. 1986. Rate of pigment modifications using reflectance spectrophotometry. J. Food Proc. Preserv. *10*, 1–18.

BROWN, W.D. and DOLEV, A. 1963. Effect of freezing on autoxidation of oxymyoglobin solutions. J. Food Sci. *28*, 211–213.

CHU, Y.H., HUFFMAN, G.R., TROUT, G.R. and EGBERT, W.R. 1987. Color and color stability of frozen restructured beef steaks: Effect of sodium chloride, tripolyphosphate, nitrogen atmosphere and processing procedures. J. Food Sci. *52*, 869–875.

DALHOFF, E. and JUL, M. 1965. In *Progress in Refrigeration Science and Technology*, Vol. I, pp. 57–66, Pergamon Press, New York.

DRAPER, N. and SMITH, H. 1981. *Applied Regression Analysis,* 2nd. Ed. pp. 471–485, John Wiley & Sons, N.Y. Chichester, Brisbane, Toronto, Singapore.

FENNEMA, O.R. 1975. Reaction kinetic in partially frozen aqueous systems. In *Water Relations in Foods.* (R.B. Duckworth, ed.) pp. 440–455.

FOX, Jr., J.B. 1966. The chemistry of meat pigments. J. Agr. Food Chem. *14*, 247–265.

HOOD, D.E. 1980. Factors affecting the rate of metamyoglobin accumulation in prepackaged beef. Meat Sci. *4*, 247–265.

HOOD, D.E. 1983. The chemistry of vacuum and gas packaging of meat. In *Recent Advances in the Chemistry of Meat*, pp. 213–230, (Allen J. Bailey, ed.) ARC Meat Research Institute.

HOOD, D.E. and RIORDAN, E.B. 1973. Discoloration in pre-packaged beef: measurement by reflectance spectrophotometry and shopper discrimination. J. Food Technol. *8*, 333–343.

IIF, International Institute of Refrigeration. 1972. *Recommendations for the Processing and Handling of Frozen Foods,* 2nd Ed. pp. 16.

JUL, M.P. 1984. *The Quality of Frozen Foods.* pp. 33–43, Academic Press, London.

KORTUM, G. 1969. *Reflectance Spectroscopy,* Springer-Verlag, New York.

LANARI, M.C. and ZARITZKY, N.E. 1988. Potassium sorbate effect on pigment concentrations of refrigerated beef. J. Food Sci. *53*, 1621–1627.

LANIER, T.C., CARPENTER, A. and TOLEDO, R.T. 1977. Effects of cold storage environment on color of exposed lean beef surfaces. J. Food Sci. *42*, 860–865.

LEDWARD, D.A. 1970. Metamyoglobin formation in beef stored in carbon dioxide enriched and oxygen depleted atmospheres. J. Food Sci. *35*, 33–37.

LEDWARD, D.A. and MACFARLANE, J.J. 1971. Some observations on myoglobin and lipid oxidation in frozen beef. J. Food Sci. *36*, 987–989.

LENTZ, C.P. 1979. Effect of light intensity and other factors on the color of frozen prepackaged beef. Can. Inst. Food Sci. and Technol. *12*, 47–50.

MACDOUGALL, D.B. 1970. Characteristics of the appearance of meat I. The luminous absorption scatter and internal transmittance of the lean of bacon manufactures from normal and pale pork. J. Sci. Food Agric. *21*, 568–571.

MACDOUGALL, D.B. 1982. Changes in color and opacity of meat. Food Chem. *9*, 75–88.

NETER, J. and WASSERMAN, W. 1974. *Applied Linear Statistical Models,* D. Pirchard Irwin, Homewood, IL.

O'KEEFE, M. and HOOD, D.E. 1980–81b. Anoxic storage of fresh beef. 1: Nitrogen and carbon dioxide storage atmospheres. Meat Sci. *5*, 27–39.

SEIDEMAN, S.C., VANDERZANT, C., SMITH, G.C., HANNA, M.O. and CARPENTER, Z.L. 1976. Effect of vacuum and length of storage on the microflora of vacuum packaged beef wholesale cuts. J. Food Sci. *41*, 738–742.

TAYLOR, A.A. 1985. Packaging of fresh meat. In *Developments in Meat Science 3.* (R.A. Lawrie, ed.) pp. 89–113. Applied Science, London.

VAN ARSDEL, W.B., 1969. *Quality and Stability of Frozen Foods,* pp. 196–197, Wiley-Interscience.

VAN DEN OORD, A.H.A. and WESDORP, J.J. 1971. Analysis of pigments in intact beef samples. J. Food Technol. *6,* 1–13.

WENDLANDT, W.N. and HECHT, H.G. 1966. *Reflectance Spectroscopy,* Interscience Publ., New York.

WILKINSON, L. 1986. *Systat: The Systèm for Statistics,* Systat Inc., Evanston, IL.

ZACHARIAH, N.Y. and SATERLEE, L.D. 1973. Effect of light, pH and buffer strength on the autoxidation of porcine, ovine and bovine myoglobins at freezing temperatures. J. Food Sci. *38,* 418–420.

ZARITZKY, N.E., AÑON, M.C. and CALVELO, A. 1982. Rate of freezing effect on the colour of frozen beef liver. Meat Science, *7,* 299–312.

EFFECT OF VOLUME CHANGE IN FOODS ON THE TEMPERATURE AND MOISTURE CONTENT PREDICTIONS OF SIMULTANEOUS HEAT AND MOISTURE TRANSFER MODELS

M. BALABAN

Food Science and Human Nutrition Department
University of Florida, Gainesville, FL 32611

Accepted for Publication April 4, 1989

ABSTRACT

Temperature and moisture content predictions of two models of simultaneous heat and moisture transfer (SHMT) in foods with and without the assumption of volume change were compared. In the first model, thermophysical and transport parameters were kept constant. In the second model, these were taken as variable functions of temperature and moisture content. Comparison of the results of both models with and without shrinkage assumption showed that there can be significant differences in predicted moisture and temperature gradients, and average moisture contents and temperatures. Biot numbers for heat and mass transfer, and the extent of overall shrinkage with moisture loss are important factors affecting these differences. The predictions of the second model were compared to experimental drying data with shrinkage. The variable-grid finite difference method can be used successfully to solve model equations involving volume changes.

INTRODUCTION

Simultaneous heat and moisture transfer (SHMT) is used extensively in food processing operations such as drying, smoking, baking, frying, and cooking. In these operations, foods undergo volume change either by shrinkage due to moisture loss, or by expansion due to gas generation. Volume change of foods during processing is well documented. Suzuki *et al.* (1976) investigated the shrinkage of root vegetables during dehydration. They suggested different relations between surface area changes and moisture content. Hwang and Hayakawa

[1]Correspondence address: M. Balaban. Food Science and Human Nutrition Department, University of Florida, Gainesville, FL 32611.
[2]Florida Agricultural Experiment Station Journal Series No. 8268

Journal of Food Process Engineering *12(1989) 67-88.* *All Rights Reserved.*
©Copyright 1989 by Food & Nutrition Press, Inc., Trumbull, Connecticut.

(1980) measured the volume change in cookies undergoing baking. They correlated densities to temperature and moisture content. Balaban (1984) and Balaban and Pigott (1986) showed that there was considerable volume shrinkage due to moisture loss during drying of fish.

Volume change is important because it causes stresses, and may result in cracks and deformations. Earle and Ceaglske (1949) identified shrinkage as the most likely cause of surface cracking in macaroni. Rao and Webb (1976) investigated the factors influencing stress cracks in frankfurters during cooking. Haghighi and Segerlind (1978) simulated the stress cracking of soybeans. Lewis *et al.* (1979) analyzed drying induced stresses in porous bodies and advanced an elastoviscoplastic model.

Jason (1958) in his pioneering work on mass transfer in fish, mentioned the problems associated with shrinkage. His main concern was the experimental determination of the effective diffusion coefficient in a shrinking material, where the calculations were based on the original dimensions. He quoted Danckwerts solution to the shrinkage problem, where the equations of diffusion were applied to shrinking systems by allowing the coordinate system to shrink with the nonaqueous material of the specimen. In this coordinate system, pseudo dimensions were introduced. They were related to the dry weight of the material. This may be applied to isothermal systems, but in SHMT other parameters such as thermal conductivity must also be "adjusted". In addition, changing the diffusion coefficient in a shrinking system to artificially keep dimensions constant will not allow for the estimation of stresses generated. Crank and Park (1968) also mention the need to correct for the diffusion coefficient if the volume of the material changes. They suggested a thermodynamic correction of the diffusion coefficient in swelling polymer systems. However, it may be more realistic to allow for changes in the dimensions, and not to artificially "adjust" physical properties.

Mathematical models are useful tools in the design and analysis of SHMT. There are many models in the literature that predict the distribution of moisture content and temperature of foods undergoing SHMT for different shapes, different compositions, and at different environmental conditions. (Mensah *et al.* 1971; Young and Whitaker 1971; Brooker *et al.* 1974; Misra and Young, 1980; Balaban 1984). In some of the models, the assumption of negligible shrinkage is made for mathematical convenience. The behavior of a SHMT model as affected by shrinkage needs to be investigated.

The objective of the present study is to compare the temperature and moisture content predictions of two mathematical models of SHMT, with and without the no-shrinkage assumption. The validity of the no-shrinkage assumption is evaluated in light of the differences in these predictions. Important parameters causing these differences are determined. The predictions of the second model are compared with experimental data.

MATERIALS AND METHODS

Two mathematical models of SHMT were evaluated to compare their predictions of moisture and temperature gradients, with and without the assumption of shrinkage. All symbols are defined in the Notation section.

Model 1

The first model was deliberately chosen as a simplified case of SHMT. Since the purpose was to evaluate the effect of only volume change on SHMT model behavior, the following assumptions were made: (1) Physical and transport properties of material are constant. (2) Water transport is in liquid phase only. (3) There is no evaporation within the material. (4) The material is a continuous infinite slab.

It is realized that these assumptions do not reflect realistic conditions for SHMT operations. However, only the effect of shrinkage on the model results is studied, and the validity of the model is not the concern at this point. Introduction of more variables would mask the effect of shrinkage. The above assumptions also simplify the solution of model equations considerably.

The model equations are:

Mass Balance:

$$\frac{\partial u}{\partial t} = D_{eff} \frac{\partial^2 u}{\partial x^2} \tag{1}$$

Heat Balance:

$$\frac{\partial T}{\partial t} = \alpha \frac{\partial^2 T}{\partial x^2} \tag{2}$$

Boundary Conditions:

At $x = 0$ (center): $t > 0$

$$\frac{\partial u}{\partial x} = 0 \text{ and } \frac{\partial T}{\partial x} = 0 \tag{3}$$

At $x = L$ (surface): $t > 0$

Mass transfer boundary condition:

$$h_m (u \rho_b - \rho_{air} u_{air}) = - D_{eff} \rho_b \frac{\partial u}{\partial x} \tag{4}$$

Heat transfer boundary condition:

$$h_T (T_{air} - T) = k_T \frac{\partial T}{\partial x} + \lambda h_m (u \rho_b - u_{air} \rho_{air}) \qquad (5)$$

Since it was assumed that initially the temperature and moisture content were uniform, the initial conditions were:

$$\text{at } t = 0 \quad T = T_0 \text{ and } u = u_0 \qquad (6)$$

The equations (1–6) were nondimensionalized, resulting in the equations:

$$\frac{\partial \omega}{\partial F_{oh}} = Lu \frac{\partial^2 \omega}{\partial Y^2} \qquad \text{for mass transfer,} \qquad (7)$$

$$\frac{\partial \theta}{\partial F_{oh}} = \frac{\partial^2 \theta}{\partial Y^2} \qquad \text{for heat transfer,} \qquad (8)$$

For boundary conditions:

$$\text{At } Y = 0 \text{ (center)} \quad \frac{\partial \omega}{\partial Y} = 0 \text{ and } \frac{\partial \theta}{\partial Y} = 0 \qquad (9)$$

$$\text{At } Y = L \text{ (surface)} :$$

$$Bi_m \{ \omega + A_1 - A_2 A_3 \} = - \frac{\partial \omega}{\partial Y} \qquad (10)$$

$$Bi_h (1 - \theta) = \frac{\partial \theta}{\partial Y} + A_4 \{ A_1 + \omega - A_2 A_3 \} \qquad (11)$$

The above system of partial differential equations (PDE) are reduced to ordinary differential equations (ODE) in time by applying the finite difference method to space derivatives. The half-thickness is divided into N nodes. The central finite difference equations are modified slightly to handle varying and unequal distances between nodes. This is called the Variable Grid Central Finite Difference (VGCFD) method (Appendix)(Balaban and Pigott 1987). With this method it is possible to analyze uneven and time dependent dimensional changes. The resulting set of 2 N ODE in time are solved by the implicit Crank-Nicholson method. The values of the temperatures and moisture contents at each mode are calculated at a given time. Additionally, VGCFD method allows for the shrinkage/expansion of the nodes with time, if the volume change of the material is known as a function of moisture content. After each time step, each node distance is adjusted according to the average moisture content for that slice.

The method provides a time and position dependent volume change. For simplicity, a linear decrease of dimension with moisture content was assumed, as seen in the f_l values in Table 1. The f_l value is the extent of shrinkage: it is zero at the initial moisture, and approaches maximum shrinkage as moisture content decreases. The linear assumption is valid in the initial stages of drying. If the experimentally determined correlation of shrinkage vs. moisture content is not linear, this would easily be incorporated into the model, and not affect the method in any way. The calculation was repeated with different maximum shrinkage levels of 70%, 50% and 30% of original.

The behavior of the first model with no volume change is also investigated. The equations are the same except that distances between nodes are now equal and constant. The same method of solution applies, except this time there is no need to adjust the node distances after each time step.

Trial runs were performed to make sure that the time step size did not affect the results. To this end, the step size was decreased 10 times, and results were compared. The difference was negligible. Therefore, the larger step size was used to save computation time.

Model 2

The SHMT model described by Balaban and Pigott (1987) was used. In this model, thermal conductivity, heat capacity, diffusion coefficient and surface water activity are experimentally determined functions of moisture content and temperature. Also, the data on dimensional shrinkage as a function of moisture loss was determined experimentally (Balaban and Pigott 1986).

Mathematical model

Mass balance:

$$\rho_l \frac{\partial u}{\partial t} = \frac{\partial}{\partial x}\left\{ D_{eff}\, \rho_l \frac{\partial u}{\partial x} \right\} \tag{12}$$

Heat balance:

$$\rho_b\, C_{pb} \frac{\partial T}{\partial t} = \frac{\partial}{\partial x}\left\{ k_T \frac{\partial T}{\partial x} \right\} \tag{13}$$

Initial conditions:

$$\text{At time} = 0 : u = u_o \text{ and } T = T_o$$

Boundary conditions:

$$\text{At } x = L/2 \text{ (center)} \quad \frac{\partial u}{\partial x} = 0 \text{ and } \frac{\partial T}{\partial x} = 0$$

$$\text{At } x = 0 \text{ (surface)} : \tag{14}$$

TABLE 1.
PARAMETERS USED FOR MODEL 1

	SET 1	SET 2	SET 3
Bi_m	5.5	5.5	55
Bi_h	62	31	6.2
C_{Pb}: J/kg K	2721.42		
D_{eff}: m^2/sec	$6.45\ 10^{-8}$	$6.45\ 10^{-8}$	$6.45\ 10^{-9}$
f_1 for 70 % shrinkage	$0.7057 - 0.904\ u$		
f_1 for 50 % shrinkage	$0.5065 - 0.649\ u$		
f_1 for 30 % shrinkage	$0.3039 - 0.389\ u$		
F_{oh} end	0.98	0.98	3.94
F_{oh} increment	$1.0\ 10^{-3}$		
h_m : m/sec	$7\ 10^{-6}$	$7\ 10^{-6}$	$7\ 10^{-6}$
h_T : w/m^2 K	500.62	250.62	50.62
k_T : w/m K	0.412		
L_o : m	$5.1\ 10^{-2}$		
N	10		
T_o: K	298		
T_{air}: K	320		
u_o : kg H_2O/kg total	0.78		
u_{air}: kg H_2O/kg air	$8.94\ 10^{-3}$		
λ : J/kg	$2.436\ 10^6$		
ρ_b: kg/m^3	1100		
ρ_{air} : kg/m^3	1.16		

$$h_m (c_{surface} - c_{air}) = D_{eff} \rho_l \frac{\partial u}{\partial x} \tag{15}$$

And:

$$h_T (T_{air} - T_{surface}) = \lambda D_{eff} \rho_l \frac{\partial u}{\partial x} - k_T \frac{\partial T}{\partial x} \tag{16}$$

Parameters used during calculations. In the above equations, the values of k_T, D_{eff}, C_{pb}, ρb, a_w were determined experimentally (Balaban 1984).

Surface Mass Transfer Coefficient (h_m). Bennett and Myers (1962) give the following relation for h_m for a flat plate with turbulent air flow parallel to the surface:

$$h_m = 8.92\ 10^{-3}\ V_o\ (Re)^{-0.2}\ \frac{c}{c - c_{air}} \tag{17}$$

The value of c at the surface is taken from the isotherm relation, assuming that the liquid and vapor water are in equilibrium.

Surface Heat Transfer Coefficient (h_T). Charm (1971) gave the following relation for the heat transfer coefficient of air flowing parallel to a flat plate:

$$h_T = 1.145\ 10^{-5}\ G^{0.8} \tag{18}$$

Thermal Conductivity (k_T). The dependence of the thermal conductivity to both moisture content and temperature was determined experimentally (Balaban 1984):

$$k_T = -8.16\ 10^{-2} + 6.49\ 10^{-4}\ T + 1.012\ 10^{-1}\ u \tag{19}$$

Heat Capacity (C_{pb}). The dependence of the heat capacity to both moisture content and temperature was determined experimentally (Balaban 1984):

$$C_{pb} = 0.9615 + 3.6872\ 10^{-1}\ u - 2.237\ 10^{-3}\ T \tag{20}$$

Water Activity (a_w) or Equilibrium Relative Humidity RH_e. The dependence of the a_w to both moisture content and temperature was determined experimentally (Balaban 1984). It was assumed that at the surface, the vapor pressure of water can be calculated from a_w by using:

$$a_w = \frac{p_v}{p_{sat}} \tag{21}$$

The empirical relation developed experimentally for a_w for Ocean Perch is:

$$a_w = \exp\left\{\frac{\frac{1}{(94\ u)^2} - 9.5018\ 10^{-5}}{3.114\ 10^{-3} - 1.3103\ 10^{-4}\ T}\right\} \tag{22}$$

The expression relating p_{sat} of water to temperature is given by Brooker (1967):

$$p_{sat} = \exp\left\{53.53 - \frac{6834.2}{T_{abs}} - 5.169 \log T_{abs}\right\} \tag{23}$$

Diffusion Coefficient of Water (D_{eff}). Jason (1958) reported that the diffusivity of fish during drying is constant with moisture down to a critical moisture content. Below this moisture, the diffusion coefficient decreased to one-fifth of its initial value. Therefore, a diffusion coefficient with a step-change with moisture content was used in this study. The critical moisture was found to be u = 0.33 experimentally (Balaban 1984). The following values were taken from Jason (1958):

$$D_{eff} = K_{lo} \exp\left(\frac{-E}{R\ T_{abs}}\right) \tag{24}$$

where:

$$E/R = 3620\ ^{\circ}K \quad \text{and} \quad K_{lo} = 2.7\ 10^{-5}\ m^2/s$$

Dimensional Changes of Fish Slab During Drying. The experimental data of Balaban (1984) were used.

Non dimensionalization of Equations. The model equations were non dimensionalized as follows:

$$\theta = \frac{(T - T_{initial})}{(T_{air} - T_{initial})} \tag{25}$$

$$Y = \frac{x}{L} \tag{26}$$

Method of Solution. The resulting system of nonlinear PDE in time and one space dimension were solved numerically by again applying the VGCFD method, reducing the PDE into a set of ODE in time. The Runge-Kutta-Gill method (Finlayson, 1980) was chosen to solve these equations. At each time step

during the solution, the values of u_i and θ_i were calculated at each node, and each node distance is decreased according to the new average moisture content for that section. This provides a time and position dependent volume change. The experimental drying conditions were: air temperature = 29.5 °C, air velocity = 0.6 m/sec, and air relative humidity = 35%.

RESULTS

The values of parameters used in the first model are given in Table 1. These values were chosen arbitrarily to represent average SHMT conditions in food processing. Figure 1 represents the comparison of predicted moisture gradients by model 1 at different times between a nonshrinking material and the same material with 70% maximum shrinkage, by using the parameters in Set 1, in Table 1. It can be seen that the moisture levels become significantly different as drying progresses. This is because internal moisture has less distance to diffuse through and reach the surface for shrinking materials. Therefore, moisture loss is faster. The shape of moisture gradients is also affected by shrinkage. It should be noted that the same figure also depicts the total shrinkage of the sample at different times. For example, at 60 min (empty triangles) the material shrunk to 80% of its original size. The individual shrinkage of each section is also visible.

Figure 2 represents the comparison of temperature gradients at different times for the same set of parameters. Again, there is a significant difference between nodal temperatures for shrinkage and nonshrinkage assumptions. Also, the shape of temperature gradients is different.

Figure 3 represents the average moisture content versus time for different maximum shrinkage levels for the parameters in Set 1, Table 1. For all maximum shrinkage levels considered, the differences become more pronounced as drying time increases. The same discussion applies to Fig. 4, average temperature versus time for different shrinkage levels.

In set 2, Table 1, the surface heat transfer coefficient and thus the Biot number for heat transfer (Bi_h) are halved, to see the effect of Bi_h on results. It is shown in Fig. 5 that there are differences in average moisture levels between different maximum shrinkage values, and that the differences become significant as drying time increases. Also, comparing Fig. 3 and 5, it can be concluded that for this simple model, Bi_h does not affect moisture levels significantly.

In Fig. 6, the same general trend for average temperature versus time is observed. As shrinkage levels are increased, the temperature values deviate from the no-shrinkage values, and the differences are significant for longer drying times. It should be noted that the model predicts the initial cooling period of the material. Since heat transfer coefficient is halved, the heat received by the material is initially less than the heat of evaporation necessary for the surface

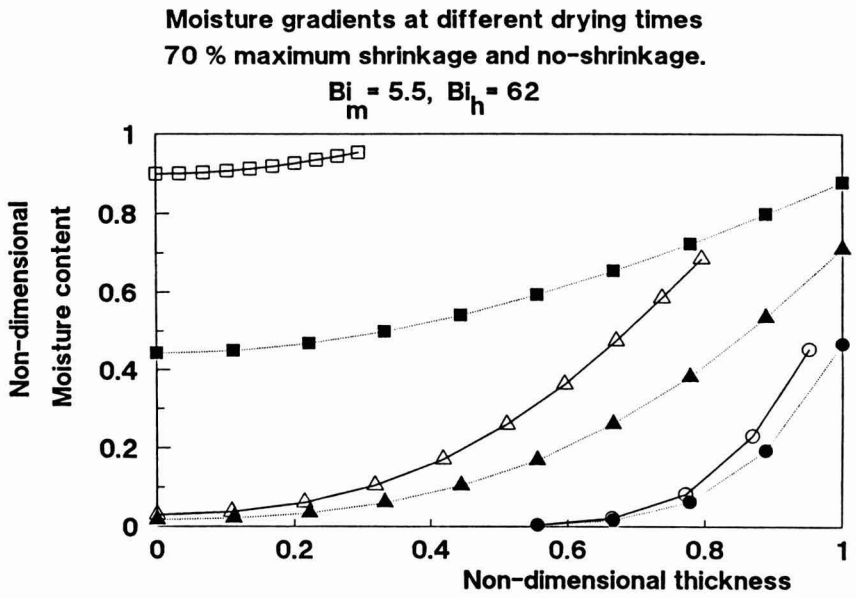

FIG. 1. MODEL. 1. COMPARISON OF MOISTURE GRADIENTS AT DIFFERENT TIMES FOR 70% MAXIMUM SHRINKAGE AND NO-SHRINKAGE CASES
Bim = 5.5, Bih = 62. °: 10 min, △: 60 min, □: 300 min ----: no shrinkage, ____: 70% shrinkage.

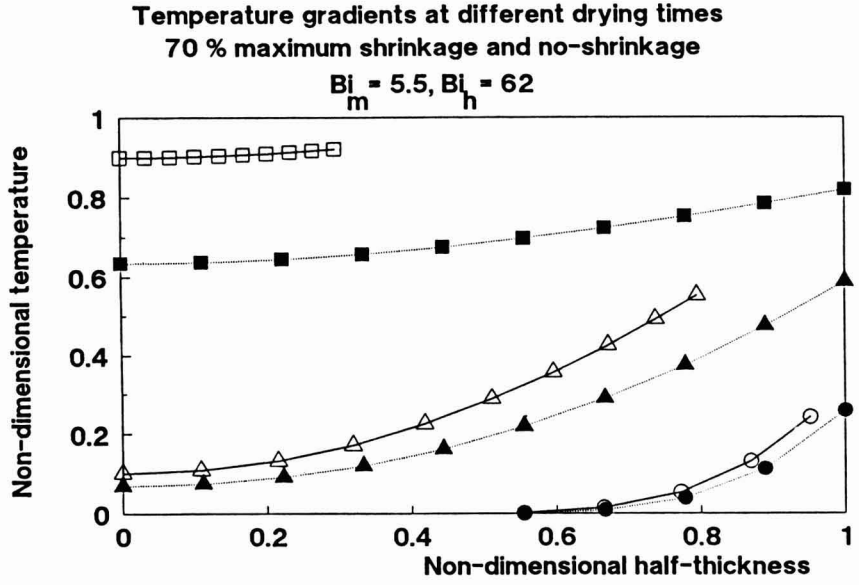

FIG. 2. MODEL. 1. COMPARISON OF TEMPERATURE GRADIENTS AT DIFFERENT TIMES FOR 70% MAXIMUM SHRINKAGE AND NO-SHRINKAGE CASES
Bim = 5.5, Bih = 62. °: 10 min, △: 60 min, □: 300 min ----: no shrinkage, ____: 70% shrinkage.

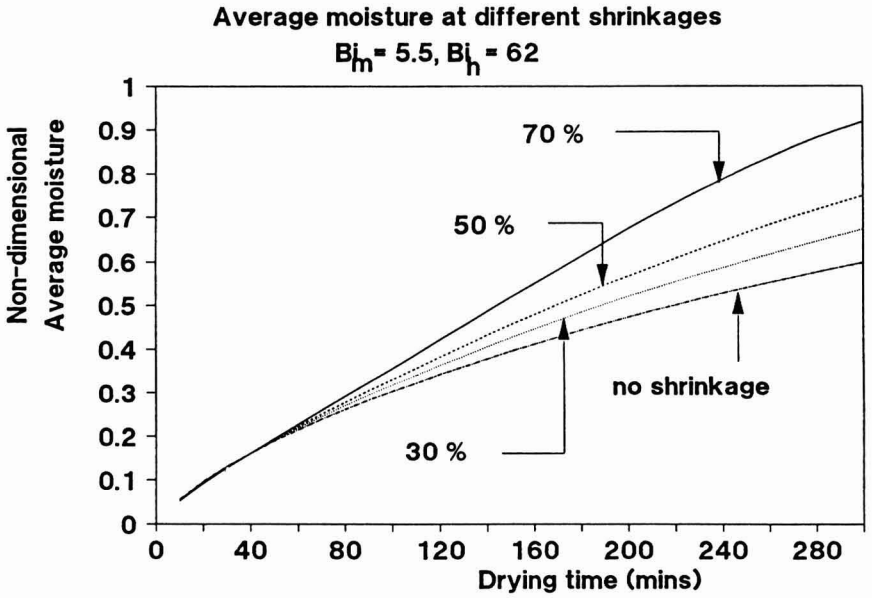

FIG. 3. MODEL. 1. COMPARISON OF AVERAGE MOISTURE VALUES VERSUS TIME FOR DIFFERENT MAXIMUM SHRINKAGE VALUES
Bim = 5.5, Bih = 62. ____: 70% shrinkage, __ __ __: 50% shrinkage, _____: 30% shrinkage, __ . __ .: no shrinkage.

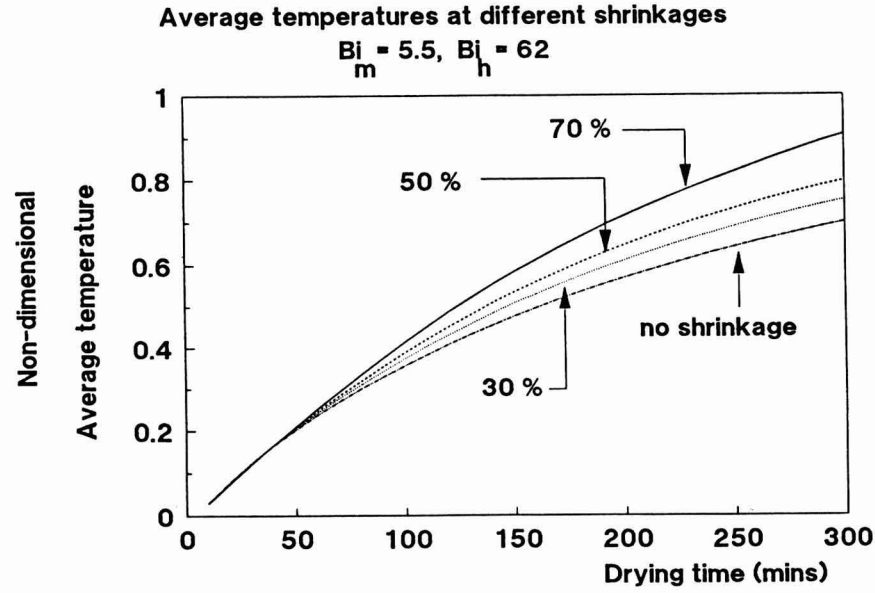

FIG. 4. MODEL. 1. COMPARISON OF AVERAGE TEMPERATURE VALUES VERSUS TIME FOR DIFFERENT MAXIMUM SHRINKAGE VALUES
Bim = 5.5, Bih = 62. ____: 70% shrinkage, __ __ __: 50% shrinkage, _____: 30% shrinkage, __ . __ .: no shrinkage.

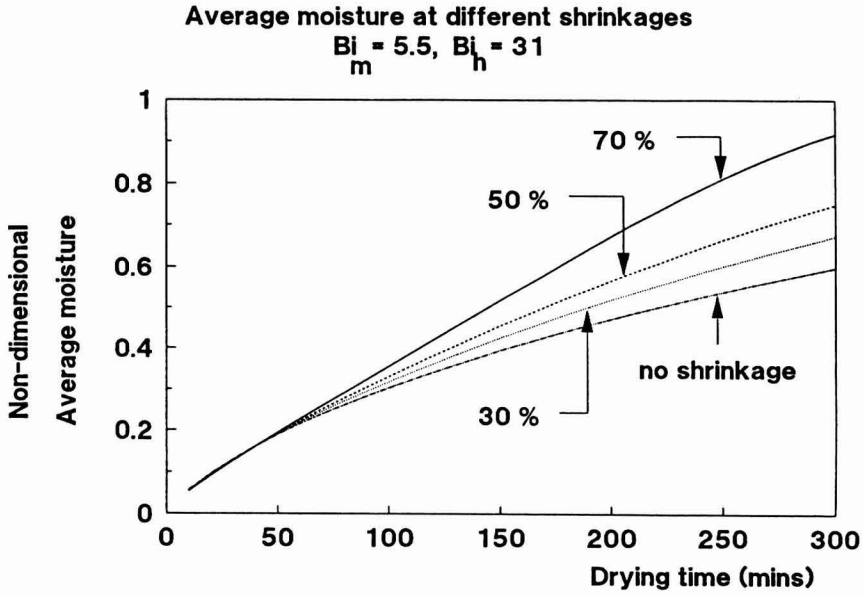

FIG. 5. MODEL. 1. COMPARISON OF AVERAGE MOISTURE VALUES VERSUS TIME FOR DIFFERENT MAXIMUM SHRINKAGE VALUES
Bim = 5.5, Bih = 31. ____: 70% shrinkage, __ __ __: 50% shrinkage, _____: 30% shrinkage, __ . __ .: no shrinkage.

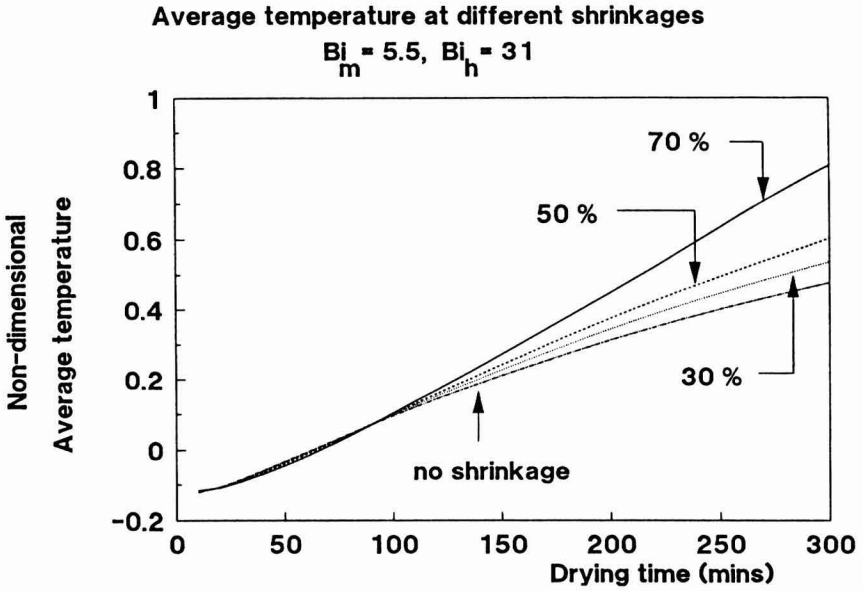

FIG. 6. MODEL. 1. COMPARISON OF AVERAGE TEMPERATURE VALUES VERSUS TIME FOR DIFFERENT MAXIMUM SHRINKAGE VALUES
Bim = 5.5, Bih = 31. ____: 70% shrinkage, __ __ __: 50% shrinkage, _____: 30% shrinkage, __ . __ .: no shrinkage.

moisture flux to evaporate, and temperature drops. Later, moisture flux decreases, and temperatures start to rise.

The effect of a change in effective moisture diffusion coefficient (and therefore Biot number for mass transfer) is also analyzed. In set 3, Table 1, the diffusion coefficient is decreased by an order-of-magnitude. This increases the Bi_m by an order-of-magnitude. Figure 7 represents the comparison of moisture gradients at different times for these data, between 70% shrinkage and no-shrinkage cases. Significant difference in both moisture levels and in moisture gradient shapes are apparent. Since surface transfer is fast, the system is diffusion controlled. Surface moisture content reaches near-equilibrium value quickly. The mass transfer then depends on how fast internal moisture diffuses to the surface. In the shrinkage case, the diffusion distance decreases, therefore initial moisture reaches the surface faster, and overall moisture approaches equilibrium faster.

In Fig. 8, temperature gradients at different times for shrinkage and no-shrinkage are compared. Since Bi_h is quite low, and surface moisture flow is small after a short time, it is expected that temperature gradients will not be steep. This means that heat transfer to the material at the surface is quickly conducted inside. Therefore, shrinkage should not have a significant effect on temperature levels. This is observed in Fig. 8.

Figure 9 represents the effect of different maximum shrinkage levels on average moisture versus time for data set 3 in Table 1. Since masss transfer is slow, the differences become significant only after long drying times.

Figure 10 confirms that there are no significant differences in average temperature versus time at different shrinkage levels for the above data set.

It should be noted that the Biot numbers presented are based on the initial dimensions. Since the transport parameters are assumed to be constant, as the material shrinks Biot numbers also decrease proportionally. In a more realistic case where transport parameters also change, the change in Biot numbers will be more complicated.

For the second model, the plot of the experimental and calculated values of the change in average final u value with and without shrinkage assumption versus time is shown in Fig. 11. It is apparent that there is a close correlation between experimental and calculated values when the shrinkage is considered. The model without shrinkage assumption predicts higher moisture contents at any given time. This is expected since nonshrinking dimensions result in longer diffusion path, and slower drying. The prediction of the moisture gradients in the slab as a function of drying time for shrinkage and nonshrinkage assumptions can be seen in Fig. 12. Since it is difficult to experimentally determine the moisture distribution within a sample with nondestructive methods, the predictions of the models could not be verified experimentally.

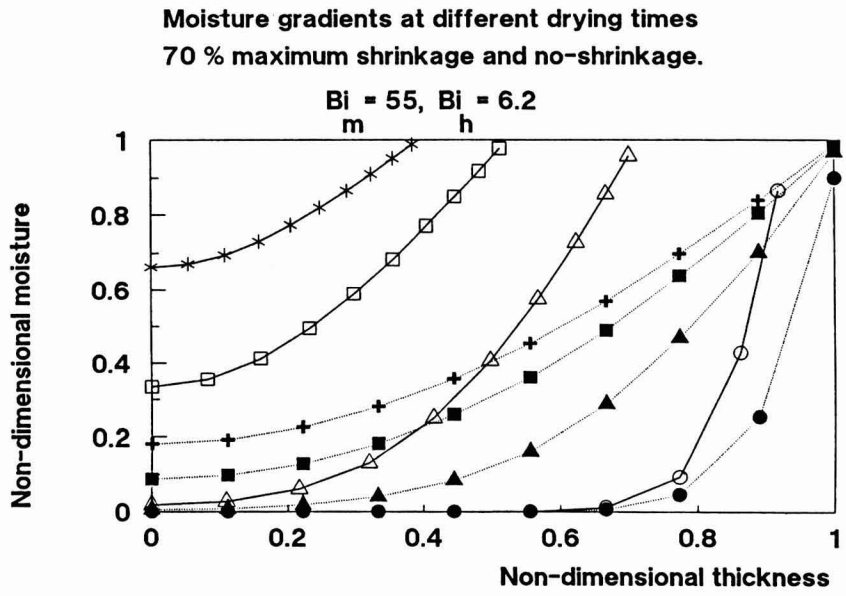

FIG. 7. MODEL. 1. COMPARISON OF MOISTURE GRADIENTS AT DIFFERENT DRYING TIMES FOR 70% MAXIMUM SHRINKAGE AND NO-SHRINKAGE CASES
Bim = 55, Bih = 6.2. °: 40 min, △: 360 min,: □ 840 min, * and +: 1200 min. -----: no shrinkage, _____:70% shrinkage.

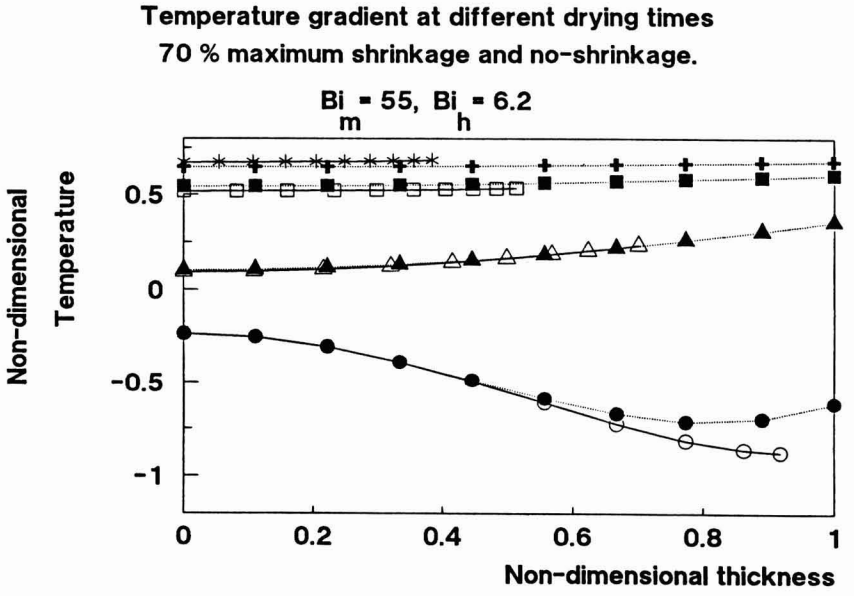

FIG. 8. MODEL. 1. COMPARISON OF TEMPERATURE GRADIENTS AT DIFFERENT DRYING TIMES FOR 70% MAXIMUM SHRINKAGE AND NO-SHRINKAGE CASES
Bim = 55, Bih = 6.2. °: 40 min, △: 360 min,: □ 840 min, * and +: 1200 min. -----: no shrinkage, _____:70% shrinkage.

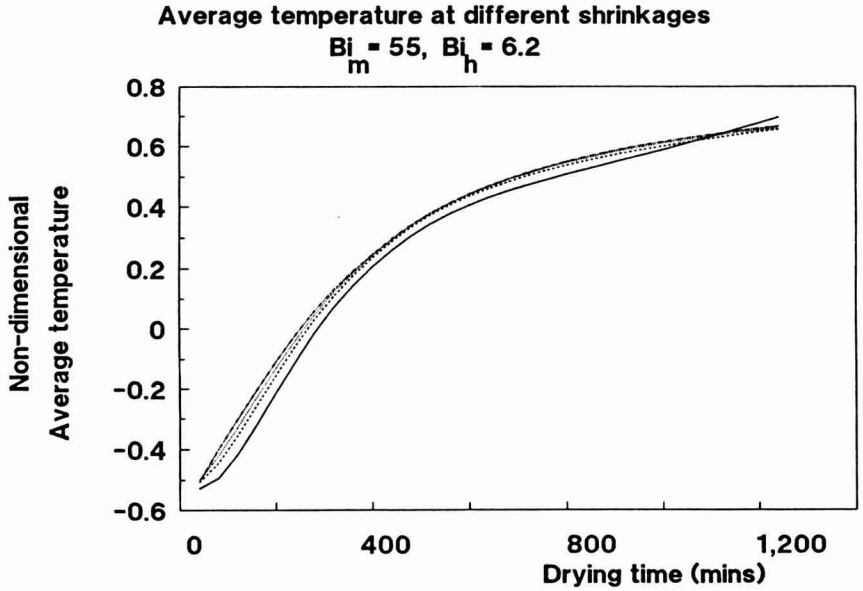

FIG. 9. MODEL. 1. COMPARISON OF AVERAGE MOISTURE VALUES VERSUS TIME FOR DIFFERENT MAXIMUM SHRINKAGE VALUES
Bim = 55, Bih = 6.2. ____: 70% shrinkage, __ __ __: 50% shrinkage, _____: 30% shrinkage, __ . __ .: no shrinkage.

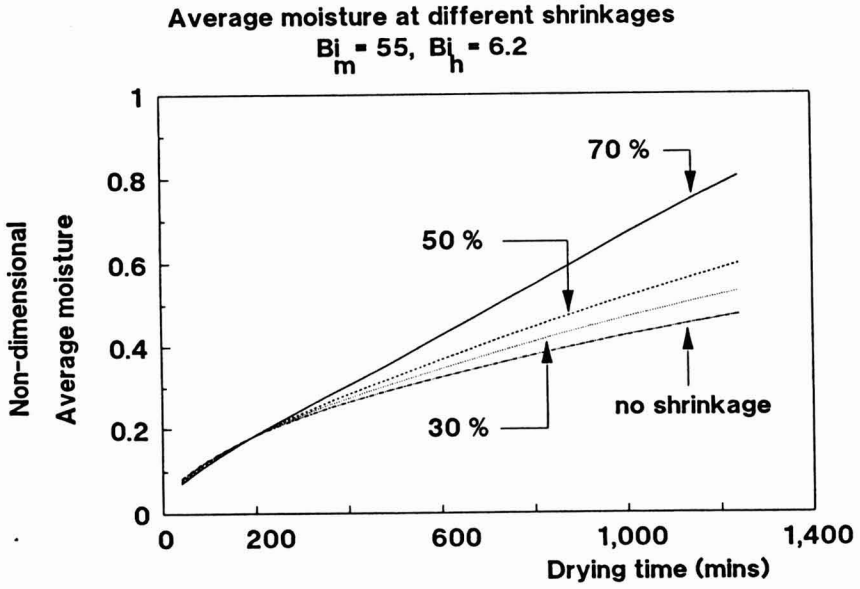

FIG. 10. MODEL. 1. COMPARISON OF AVERAGE MOISTURE VALUES VERSUS TIME FOR DIFFERENT MAXIMUM SHRINKAGE VALUES
Bim = 55, Bih = 6.2. ____: 70% shrinkage, __ __ __: 50% shrinkage, _____: 30% shrinkage, __ . __ .: no shrinkage.

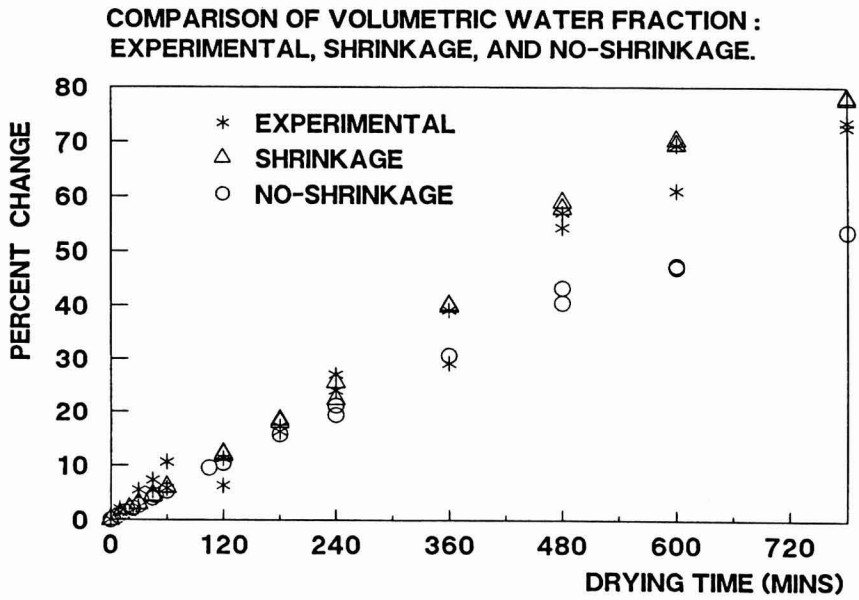

FIG. 11. MODEL. 2. COMPARISON OF EXPERIMENTAL, AND CALCULATED (WITH AND WITHOUT SHRINKAGE) PERCENT CHANGES IN VOLUMETRIC WATER FRACTION WITH DRYING TIME*: experimental, △: calculated, with shrinkage, __: calculated, no shrinkage.

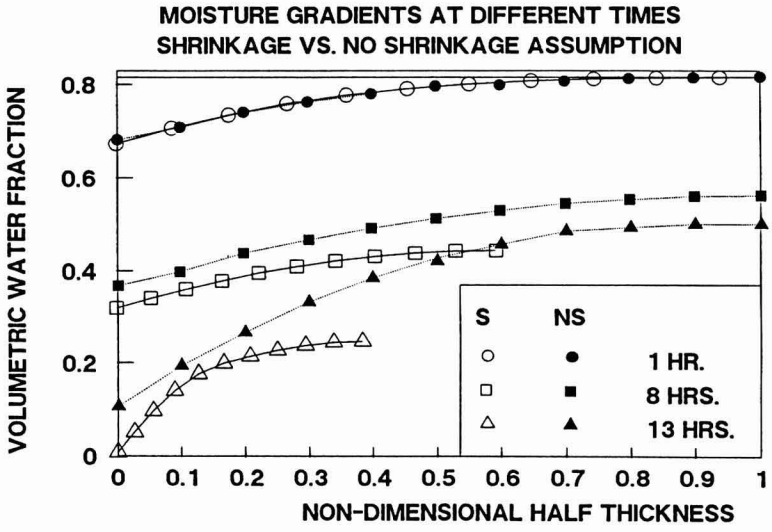

FIG. 12. MODEL 2. PREDICTED MOISTURE GRADIENTS AT DIFFERENT DRYING TIMES °: 1 h, □: 8 h, △: 13h.

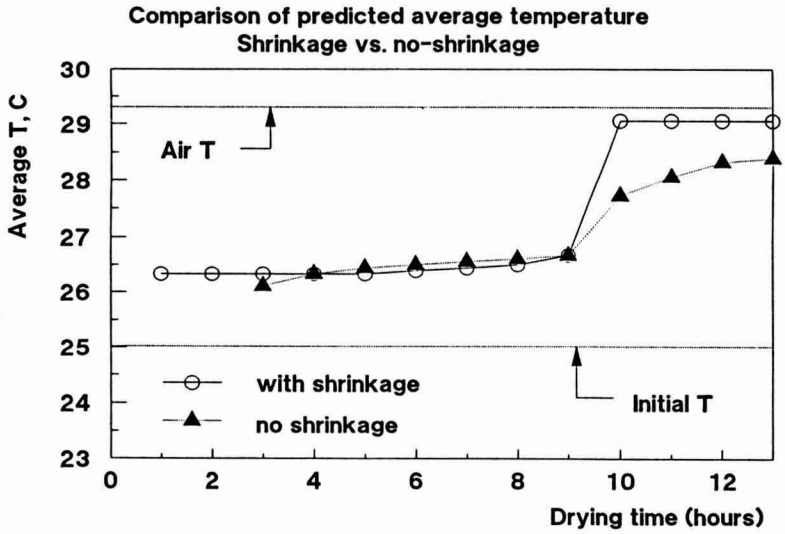

FIG. 13. MODEL 2. COMPARISON OF PREDICTED AVERAGE TEMPERATURES
△: no shrinkage, : "with shrinkage.

The drying model also predicted the temperature distribution of the slab at different drying times. However, due to the small thickness of the samples (less than 0.5 cm), it was not possible to determine the temperature distribution experimentally. The predicted values of models with and without shrinkage are shown in Fig. 13.

CONCLUSION

The assumption of no shrinkage in SHMT models may cause significant differences between actual values of temperature and moisture gradients and results predicted by the model. The factors affecting the magnitude of this difference include the maximum level of shrinkage, heat and mass transfer coefficients at the surface, and values of other transport parameters such as diffusion coefficient and thermal conductivity. An easy method to incorporate shrinkage into the model is to use variable-grid central finite difference method.

NOTATION

$$A_1 = \frac{u_o}{u_{air} - u_o} \text{ dimensionless}$$

$$A_2 = \frac{u_{air}}{u_{air} - u_o} \text{ dimensionless}$$

$$A_3 = \frac{\rho_{air}}{\rho_b} \text{ dimensionless}$$

$$A_4 = \frac{\lambda \; h_m \; (u_{air} - u_o) \; L_o \; \rho_b}{k_T \; (T_{air} - T_o)} \text{ dimensionless}$$

a_w : Water activity, dimensionless

$$Bi_m = \frac{h_m \; L_o}{D_{eff}} \text{ Biot number for mass transfer, dimensionless}$$

$$Bi_h = \frac{h_T \; L_o}{k_T} \text{ Biot number for heat transfer, dimensionless}$$

c Concentration of water at the surface, kg/m^3

c_{air} : Concentration of water in the air, kg/m^3

C_{pb} : Bulk heat capacity of material, $J/kg\ ^\circ K$

D_{eff} : Effective mass diffusion coefficient of water, m^2/sec

E/R : $^\circ K$

f_1 : Known function of shrinkage with u, dimensionless

$$F_{oh} = \frac{k_T \; t}{C_p \; \rho_b \; (L_o)^2} \text{ Fourier number for heat transfer, dimensionless}$$

G : Mass velocity of air, $kg/sec\text{–}m^2$

h_m : Convective surface mass transfer coefficient, m/sec

h_T : Convective heat transfer coefficient, $w/m^2\text{–}^\circ K$

k_T : Thermal conductivity, w/m–°K

$Lu = \frac{D_{eff}}{\alpha}$ Luikov number, dimensionless

L : Half–thickness at time t, m

N : Number of finite difference nodes

P_v : Partial pressure of water, KPa

P_{sat} : Vapor pressure of water, KPa

Re : Reynolds number, dimensionless

t : Time, sec

T : Temperature, °C

T_o : Initial temperature, °C

T_{air} : Air temperature, °C

T_{abs} : Absolute temperature, °K

u : wet basis moisture content, kg water/ kg total (model 1)

u_o : Initial wet basis moisture content, kg water/ kg total (model 1)

u_{air} : wet basis moisture content of air, kg water/ kg total (model 1)

u : Volume fraction of water in fish, dimensionless (model 2)

u_o : Initial volume fraction of water, dimensionless (model 2)

V_o : Velocity of air, m/sec

x : Space dimension in the direction of thickness, m

$Y = \frac{x}{L_o}$: Nondimensional space variable

$\alpha = \frac{k_T}{C_p \rho_b}$. Thermal diffusivity, m^2/sec

λ : Heat of evaporation of water, J/kg

ρ_b : Bulk density of material, kg/m^3

ρ_{air} : Density of air, kg/m^3

ρ_l : Density of liquid, kg/m^3

$$\theta = \frac{(T - T_o)}{(T_{air} - T_o)}$$ Nondimensional temperature

$$\omega = \frac{(u - u_o)}{(u_{air} - u_o)}$$ Nondimensional moisture content (model 1)

APPENDIX

Application of variable–grid central finite difference to partial derivatives :

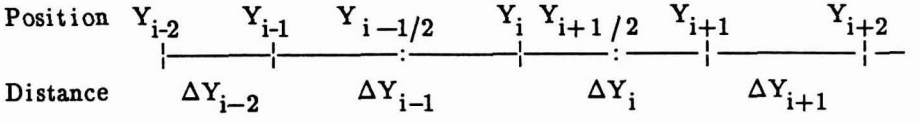

The values of the dependent variables θ and ω are evaluated at the nodes Y_i.

The equations are:

$$\frac{\partial \omega_i}{\partial Y} = \frac{\omega_{i+1} - \omega_{i-1}}{\Delta Y_i + \Delta Y_{i-1}} \qquad [A1]$$

$$\frac{\partial \theta_i}{\partial Y} = \frac{\theta_{i+1} - \theta_{i-1}}{\Delta Y_i + \Delta Y_{i-1}} \qquad [A2]$$

For second order derivatives :

$$\frac{\partial^2 \omega_i}{\partial Y^2} = \frac{\dfrac{\omega_{i+1} - \omega_i}{\Delta Y_i} - \dfrac{\omega_i - \omega_{i-1}}{\Delta Y_{i-1}}}{0.5\,(\Delta Y_i + \Delta Y_{i-1})} \qquad [A3]$$

$$\frac{\partial^2 \theta_i}{\partial Y^2} = \frac{\dfrac{\theta_{i+1} - \theta_i}{\Delta Y_i} - \dfrac{\theta_i - \theta_{i-1}}{\Delta Y_{i-1}}}{0.5\,(\Delta Y_i + \Delta Y_{i-1})} \qquad [A4]$$

REFERENCES

BALABAN, M. 1984. Mathematical model of air drying applied to fish. Ph.D. Dissertation. University of Washington, Seattle, WA.

BALABAN, M. and PIGOTT, G. 1986. Shrinkage in fish muscle during drying. J. Food Sci. *51*, 510.

BALABAN, M. and PIGOTT, G. 1987. Mathematical model of simultaneous heat and mass transfer in food with dimensional changes and variable transport parameters. J. Food Sci. *53*(3), 395.

BENNETT, C.O. and MYERS, J.E. 1962. *Momentun, Heat and Mass Transfer,* p. 483, McGraw-Hill, New York.

BROOKER, D.B. 1967. Mathematical model of the psychrometric chart. Trans. ASAE. *10*, 558.

BROOKER, D.B., BAKKER-ARKEMA, F.W. and HALL, C.W. 1974. *Drying of Cereal Grains*, Van Nostrand Reinhold/AVI, New York.

CHARM, S.E. 1963. Dehydration of foods. In *Food Engineering*, Van Nostrand Reinhold/AVI, New York.

CRANK, J. and PARK, G.S. (Eds.) 1968. *Diffusion in Polymers,* Academic Press, New York.

EARLE, P.L. and CEAGLSKE, N.H. 1949. Factors causing cracking of macaroni. Cereal Chem. *26*, 267.

FINLAYSON, B.A. 1980. *Nonlinear Analysis in Chemical Engineering*, McGraw-Hill, New York.

HAGHIGHI, K. and SEGERLIND, L.J. 1978. Computer simulation of the stress cracking of soybeans. ASAE paper No. 78-3560, ASAE, St. Joseph, MI.

HWANG, M.P. and HAYAKAWA, K.I. 1980. Bulk densities of cookies undergoing commercial baking processes. J. Food Sci. *45*, 1400.

JASON, A.C. 1958. A study of evaporation and diffusion process in the drying of fish muscle. In *Fundamental Aspects of the Dehydration of Foodstuffs*, Soc. Chem. Ind., London.

LEWIS, R.W., MORGAN, K., THOMAS, H.R. and STRADA, M. 1979. Drying induced stresses in porous bodies — An elastoviscoplastic model. Computer Methods in Applied Mech. eng. *20*, 291.

MENSAH, J.K., NELSON, G.L., HAMDY, M.Y. and RICHARD, T.G. 1985. A mathematical model for predicting soybean seedcoat cracking during drying. Trans. ASAE. *28*, 580.

MISRA, R.N. and YOUNG, J.H. 1980. Numerical solution of simultaneous moisture diffusion and shrinkage during soybean drying. Trans. ASAE. *23*, 1277.

RAO, V.N.M. and WEBB, N.B. 1976. Factors influencing stress cracks in frankfurters during cooking and in storage. J. Food Sci. *41*, 427.

SUZUKI, K., KUBOTA, K., HASEGAWA, T. and HOSAKA, H. 1976. Shrinkage in dehydration of root vegetables. J. Food Sci. *41*, 1189.

YOUNG, J. and WHITAKER, T.G. 1971. Numerical analysis of vapor diffusion in a porous composite sphere with concentric shells. Trans. ASAE. *14*, 1051.

ERRATA

Morgan, R.G., Steffe, J.F., and R.Y. Ofoli. 1989. A generalized viscosity model for extrusion of protein doughs. J. Food Process Engineering 11: 55–78.

1. *Add to Table 1, pg. 67:*

ΔE_d	Activation energy for protein denaturation

2. *Add to Table 3, pg. 71:*

ΔE_d*(Kcal/gmole)*	27.7	Within range commonly reported for proteins

F
N
P

PUBLICATIONS IN FOOD SCIENCE AND NUTRITION

Journals

JOURNAL OF MUSCLE FOODS, N.G. Marriott and G.J. Flick, Jr.
JOURNAL OF SENSORY STUDIES, M.C. Gacula, Jr.
JOURNAL OF FOOD SERVICE SYSTEMS, O.P. Snyder, Jr.
JOURNAL OF FOOD BIOCHEMISTRY, J.R. Whitaker, N.F. Haard and H. Swaisgood
JOURNAL OF FOOD PROCESS ENGINEERING, D.R. Heldman and R.P. Singh
JOURNAL OF FOOD PROCESSING AND PRESERVATION, D.B. Lund
JOURNAL OF FOOD QUALITY, R.L. Shewfelt
JOURNAL OF FOOD SAFETY, T.J. Montville and A.J. Miller
JOURNAL OF TEXTURE STUDIES, M.C. Bourne and P. Sherman

Books

CONTROLLED/MODIFIED ATMOSPHERE/VACUUM PACKAGING OF FOODS, A.L. Brody
NUTRITIONAL STATUS ASSESSMENT OF THE INDIVIDUAL, G.E. Livingston
QUALITY ASSURANCE OF FOODS, J.E. Stauffer
THE SCIENCE OF MEAT AND MEAT PRODUCTS, 3RD ED., J.F. Price and B.S. Schweigert
HANDBOOK OF FOOD COLORANT PATENTS, F.J. Francis
ROLE OF CHEMISTRY IN THE QUALITY OF PROCESSED FOODS, O.R. Fennema, W.H. Chang and C.Y. Lii
NEW DIRECTIONS FOR PRODUCT TESTING AND SENSORY ANALYSIS OF FOODS, H.R. Moskowitz
PRODUCT TESTING AND SENSORY EVALUATION OF FOODS, H.R. Moskowitz
ENVIRONMENTAL ASPECTS OF CANCER: ROLE OF MACRO AND MICRO COMPONENTS OF FOODS, E.L. Wynder *et al.*
FOOD PRODUCT DEVELOPMENT IN IMPLEMENTING DIETARY GUIDELINES, G.E. Livingston, R.J. Moshy, and C.M. Chang
SHELF-LIFE DATING OF FOODS, T.P. Labuza
RECENT ADVANCES IN OBESITY RESEARCH, VOL. V, E. Berry, S.H. Blondheim, H.E. Eliahou and E. Shafrir
RECENT ADVANCES IN OBESITY RESEARCH, VOL. IV, J. Hirsch *et al.*
RECENT ADVANCES IN OBESITY RESEARCH, VOL. III, P. Bjorntorp *et al.*
RECENT ADVANCES IN OBESITY RESEARCH, VOL. II, G.A. Bray
RECENT ADVANCES IN OBESITY RESEARCH, VOL. I, A.N. Howard
ANTINUTRIENTS AND NATURAL TOXICANTS IN FOOD, R.L. Ory
UTILIZATION OF PROTEIN RESOURCES, D.W. Stanley *et al.*
FOOD INDUSTRY ENERGY ALTERNATIVES, R.P. Ouellette *et al.*
VITAMIN B_6: METABOLISM AND ROLE IN GROWTH, G.P. Tryfiates
HUMAN NUTRITION, 3RD ED., F.R. Mottram
FOOD POISONING AND FOOD HYGIENE, 4TH ED., B.C. Hobbs *et al.*
POSTHARVEST BIOLOGY AND BIOTECHNOLOGY, H.O. Hultin and M. Milner

Newsletters

FOOD INDUSTRY REPORT, G.C. Melson
FOOD, NUTRITION AND HEALTH, P.A. Lachance and M.C. Fisher
FOOD PACKAGING AND LABELING, S. Sacharow

GUIDE FOR AUTHORS

Typewritten manuscripts in triplicate should be submitted to the editorial office. The typing should be double-spaced throughout with one-inch margins on all sides.

Page one should contain: the title, which should be concise and informative; the complete name(s) of the author(s); affiliation of the author(s); a running title of 40 characters or less; and the name and mail address to whom correspondence should be sent.

Page two should contain an abstract of not more than 150 words. This abstract should be intelligible by itself.

The main text should begin on page three and will ordinarily have the following arrangement:

Introduction: This should be brief and state the reason for the work in relation to the field. It should indicate what new contribution is made by the work described.

Materials and Methods: Enough information should be provided to allow other investigators to repeat the work. Avoid repeating the details of procedures which have already been published elsewhere.

Results: The results should be presented as concisely as possible. Do not use tables *and* figures for presentation of the same data.

Discussion: The discussion section should be used for the interpretation of results. The results should not be repeated.

In some cases it might be desirable to combine results and discussion sections.

References: References should be given in the text by the surname of the authors and the year. *Et al.* should be used in the text when there are more than two authors. All authors should be given in the Reference section. In the Reference section the references should be listed alphabetically. See below for style to be used.

DEWALD, B., DULANEY, J.T., and TOUSTER, O. 1974. Solubilization and polyacrylamide gel electrophoresis of membrane enzymes with detergents. In *Methods in Enzymology,* Vol. xxxii, (S. Fleischer and L. Packer, eds.) pp. 82–91, Academic Press, New York.

HASSON, E.P. and LATIES, G.G. 1976. Separation and characterization of potato lipid acylhydrolases. Plant Physiol. *57,*142–147.

ZABORSKY, O. 1973. *Immobilized Enzymes,* pp. 28–46, CRC Press, Cleveland, Ohio.

Journal abbreviations should follow those used in *Chemical Abstracts.* Responsibility for the accuracy of citations rests entirely with the author(s). References to papers in press should indicate the name of the journal and should only be used for papers that have been accepted for publication. Submitted papers should be referred to by such terms as "unpublished observations" or "private communication." However, these last should be used only when absolutely necessary.

Tables should be numbered consecutively with Arabic numerals. The title of the table should appear as below:

Table 1. Activity of potato acyl-hydrolases on neutral lipids, galactolipids, and phospholipids

Description of experimental work or explanation of symbols should go below the table proper. Type tables neatly and correctly as tables are considered art and are not typeset. Single-space tables.

Figures should be listed in order in the text using Arabic numbers. Figure legends should be typed on a separate page. Figures and tables should be intelligible without reference to the text. Authors should indicate where the tables and figures should be placed in the text. Photographs must be supplied as glossy black and white prints. Line diagrams should be drawn with black waterproof ink on white paper or board. The lettering should be of such a size that it is easily legible after reduction. Each diagram and photograph should be clearly labeled on the reverse side with the name(s) of author(s), and title of paper. When not obvious, each photograph and diagram should be labeled on the back to show the top of the photograph or diagram.

Acknowledgments: Acknowledgments should be listed on a separate page.

Short notes will be published where the information is deemed sufficiently important to warrant rapid publication. The format for short papers may be similar to that for regular papers but more concisely written. Short notes may be of a less general nature and written principally for specialists in the particular area with which the manuscript is dealing. Manuscripts which do not meet the requirement of importance and necessity for rapid publication will, after notification of the author(s), be treated as regular papers. Regular papers may be very short.

Standard nomenclature as used in the engineering literature should be followed. Avoid laboratory jargon. If abbreviations or trade names are used, define the material or compound the first time that it is mentioned.

EDITORIAL OFFICES: DR. D.R. HELDMAN, COEDITOR, *Journal of Food Process Engineering,* National Food Processors Association, 1401 New York Avenue, N.W., Washington, D.C. 20005 USA; or DR. R.P. SINGH, COEDITOR, *Journal of Food Process Engineering,* University of California, Davis, Department of Agricultural Engineering, Davis, CA 95616 USA.

JOURNAL OF FOOD PROCESS ENGINEERING VOLUME 12, NUMBER 1

CONTENTS